MAGNETIC ANISOTROPY OF CRETACEOUS DEEP SEA SEDIMENTARY ROCKS FROM THE PACIFIC PLATE

SATRIA BIJAKSANA

MAGNETIC ANISOTROPY OF CRETACEOUS DEEP SEA SEDIMENTARY ROCKS FROM THE PACIFIC PLATE

by

Satria Bijaksana, B.Sc.Hon.

A Thesis submitted to the School of Graduate
Studies in partial fulfilment of the
requirements for the degree of
Master of Science

Department of Earth Sciences
Memorial University of Newfoundland

1991

St.John's Newfoundland

ISBN 0-315-82610-X

ABSTRACT

Palaeomagnetism and magnetic anisotropy are measured for Cretaceous deep sea sedimentary rocks cored from the Pacific plate by the Deep Sea Drilling Project. The objective is to use magnetic anisotropy to test whether sediment compaction during burial is responsible for the shallowing of remanence inclination reported previously for these rocks.

The present palaeomagnetic study confirms that except at site 463 remanence inclination is shallower than expected. Careful alternating field demagnetization shows that the inclination shallowing is not likely due to a shallow overprint.

Anisotropy of anhysteretic susceptibility (AAS) measurements reported in this thesis show that most specimens (except those from site 463) have a high degree of magnetic anisotropy (averaging 15%) with strong foliation in the bedding plane as would be expected from sediment compaction. Correlation found between degree of magnetic anisotropy and density for both claystones and limestones suggests that the anisotropy was enhanced by compaction. For the claystone specimens, the hypothesis of sediment compaction causing inclination shallowing is supported by a correlation found between the inclination shallowing and the AAS degree of

anisotropy. No such correlation is found for the limestones perhaps because they magnetized earlier in the compaction process. The claystone results suggest that at mid-palaeo-latitudes claystones with AAS degree of anisotropy of about 15% may show a compaction-induced inclination error of 5° leading to an underestimation of palaeolatitude of 4°.

Both claystones and limestones seem to show an inclination shallowing of about 12°, which is independent of anisotropy and thus is probably not compaction-induced. Perhaps inaccuracies in the apparent polar wander path for the Pacific plate are responsible.

The axis of minimum anhysteretic susceptibility deviates an average of only 5° (± 3°) from vertical orientation in the DSDP specimens with about 15% anisotropy. Perhaps AAS could be used to locate the bedding plane in massive sediments.

The magnetic susceptibility of most specimens was too weak for its anisotropy to be reliably measured. However, the susceptibility anisotropy of the stronger specimens did resemble the AAS but was weaker.

Key words: palaeomagnetism, Pacific plate, Cretaceous, deep-sea sedimentary rocks, remanence inclination shallowing, magnetic anisotropy, sediment compaction.

ACKNOWLEDGEMENTS

I am grateful to my supervisor, Dr. J.P. Hodych, for suggesting the thesis topic, for his constant encouragement and guidance in carrying out this research.

Among the faculty members of the Department of Earth Sciences, I would like to thank Drs. E.R. Deutsch and G.S. Murthy for introducing me to the ideas and methods in palaeomagnetism and rock magnetism.

I am indebted to Mr. R. Pätzold and Mr. M. Tubrett of the Palaeomagnetic and Rock Magnetic Laboratory of the Department of Earth Sciences for their assistance in the laboratory.

The privilege to use DSDP specimens was granted kindly by the Ocean Drilling Program. I thank Mr. G. Bode and Mr. S. Prinz of the ODP West-Coast Repository in La Jolla California for their cooperation and assistance during my sampling of DSDP cores.

I am thankful to Dr. C. Hale of the Department of Geology University of Toronto for allowing me to use his magnetic susceptibility meter. I also thank Dr. Hale and Miss J. King for their assistance in using the instrument.

Among graduate students in the Department of Earth Sciences, I would like to thank Mr. D. van Everdingen and Mr. J. van Gool for allowing me to use their computer program, QUICKPLOT, to plot figures 5.1 and 5.2. I thank Mr. S. O'Brien, my office-mate and friend, not only for making available his computational expertise, but also for his encouragement and understanding.

Throughout my tenure as a graduate student, I held a scholarship from the Higher Education Development Project (HEDP) for which I am thankful to the Directorate General of Higher Education of the Ministry of Education and Culture of the Republic of Indonesia and to the Head of the Project, Dr. O. Simbolon. Thanks are also due to Prof. M.T. Zen of Bandung Institute of Technology who nominated me for this scholarship. I am also thankful to World University Service of Canada (WUSC) for administering this scholarship in Canada. Additional financial support was received in the form of travel allowances through the operating grant from the Natural Sciences and Engineering Research Council of Canada (NSERC) to Dr. J.P. Hodych. All this assistance is gratefully acknowledged.

I like to thank Bandung Institute of Technology for granting me leave of absence for my study in Canada.

Finally, I am indebted to my wife, Tintin, and members of my family for their understanding and encouragement.

TABLE OF CONTENTS

Page

LIST OF TABLES

LIST OF FIGURES

Page

CHAPTER 1

INTRODUCTION

1.1 Magnetization of Marine Sediments

The presence of ferromagnetic grains allows marine sediments to acquire a remanent magnetism. Various rock magnetic studies (e.g., Løvlie et al., 1971; Worm and Weinrich, 1988) have shown that the dominant magnetic mineral in most marine sediments is magnetite (Fe_3O_4). The concentration of magnetite is only a few parts per million of the bulk material. Nevertheless, its high saturation magnetization, typically 48 milliteslas, makes fine-grained magnetite a main carrier of natural remanent magnetization (NRM) observed in marine sediments.

Recent studies have shown that magnetite in deep-sea sediments can have organic as well as inorganic origins. Organic magnetite is formed by magnetotactic bacteria and other magnetite-precipitating organisms living in the sea including a variety of pelagic fishes (Chang and Kirschvink, 1989; Stolz et al., 1990). On the other hand, inorganic magnetite is derived mainly from continental sources and oceanic volcanism although some larger particles (> 63 μm) may originate from extraterrestrial input (Bornhold and Bonardi, 1979). Factors such as sedimentation rate, ocean bottom current, turbidity, volcanism etc. control the magnetite input from both organic and inorganic sources. The formation and the chemical composition of deep-sea sediments were discussed in detail by Chester (1990).

The magnetization process in marine sediments begins during sedimentation when fine-grained magnetic particles, carrying a magnetic remanence, align with the Earth's magnetic field as they settle to the bottom. Further sedimentation buries these particles and may prevent their subsequent rotation preserving a detrital remanent magnetization (DRM) (Verosub, 1977; Piper, 1987).

There are two stages of DRM acquisition. The first stage occurs during the depositional processes. It arises from interaction between the magnetic carriers and the substrate at the sediment/water interface. Magnetization acquired at this stage is termed depositional DRM. Fine magnetic grains within fluid filled voids in the sediments remain able to rotate into the direction of the Earth's field. However, as sedimentation proceeds, the increase of overburden load compresses the grains into a tighter configuration and expels the inter-granular water. This fixes the directions of the fine magnetic grains producing a remanence termed post-depositional DRM.

Bioturbation (mixing of near surface-sediments by organisms) destroys depositional DRM tending to replace it by post-depositional DRM.

The orientation of magnetic and non-magnetic particles, in natural sediments is also controlled by the gravitational field and by hydrodynamic factors such as water currents. The impact of these factors is stronger on large particles whereas the Earth's field only affects grains smaller than about 0.03 millimetres (Hrouda, 1982).

Deep-sea soft sediments have been more commonly used than near-shore soft sediments in palaeomagnetic and geomagnetic studies as they preserve a more continuous record of the Earth's magnetic field. The sedimentation rates of deep sea sediments vary from a few millimetres to a few centimetres per 1000 years. Unlike lake and marginal sea sediments whose sedimentation rates are much higher, this low sedimentation rate prohibits deep-sea sediments from recording geomagnetic secular variation. Therefore their magnetization is expected to record only the dipole features of the earth's magnetic field (Verosub, 1977).

1.2 The Use of Deep-Sea Sediments in Palaeomagnetic and Geomagnetic Studies

Prior to the 1960s, drilling to recover deep-sea rock specimens for scientific study was uncommon. In 1968, JOIDES (Joint Oceanographic Institutions for Deep Earth Sampling) started an extensive drilling program termed the Deep Sea Drilling Project (DSDP). This was succeeded in 1983 by the Ocean Drilling Program (ODP). Hundreds of sites have been drilled world wide and many institutions and nations have joined JOIDES. Today, DSDP and ODP samples provide very important research material for marine geology and geophysics.

Opdyke and Phillips (1969) showed the feasibility of palaeomagnetic and geomagnetic studies using deep-sea sedimentary rock cores when they reported the palaeomagnetic stratigraphy derived using specimens from the first seven DSDP sites. Although the cores were not oriented in azimuth, the changes in the sign of inclination or the changes of 180° in declination were sufficient to mark the polarity changes. The polarity change record supported the geomagnetic reversal sequences observed on land and extended the sequences back to 10 Ma or more (Opdyke et al., 1974). Foster and Opdyke (1970) showed that the marine polarity record was in agreement with the pattern of sea-floor magnetic anomalies produced by sea-floor spreading.

Magnetic inclination records also give palaeolatitude data for the drilling sites. Magnetically derived palaeolatitude data for rock core of known age can be used to estimate the latitudinal component of the absolute motion of the DSDP sites (Sclater and Cox, 1970). Palaeolatitude data from several representative sites may be used to reconstruct the motion of the oceanic plates. Opdyke (1972) discussed the use of deep-sea cores in palaeomagnetism in great detail.

1.3 Reliability of the Palaeolatitude Data Determined from Palaeomagnetic Study of Deep-Sea Sediments

The main question in the study of magnetization in sediments, including deep sea sediments, is how accurately the magnetization records the direction of the Earth's magnetic field at the time the sediments formed. Early experimental studies suggested that although the declination of remanence in sediments parallels the applied field, the inclination of remanence is shallower than the field (e.g., Johnson et al., 1948). A few physical mechanisms that may be responsible for this inclination error have been proposed (for a review, see Nagata, 1962 and Verosub, 1977).

First, inclination error may arise because some magnetic grains are not perfectly spherical. Disk-shaped grains, for example, will align horizontally parallel to the bedding plane, instead of aligning with the applied field inclination. Inclination error may also occur if particles are deposited on a dipping bed. Also, the velocity gradient of the flow may induce an inclination error; it can exert a shear stress on a particle rotating the particle about a horizontal axis perpendicular to the direction of flow.

The above proposed mechanisms imply that inclination error is an intrinsic property of sediments. However, Verosub (1977) and Levi and Banerjee (1990) argued that these mechanisms are not realistic for natural sediments because the sedimentation rates used to produce the artificial sediments were much higher than usually encountered in nature.

Inclination error may also occur during sediment compaction. Elongated magnetic particles may be rotated into a more horizontal orientation causing a shallowing of the sample's remanence. Inclination shallowing accompanying compaction in synthetic and natural sediments has been demonstrated by Anson and Kodama (1987), Celaya and Clement (1988), Deamer and Kodama (1990), and Arason and Levi (1990a).

One type of commonly used synthetic sediment in compaction experiments is the single clay slurry consisting of magnetite mixed with one type of clay (Anson and Kodama, 1987; Deamer and Kodama, 1990). During compaction, magnetite grains are either attached to clay particles or incorporated into clay domains. Magnetite grains then rotate as the flat clay particles align horizontally during compaction. Anson and Kodama(1987) suggested that electrostatic attraction between positively charged smaller magnetite grains and negatively charged larger clay particles produce the attachment. However, Deamer and Kodama (1990) suggested that Van der Walls attraction produces the attachment. Arason and Levi (1990b) provided general models of inclination shallowing during sediment compaction.

Inclination shallowing in deep-sea sediments has been observed by Celaya and Clement (1988) and Arason and Levi (1990a). Celaya and Clement (1988) used deep-sea sediments from the North Atlantic to show that inclination shallowing correlates with a downhole decrease in water content presumably due to compaction. Arason and Levi (1990a) showed a correlation between inclination shallowing and decrease in average porosity at DSDP sites in the Pacific Ocean suggesting that the correlation was caused by sediment compaction.

There are a few other reasons why palaeolatitude data from magnetism of deep-sea sedimentary rock cores may not be as reliable as from continental samples (Peirce, 1976; Gordon and Cox, 1980). First, it is possible that the cores were not drilled vertically (Ogg, 1986) requiring an additional correction based on the measured vertical deviation of the hole. Secondly, the quantity of material at a given level may not be sufficient due to poor core recovery. Third, palaeomagnetic inclination averages without declination control may provide a low estimate of the true palaeolatitude. Methods of correcting this have been suggested by Kono (1980) and McFadden and Reid (1982).

One study that questions the reliability of palaeolatitude data determined from palaeomagnetic study of deep sea sedimentary rock cores was done by Gordon (1990). He showed that the Cretaceous palaeolatitudes estimated palaeomagnetically using sediment cores at nine DSDP sites from the Pacific plate were mostly significantly shallower than the palaeolatitudes predicted from the apparent polar wander path (APWP) constructed using all other palaeomagnetic data (Figure 1.1).

Gordon (1990) proposed several mechanisms that could account for this remanence shallowing. These were (1) a shallow overprint or an unremoved recent viscous remanent magnetization (VRM), (2) coring-related process, (3) delayed magnetization and (4) compaction of sediments in post depositional processes. Later, Tarduno (1990) reexamined the data in detail and showed that the only possible mechanism for this remanence shallowing is compaction of sediments after deposition.

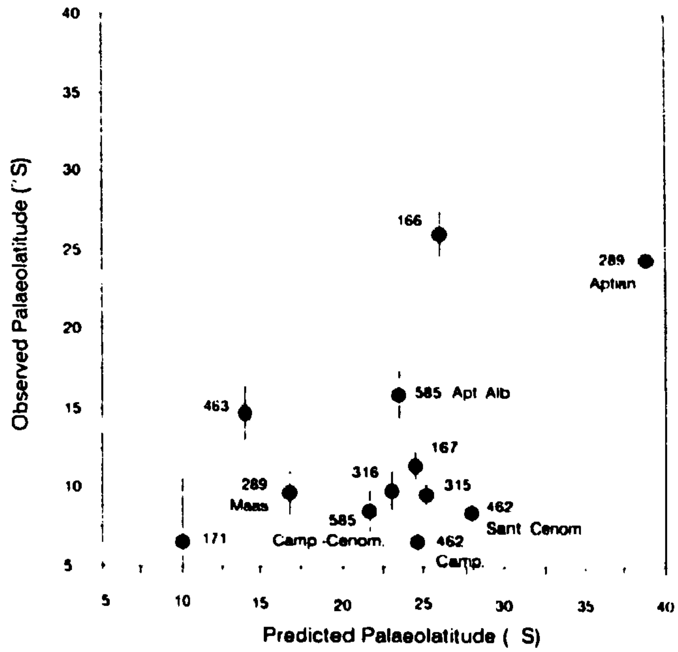

Fig.1.1 Comparison of palaeolatitude observed by palaeomagnetic study of sediments recovered by the DSDP with the palaeolatitude predicted by the APWP constructed using all other palaeomagnetic data. After Gordon (1990).

1.4 The Objectives of this Study

The primary objective of the present investigation was to use magnetic anisotropy to test whether the inclination shallowing of remanence in the Cretaceous DSDP sedimentary rock cores reported by Gordon (1990) is caused by compaction during burial. If so, one expects a correlation between magnetic anisotropy and remanence inclination shallowing. A correlation between compaction and magnetic anisotropy was shown by Kodama and Sun (1990) for artificial kaolinite-magnetite samples compacted in the laboratory. They used two magnetic anisotropy methods namely anisotropy of magnetic susceptibility (AMS), and anisotropy of anhysteretic susceptibility (AAS)(McCabe et al., 1985). Kodama and Sun (1990) showed that compaction caused an AMS of about 2-5 % and an AAS of about 15-30 %.

Cockerham and Jarrad (1976) measured the AMS of DSDP sediments but concluded that the measured magnetic anisotropy was too small to generate an inclination error. Although both AAS and AMS were measured in the present investigation, the former was considered as the main technique since it was expected to be larger and to be applicable to rocks of very low magnetite content (McCabe et al., 1985; Potter and Stephenson, 1986).

In the present investigation, 43 specimens from six DSDP sites in the equatorial Pacific (Chapter 2) were studied. The NRMs of specimens were measured to obtain the magnetic inclination of the sites (Chapter 3). Later, the mean inclination of each site was compared with the published palaeomagnetic poles to determine the occurrence of remanence inclination shallowing. Chapter 4 discusses briefly the nature of magnetic anisotropy including differences between AAS and AMS. The methods and results of AAS and AMS measurement are described in Chapter 5. The palaeomagnetic data were then correlated with the anisotropy data. Chapter 6 discusses this correlation as well as other aspects of the anisotropy data.

CHAPTER 2

GEOLOGY AND SAMPLING

2.1 General Geology of the Pacific Plate

The Pacific is the world's oldest and largest ocean. It was a *superocean* known as Phantalassa in the Early Mesozoic when the continents were clustered together as Gondwana and Laurasia. The generation of the Indian and Atlantic Oceans forced the ancestral Pacific to grow smaller (Dietz and Holden, 1970) as the North and South American plates moved westward and the Australian plate moved northward.

The Pacific Ocean consists of several plates, with the Pacific plate as the largest (Figure 2.1). The Pacific plate is bounded to the east by the constructive East Pacific rise that extends northward to the complex North American boundary. To the north and west, the Pacific plate is bounded by a trench system extending from the Aleutian and Kurile trenches to the Japan Trench, Mariana Trench, and the New Hebrides Trench, and then southwest through the Kermadec-Tonga Trench. The Macquarie and the Pacific-Antarctic ridges mark the southern boundary of the Pacific plate.

Fracture zones, magnetic isochrons, palaeomagnetism, palaeoclimatology and hotspot tracks have been used to

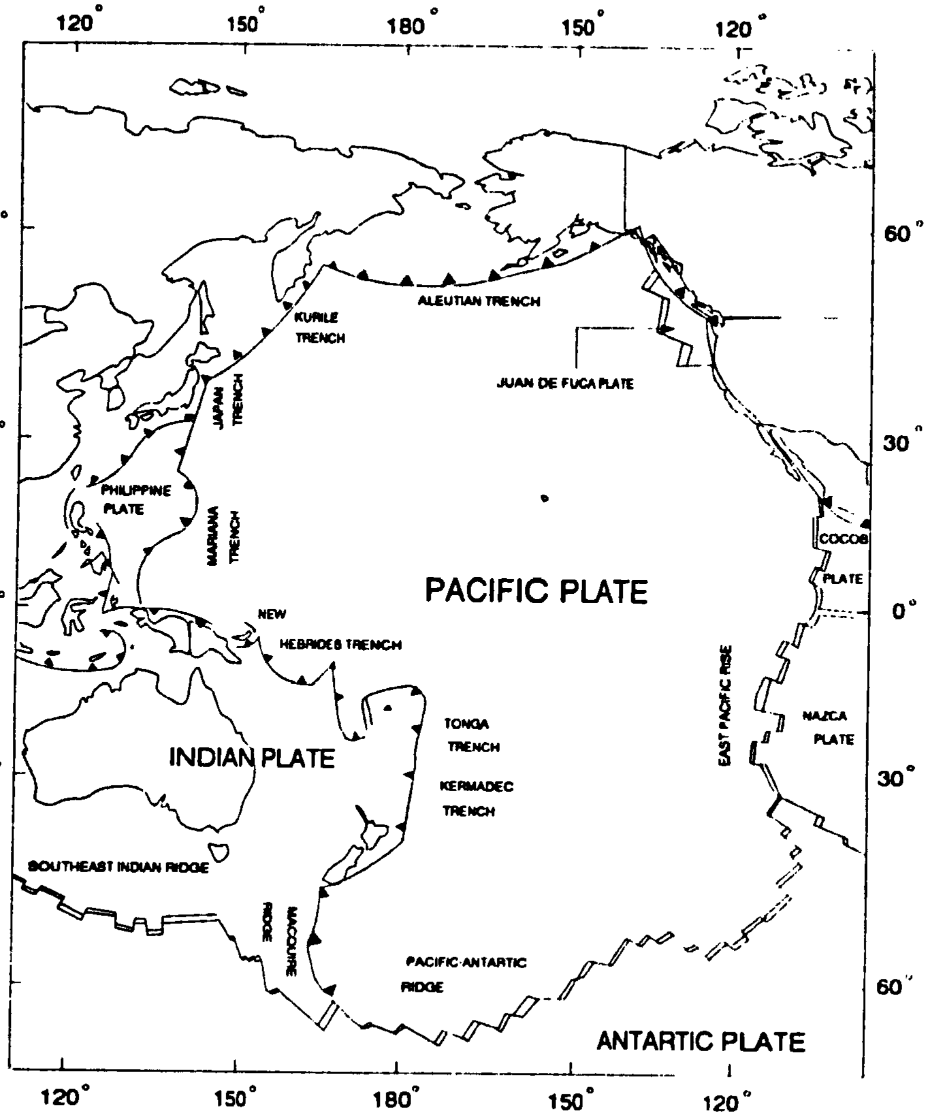

Fig.2.1 The major tectonic plates, mid-ocean ridges, trenches and transform faults in the Pacific region.

reconstruct the interactions between oceanic and continental plates in and around the Pacific basin during the last 140 million years (e.g., Hilde et al., 1977; Engebretson et al., 1987; Zonenshain et al., 1987; Cox et al., 1989). Although these reconstructions differed in detail, they agreed that the northernmost part of the Pacific plate was in the southern hemisphere at 140 Ma. The Pacific plate has since moved almost northwestward as the older oceanic plates were subducted and destroyed beneath North America, Northeastern Asia and the Bering Sea.

The tectonic history of the Pacific plate has been summarized in many text books (e.g., Condie, 1982; Kennett, 1982; Fowler, 1990). Cox and Hart (1986) have clearly outlined the methods used in producing these reconstructions.

2.2 Sampling Sites

The present investigation uses specimens from six DSDP sites in the equatorial Pacific (Figure 2.2). Palaeomagnetic studies of these sites have been done by Jarrad (1973) for site 167, Cockerham and Jarrad (1976) for site 315, Cockerham (1979) for sites 167, 315 and 316, Steiner (1981) for site 462, Sayre (1981a) for site 463, and Tarduno (1990) for sites 167, 288, 315, 316 and 463. Gordon (1990) and Tarduno (1990) showed that for all these sites except site 463, the observed magnetic inclinations are shallower than magnetic inclinations predicted by the APWP from all other data (see Fig.1.1).

Site 167 is located on the Magellan Rise in the Central Pacific Basin. The cores taken from this site indicate that

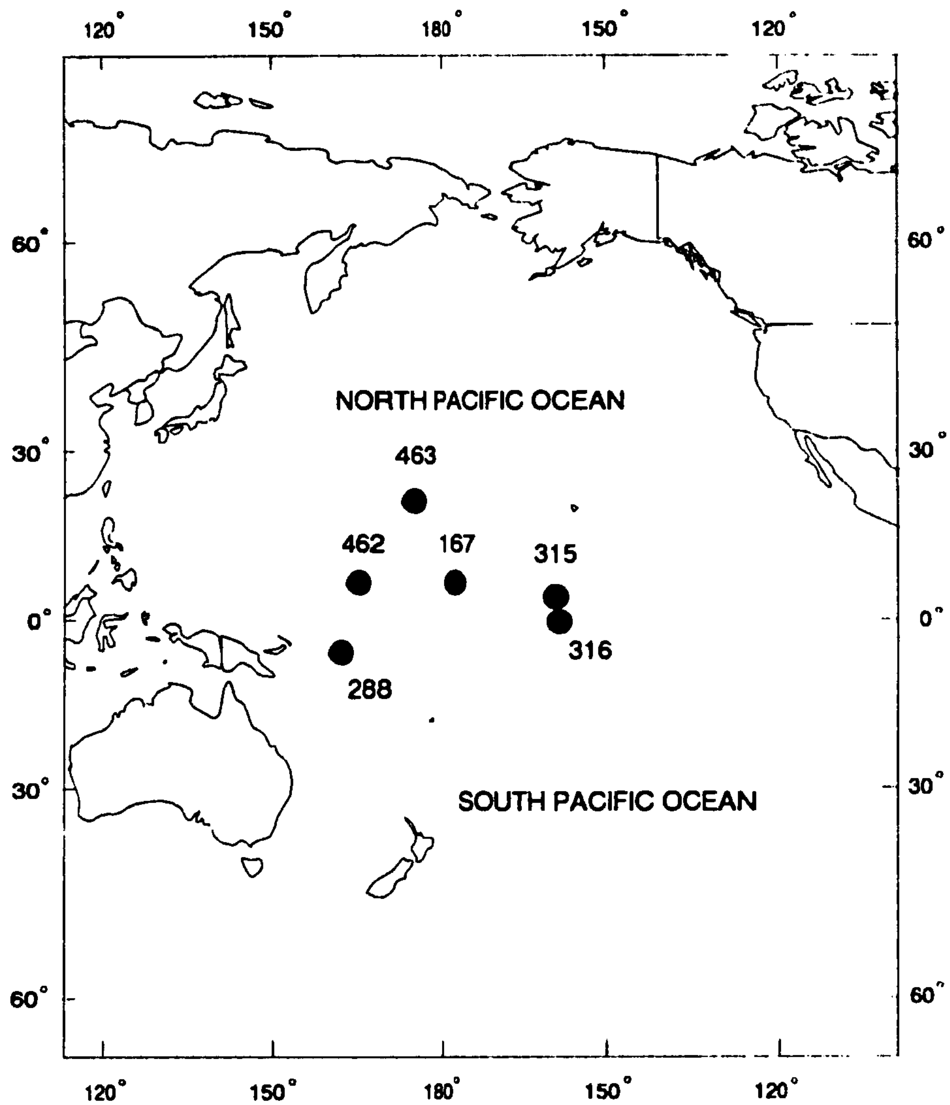

Fig.2.2 Location map of Pacific plate DSDP sites analyzed in the present investigation.

the Magellan Rise is covered by old sediments. The oldest datable sediments were Early Cretaceous or Late Jurassic in age. The curve of accumulation rate suggested that site 167 was in the equatorial zone during about 25 to 30 Ma, and has since moved northward at an average rate of about 1 degree per 4 million years (Winterer et al., 1973).

Site 288 is located on the southeastern flank of the Ontong Java Plateau. The underlying oceanic crust beneath the plateau has an unusual thickness of up to 40 kilometres (Kroenke, 1972). The thick accumulation of biogenic sediment above the plateau was probably caused by shallow water depth and its tropical location. The cores range in age from Aptian at the base to Pleistocene at the top with an interval of unrecovered core that is probably Palaeocene to Early Oligocene in age (Andrews et al., 1975). Figure 2.3 shows the geologic linear time scale from Cretaceous to the present time.

Sites 315 and 316 are located on the Line Islands seamount chain, which stretches southeast across the Central Pacific from the Mid Pacific Mountain to the equator. Winterer (1976) suggested that this chain of volcanos was built by mid plate volcanism at the abandoned spreading centre of the Pacific-Farallon Ridge about 105 million years ago. The age of the oldest datable sediments was Santonian at site 315 and Campanian at site 316 (Schlanger et al., 1976a and 1976b).

Site 462 is located on the northern part of Nauru Basin. It is the location of a mid-Cretaceous volcanic complex at least 500 meters thick composed of sills, flows, and volcani-

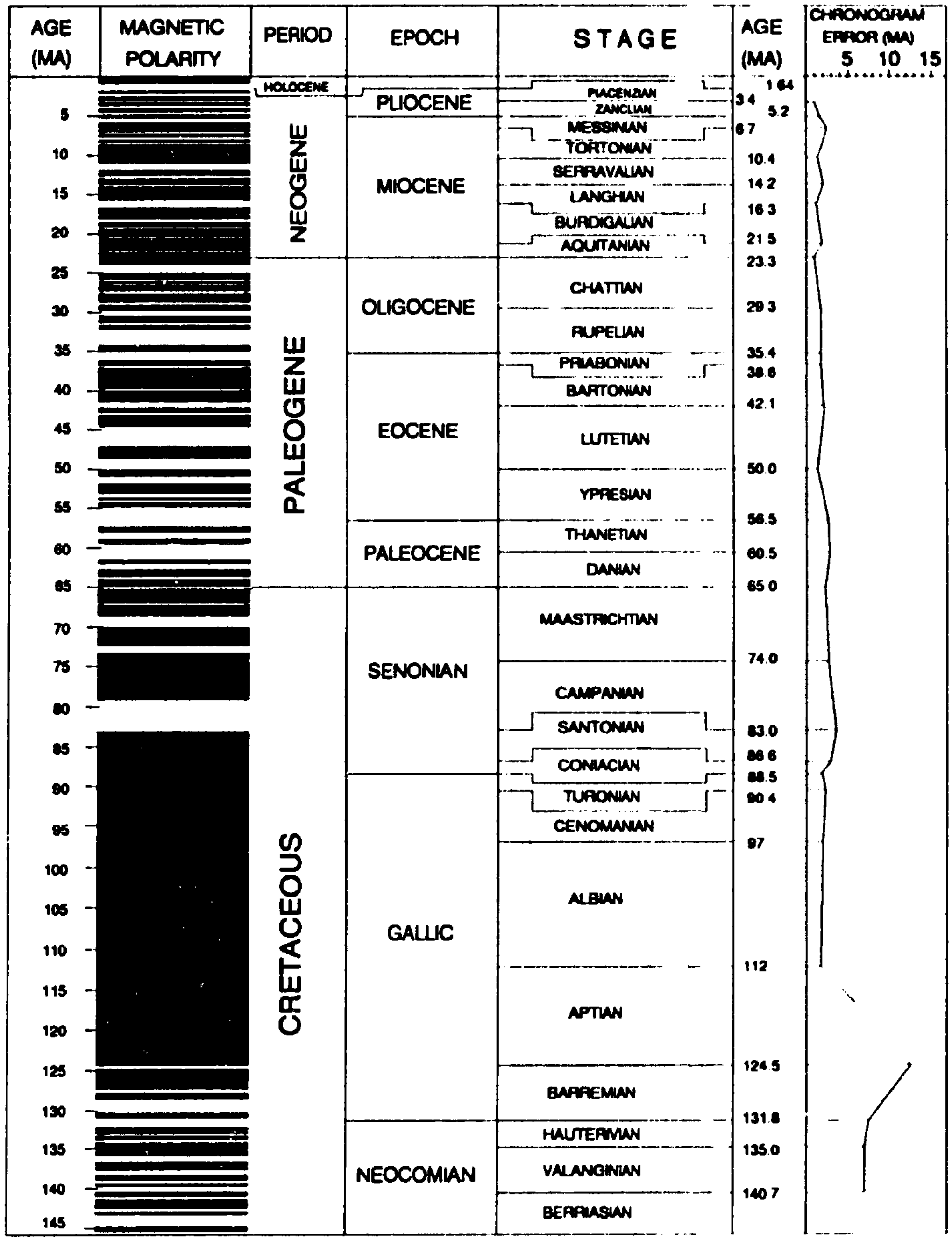

Fig.2.3 Geologic linear time scale from Cretaceous to the present time (modified from Harland et al., 1990).

clastic sediments (Larson et al., 1981). The Jurassic(?) basement of the basin subsided due to loading of the Cretaceous volcanic pile and subsequent sedimentation (Larson and Schlanger, 1981). The oldest sediment cored at site 462 was Cenomanian in age (Larson et al., 1981).

Site 463 is located on the western part of the Mid-Pacific Mountains. This is the largest aseismic rise in the central North Pacific Ocean. It rests on top of probable Lower Cretaceous and Jurassic crust (Thiede et al., 1981a). The curve of accumulation rate indicates that the site might have crossed the equator during the late Campanian and early Maastrichtian (Thiede et al., 1981b). The oldest sediment cored was Barremian in age (Thiede et al., 1981b).

2.3 Sampling Techniques

The West Coast Repository of the ODP at Scripps Institution of Oceanography in La Jolla California provided 83 specimens from sites 167, 288, 315, 316, 462, 463 and 585. The specimens were selected based on their ages, lithology, and material condition. The numbering of specimens follows the method that is used by DSDP and ODP.

Each DSDP/ODP drilling site is assigned a number, for example, site 167. The first hole of the site carries the site name, whereas additional holes have a letter following the number; A for the second, B for the third and so on. From each hole, many cores were taken. Each core, normally 9 meters in length, consists of six 150 cm sections. Specimen 315A-19-5-50, for example, is obtained from the second hole of site 315 core 19 section 5 and 50 cm from the top of the section.

The specimens were obtained by travelling to Scripps and subsampling the split core collection in the repository workshop. Prior to drilling, both vertical and horizontal orientations were marked on each proposed sample. The core (of 2.44 inch diameter) was then drilled perpendicular to its vertical axis using a ¾ inch (about 19 mm) diamond drill bit. Later, in the palaeomagnetic and rock magnetic laboratory at Memorial University, the resultant 19 mm diameter cores were trimmed to 19 mm length using a diamond wheel. Only the up-down axis is known. Nevertheless, for simplicity, the horizontal orientation mark made before drilling was nominally called the 'east-west' axis whereas the cylinder axis of the specimen was denoted the 'north-south' axis. See Figure 2.4.

Later, specimens from site 585 were excluded because they were soft and brittle making them difficult to measure with the existing apparatus. Some specimens from other sites were also excluded either because they shattered during drilling and cutting or because they were not magnetic enough to measure their remanences to acceptable accuracy.

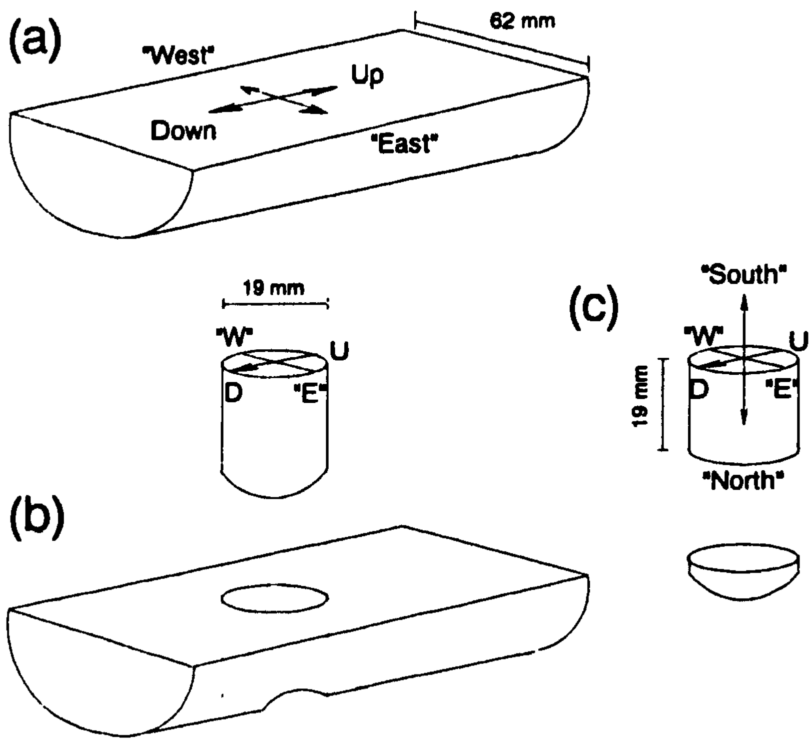

Fig.2.4 Schematic of sampling technique. (a) The vertical and horizontal orientations are marked on the split core sample. (b) The core is then drilled perpendicular to the up-down axis using a ¾ inch diamond drill bit. (c) The drilled specimen is trimmed to 19 mm length. Note that the 'east-west' and the 'north-south' axes are nominal since the core's azimuth is unknown.

In total, magnetic anisotropies of 43 specimens were measured. The locations of the sites, number of specimens taken from each site, and geological stages and lithology of specimens are summarized in Table 2.1.

Table 2.1 Summary of Sampling Sites

SITE	LONGITUDE	LATITUDE	N	STAGE#	LITHOLOGY#
167	176°49.50'W	07°04.10'N	8	Albian to Hauterivian	Marly Limestones - Limestones
288A	161°49.53'E	05°58.35'S	8	Turonian to Albian	Limestones
315A	158°31.54'W	04°10.26'N	8	Campanian to Santonian	Claystone - Clayey Limestones
316	157°07.71'W	00°05.44'N	7	Maastrichtian to Campanian	Foraminiferal Limestones
462	165°01.83'E	07°14.25'N	5	Campanian	Claystones
463	174°40.07'E	21°21.01'N	7	Albian to Aptian	Silicified Limestones

Winterer et al. (1973) for site 167; Andrews et al. (1975) for site 288; Schlanger et al. (1976a) for site 315; Schlanger et al. (1976b) for site 316; Larson et al. (1981) for site 462; Thiede et al. (1981b) for site 463. N is the number of specimens taken from each site.

CHAPTER 3

PALAEOMAGNETIC STUDY

3.1 Introduction

The natural remanent magnetization present in a rock specimen is often the resultant of two major components namely the primary or characteristic magnetization and the secondary magnetization. In sediments, the former is the magnetization acquired during sediment formation, while the latter refers to magnetizations acquired during subsequent geological time. The objective is to isolate the primary magnetization of each specimen and measure its characteristic inclination. The inclination data of specimens close to the same known age will be averaged site by site.

To isolate the primary magnetization, the remanence is measured after each step in a gradual demagnetization that removes the soft or unstable component before the hard or stable component. The primary component is assumed to be magnetically more stable against demagnetization than the secondary component. There are two common demagnetization methods, namely alternating field (AF) and thermal demagnetization.

In AF demagnetization, a specimen is exposed to an alternating magnetic field in a space that is otherwise field-free. Its magnetization of low coercivity follows the applied field and is erased by being randomized as the field is reduced to zero. The intensity of alternating field is increased in steps, with the remanence of the specimen being measured after each step. The remanence remaining is of higher and higher coercivity after each step and should approach closer and closer to a stable "characteristic" direction which is often assumed to be primary.

In thermal demagnetization, the specimen is heated and cooled in field-free space using higher and higher temperatures. In the present investigation, AF rather than thermal demagnetization was used for two reasons. First, the main magnetic mineral in deep-sea sediments is magnetite whose range of coercivities lies within the range of the available AF demagnetizer. Secondly AF demagnetization will not chemically alter the specimen whereas thermal demagnetization will.

3.2 Techniques of Remanence Measurement

All remanence measurements were performed with a superconducting magnetometer built by CTF Systems Inc. (Port Coquitlam, British Columbia). The instrument has two detecting units - one to measure the horizontal component of the specimen's magnetic moment and the other to measure the vertical component. Each detecting unit has a SQUID (Superconducting Quantum Interference Device) sensor and a superconducting pick-up coil. The detecting units and the specimen access region are surrounded by superconducting shields to enhance the sensitivity of the instrument. Each of these shields is a closed shell that traps whatever magnetic field is present when the shell becomes superconducting. The shells are in an almost field-free space provided by a 3-layered mu-metal shield enclosing the entire instrument. The superconducting shield in the sample access region attenuates external field changes by a factor $\geq 10^7$ in the transverse direction and $\geq 10^9$ in the axial direction. A 30-litre superinsulated Dewar flask containing liquid helium houses the superconducting shields and the detecting assembly. Liquid helium, with a boiling point of 4.2°K, is the cryogen for the superconducting shields and the detecting assembly.

The measurement begins by lowering the specimen into the centre of the superconducting pick-up coils using the sample access hole. A reading of the vertical (up-down) component of the sample's magnetic moment and one of its horizontal components is then taken through an on-line computer. Rotating the specimen through 90° about a vertical axis gives a reading of the other horizontal component of the sample's magnetic moment. The specimen is rotated through 360° in successive 90° steps about the vertical axis taking readings after each step. The same procedure is then repeated with the specimen turned upside down. This provides four values each for the North and the East component and two values for the Down component. The computer then calculates and prints the output in terms of declination, inclination and the intensity of the sample's magnetic moment.

The magnetic moment of the specimen holder used in this investigation was of the order of 5 to 10 x 10^{-12} Am^2 and was measured every four operating hours. Although this holder moment was negligible compared to the NRMs of specimens (which vary from 1 x 10^{-9} to 5 x 10^{-7} Am^2), it was routinely subtracted from the resultant moment in each remanence measurement of a specimen.

3.3 Alternating Field (AF) Demagnetization

In the present investigation, the alternating field demagnetization was carried out on a Schonstedt GDS-1 AF demagnetizer. It consists of a solenoid that can produce a peak alternating field of 100 mT. The field strength and its decay rate are selected on a control panel. The solenoid is enclosed in a 3-layer mu-metal magnetic shield to exclude the Earth's magnetic field.

Each specimen was demagnetized along three orthogonal directions (N, E, D) in turn and then its residual magnetic moment was measured with the magnetometer. The demagnetization started with a peak alternating field of 2.5 mT. Successively higher fields were then applied to reduce the magnetic moment further until it went down to approximately 10% or less of its original (NRM) value. By then, the remanence of most specimens was heading reliably toward the origin. The maximum field used was usually 60 mT. However, magnetic moment in some specimens required significantly less or significantly more than 60 mT for demagnetization to 10% of NRM.

3.4 Results

Since the true azimuths of the specimens are unknown, their declinations are given relative to the nominal "east-west" axis marked on the split core (Section 2.3). The characteristic magnetic inclination and this 'relative' or nominal characteristic magnetic declination (Columns 6 and 7 on Table 4.1) were determined for each specimen by simple least-squares fit (forced through the origin) calculations since the demagnetization vector plots of most specimens (except those from site 463) point toward the origin. This was done using spreadsheet software (LOTUS 123 version 2.2). This is illustrated by least squares fit dashed lines in the vector plots of Figure 3.1. As an example, the characteristic magnetic inclination and the nominal characteristic magnetic declination of specimen 167-62-4-64 determined using this method are illustrated in Figure 3.1.a.

Some specimens carry a stable single component of magnetization as shown by the magnetization direction hardly changing during AF demagnetization (specimen 315-20-5-17 in Fig. 3.1.c, for example). Other specimens carry a multi-component magnetization and the magnetization direction changes significantly during demagnetization (specimen 167-62-4-64 in Fig. 3.1.a, for example). The palaeomagnetic results are listed in Table 3.1, while their details are in Appendix 1. The results are summarized as follows:

Site 167

The remanence inclinations of most specimens from site 167 steepened as the demagnetizing field increased. On the other hand, only a few specimens showed significant remanence declination change during demagnetization. The remanence intensities of the specimens were easily reduced to 10% by a demagnetizing field of 40-50 mT. Specimen 167-62-4-64 is typical of the specimens from site 167 (see Fig.3.1.a).

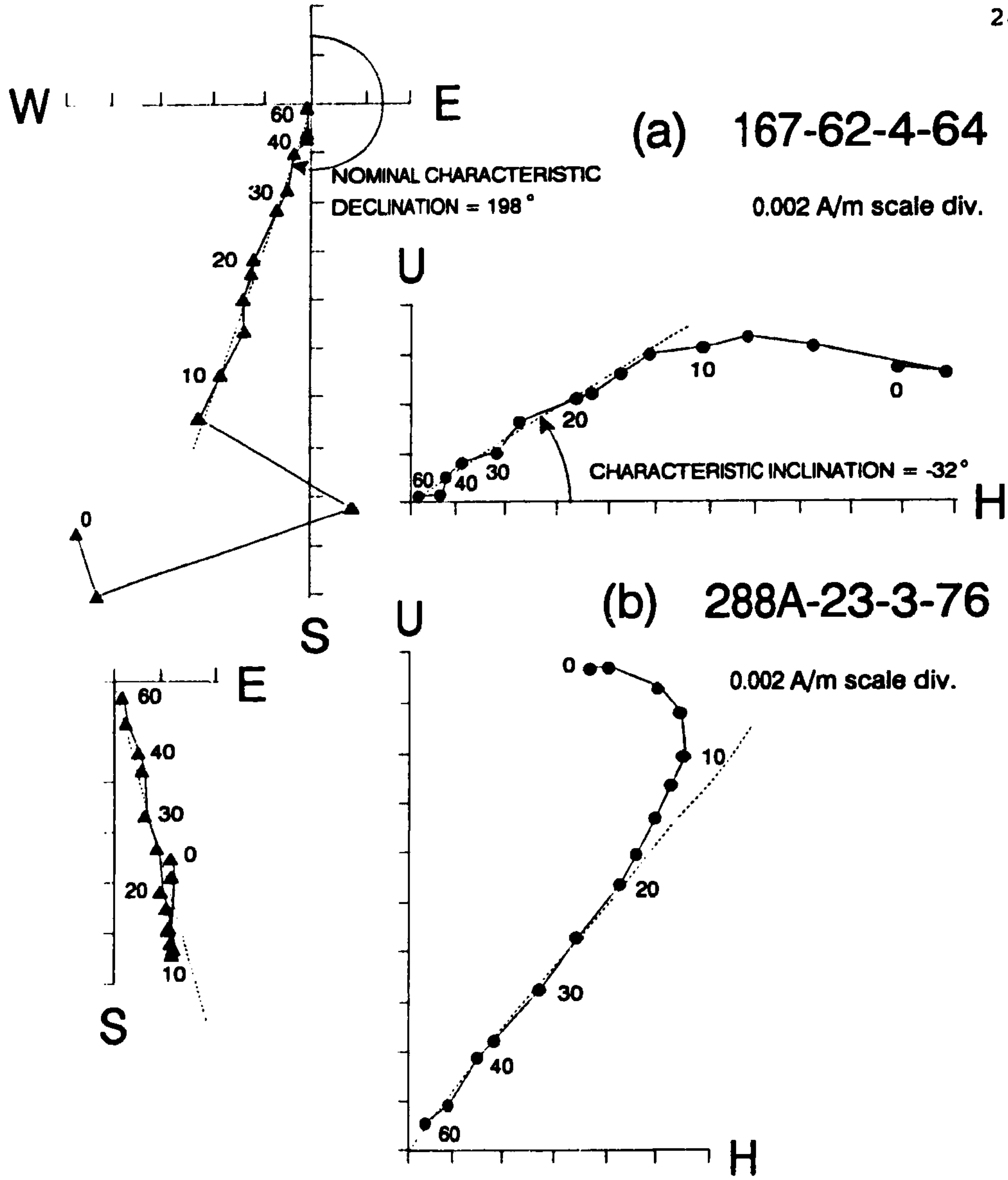

Fig. 3.1 Vector (Roy) plots of horizontal (solid triangle) and vertical (solid circle) components of natural magnetic remanence of selected specimens (a) 167-62-4-64, (b) 288A-23-3-76, (c) 315A-20-5-17, (d) 316-20-4-67, (e) 462-55-1-114 and (f) 463-60-2-33. Numbers indicate the demagnetizing field in mT. U = up, D = down, H = horizontal, N = north, E = east, S = south and W = west. Dashed lines obtained from least squares method illustrate the characteristic magnetic inclination and the nominal characteristic magnetic declination of the specimens.

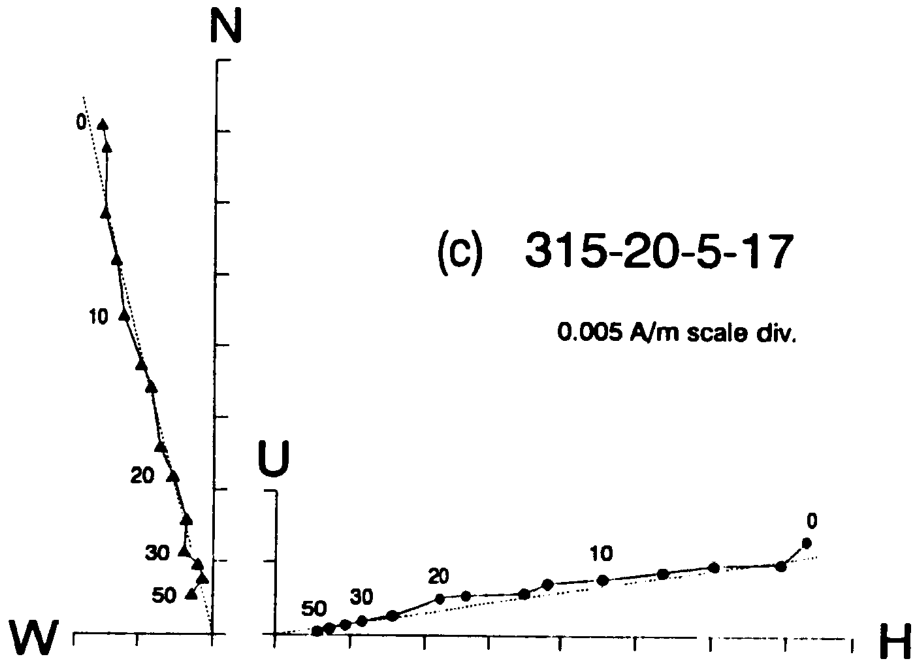
N
(c) 315-20-5-17
0.005 A/m scale div.
U
W
H
0
10
20
30
50

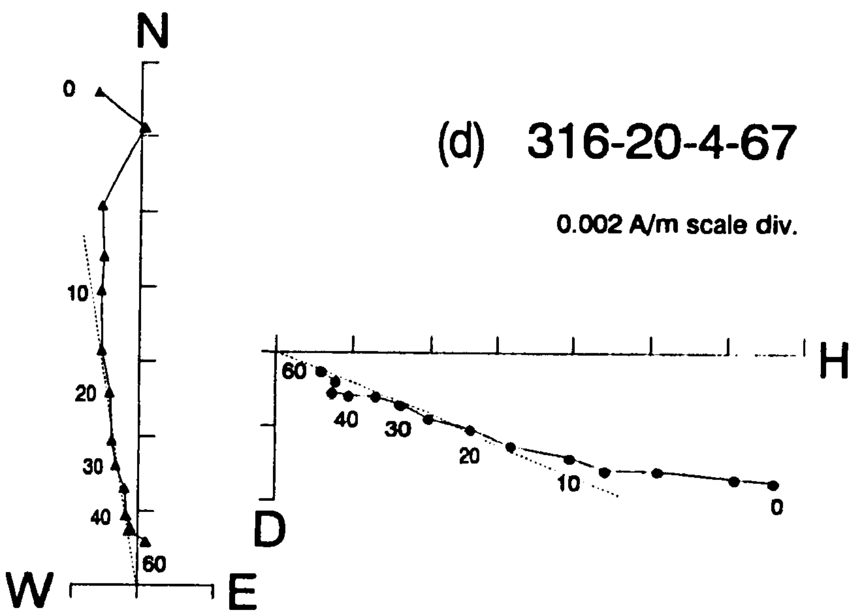
N
(d) 316-20-4-67
0.002 A/m scale div.
H
D
W
E
0
10
20
30
40
60

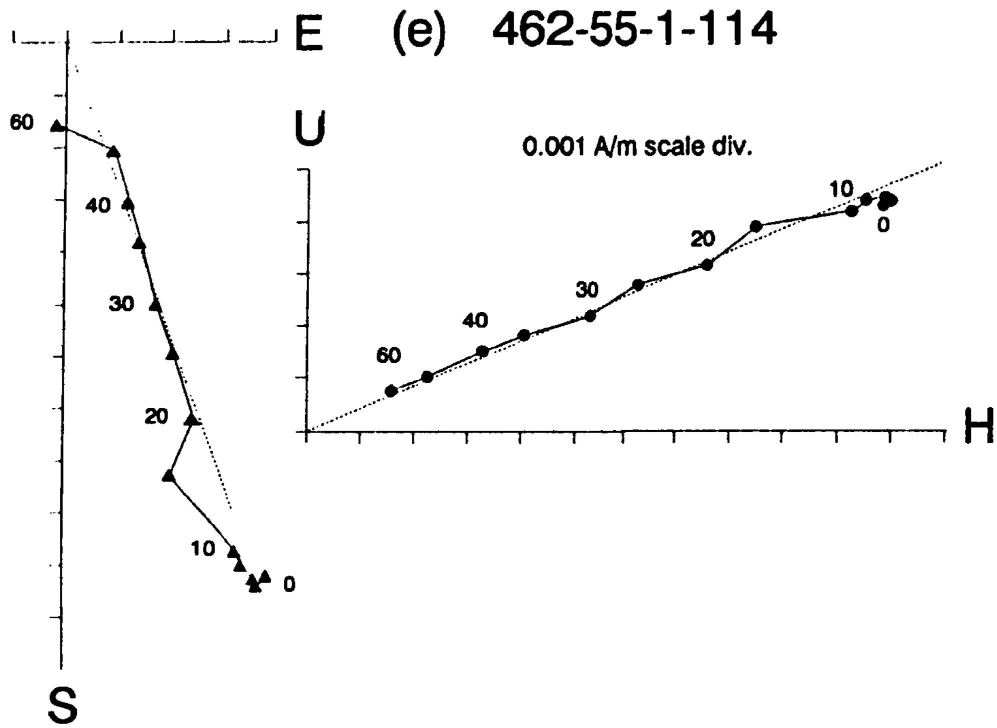
E
(e) 462-55-1-114
U
0.001 A/m scale div.
60
40
30
20
10
0
H
S

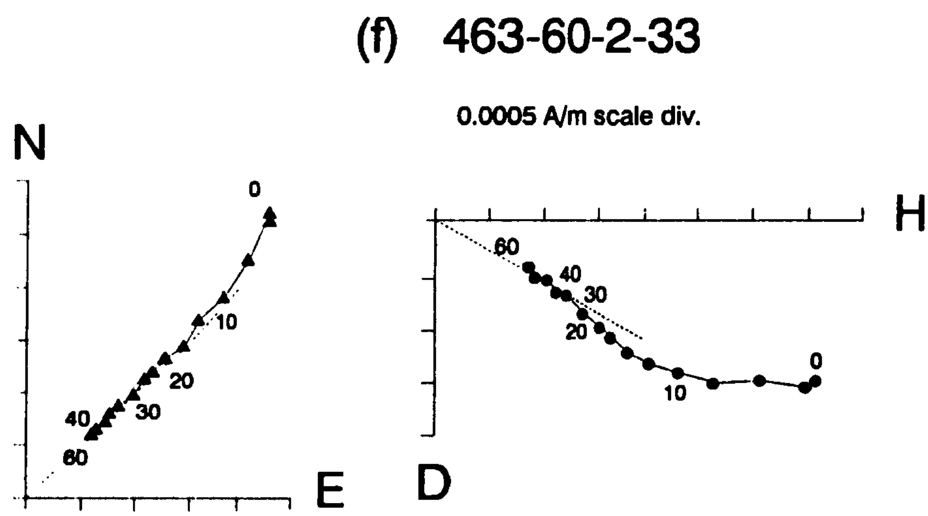
(f) 463-60-2-33
0.0005 A/m scale div.
N
0
10
20
30
40
60
E
H
D

TABLE 3.1 Palaeomagnetic results

SITE/SPECIMEN	NRM			CHAR.DIRECTION#	
	MOMENT(A.m^2)	DEC.*	INC.	DEC.*	INC.
167					
167-62-4-64	1.104e-07	208.2	-15.3	197.8	-32.0
167-63-4-75	4.543e-07	5.5	3.4	3.2	-27.3
167-65-3-42	8.273e-08	266.0	-66.0	245.4	-45.8
167-67-3-36	1.403e-07	22.3	-9.1	36.5	-28.2
167-69-4-133	5.021e-08	70.7	16.2	85.1	14.3
167-71-2-63	1.854e-07	330.4	-12.0	297.6	-20.9
167-72-2-63	4.028e-08	27.8	-10.4	28.1	-17.0
167-73-2-121	9.077e-09	12.1	-4.4	10.2	-18.2
288A					
288A-21-2-98	5.567e-08	41.4	-49.7	92.5	-52.5
288A-21-3-18	4.913e-08	193.2	-68.6	181.3	-51.8
288A-22-2-84	1.246e-07	56.3	-51.5	89.7	-47.3
288A-23-1-79	1.783e-08	145.6	-66.3	140.4	-55.1
288A-23-2-115	9.331e-08	334.5	-8.6	337.3	-11.9
288A-23-3-76	1.119e-07	161.6	-69.0	164.8	-50.9
288A-26-1-28	2.023e-07	217.8	-48.7	216.3	-48.4
288A-29-1-47	1.433e-07	88.4	-55.2	115.0	-38.5
315A					
315A-19-5-50	1.756e-07	217.4	-14.1	218.5	-16.5
315A-20-2-21	3.246e-07	356.8	-10.8	354.4	-15.9
315A-20-2-131	3.324e-07	105.7	-24.8	119.7	-20.6
315A-20-5-17	1.988e-07	347.5	-10.9	345.3	-8.6
315A-21-2-11	5.010e-07	266.1	-5.4	265.5	-5.2
315A-21-5-8	1.330e-07	98.4	-15.6	111.1	-14.9
315A-21-6-108	8.956e-08	138.0	-31.9	143.0	-31.8
315A-26-2-123	1.489e-07	75.8	-14.6	80.0	-13.1

TABLE 3.1 (Continued)

SITE/SPECIMEN	NRM			CHAR.DIRECTION#	
	MOMENT(A.m^2)	DEC.*	INC.	DEC.*	INC.
316					
316-19-2-108	9.159e-08	342.8	29.5	339.4	35.4
316-19-4-74	5.625e-08	338.4	4.5	328.9	38.1
316-20-4-67	7.345e-08	354.6	14.6	350.1	22.4
316-22-2-77	1.322e-07	321.8	10.2	312.1	12.0
316-23-3-107	1.566e-07	353.3	9.6	332.4	22.0
316-24-3-59	5.496e-08	70.2	-43.7	107.5	-32.4
316-25-5-40	2.519e-07	91.8	-21.2	95.2	-25.5
462					
462-55-1-28	3.350e-07	81.0	-13.6	82.7	-13.7
462-55-1-114	6.329e-08	160.7	-21.6	160.6	-23.3
462-55-2-128	2.874e-07	19.4	-2.1	17.0	-12.7
462-55-3-29	8.679e-07	204.5	13.1	205.3	14.7
462-55-3-132	1.157e-07	287.8	12.1	263.2	19.7
463					
463-58-1-31	8.798e-09	62.4	-20.4	75.5	-19.1
463-58-2-82	1.280e-08	45.8	-20.2	53.1	-34.9
463-59-2-104	5.581e-09	298.7	-26.0	245.1	-29.6
463-60-2-33	2.088e-08	39.8	22.5	44.4	29.2
463-61-1-105	4.711e-08	341.7	-31.2	279.8	-33.0
463-64-1-60	1.074e-08	297.8	-18.6	294.6	-44.5
463-67-2-103	1.950e-09	147.1	-26.3	164.4	-32.0
463-70-1-78	4.672e-09	9.4	-29.1	11.0	-22.9

CHAR. DIRECTION# is characteristic direction of specimen's magnetic remanence after AF demagnetization determined from the directions of the stable residual remanences using the least squares method. DEC* is relative or nominal declination. See text for explanation.

Site 288 Hole A

In contrast to site 167, for most specimens from site 288 hole A, remanence inclination shallowed as the demagnetizing field increased. Upon completion of the demagnetization steps, the remanence declination of some specimens had changed by as much as 50°. A demagnetizing field of 50-60 mT was required to reduce the remanence intensity of the specimens to 10%. Specimen 288A-23-3-76 is typical of the specimens from site 288 hole A (see Fig.3.1.b).

Site 315 Hole A

Demagnetization to 60 mT did not significantly change the magnetic inclinations and declinations of specimens from site 315 hole A. Specimen 315A-20-5-17 is typical of the specimens from this site (see Fig.3.1.c).

Site 316

Like specimens of site 167, most specimens of site 316 showed remanence inclination steepening as the demagnetizing field increased. Remanence declinations only changed slightly. Unlike specimens from any other site, most specimens of site 316 have positive magnetic inclination suggesting reverse polarity. This may correspond to one or more periods of reversed magnetic field during Upper Campanian-Midlle

Maastrichtian. The remanence intensity was lowered to 10% of NRM on demagnetization to 60 mT. Specimen 316-20-4-67 is typical of the specimens of site 316 (see Fig.3.1.d).

Site 462

The remanence inclinations and declinations of specimens of site 462 were not significantly affected by demagnetization. Since all specimens are Campanian, the positive inclination shown by the last two specimens may correspond to the Campanian reversed period. The maximum demagnetizing field required was typically 60 mT. One specimen (462-55-4-42) was rejected because it retains a magnetization of very high coercivity beyond the 100 mT range of the AF demagnetizer perhaps carried by hematite. Specimen 462-55-1-114 is typical of the specimens from site 462 (see Fig.3.1.e).

Site 463

The remanence inclinations and declinations of specimens from site 463 were changed slightly by demagnetization. As their coercivities are higher than those from other sites (at a demagnetizing field of 60 mT, some specimens retain about 30% of their original remanence), the method of inclination and declination determination described above requires specimens from site 463 to be demagnetized to higher fields. However, this may not have helped significantly because the remaining magnetic moments were already very weak approaching the noise level of the magnetometer (for example, see specimen 463-70-1-78, Appendix 1). Specimen 463-60-2-33 is typical of the specimens from site 463 (see Fig.3.1.f).

3.5 Estimating Inclination Shallowing of Remanence Observed at the Sites

In this investigation, it is important to determine not only the characteristic remanence inclination at a given site but also the age of specimens at that site. The latter would be used to estimate the palaeoinclination of the Earth's field at the site expected from the APWP of the Pacific plate (see Table 3.2). An observed remanence inclination less than the predicted palaeoinclination of the Earth's field would suggest the presence of inclination shallowing.

At some sites, the geological ages of specimens vary significantly. Therefore, each specimen was assigned a median age by averaging the upper and lower boundary ages of its geological stage given by Harland et. al's time scale (1990). The median ages of Cretaceous geological stages and their errors are listed in Table 3.3. These median ages of individual specimens within a particular site were then averaged to obtain the site's mean age (see Table 3.4) used to calculate the position of the corresponding palaeomagnetic pole.

TABLE 3.2 The APWP of the Pacific Plate

AGE (MA)	POLE LAT.	POLE LON.	SEMI AXIS[§] MAJ.[#]	ORT.[*]	MIN.[†]	SOURCE
66	71°N	9°E	6°	91°	2°	Gordon (1983)
81	57°N	4°W	5°	88°	4°	Gordon (1983)
94	58.6°N	30.9°W	7.0°	35°	6.2°	Sager & Pringle (1988)
125	51.4°N	36.9°W	9.8°	63°	3.2°	Gordon (1990)

§: the semiaxes of the 95% confidence limit. #: the length of the major semiaxis. *: the orientation of the major semiaxis clockwise of north. †: the length of the minor semiaxis. The position of the pole at any time is determined by extrapolating its past and future positions listed above assuming that it propagated steadily in a straight path.

The geographic latitude (λ_p) and longitude (ϕ_p) of the palaeomagnetic pole at the any given time is determined by interpolating between its previous and subsequent known positions (Table 3.2) assuming that the pole propagated steadily in a straight path. For example, the latitude and longitude of the pole at 115.8 MA ($\lambda_{115.8}$ and $\phi_{115.8}$) required to estimate the palaeoinclination of the Earth's magnetic field at site 167 are calculated from the known positions of the pole at 94 MA (58.6°N 30.9°W) and at 125 MA (51.4°N 36.9°W) as follows:

$$\lambda_{115.8} = \frac{115.8 - 94}{125 - 94} (\lambda_{125}-\lambda_{94}) + \lambda_{94} = 53.5°N$$

$$\phi_{115.8} = \frac{115.8 - 94}{125 - 94} (\phi_{125} - \phi_{94}) + \phi_{94} = -35.1° = 35.1°W$$

where λ_{94} and ϕ_{94} are the known latitude and longitude of the pole at 94 MA and λ_{125} and ϕ_{125} at 125 MA.

The predicted palaeoinclination (I), the predicted palaeolatitude (λ), and the predicted palaeodeclination (D) can then be calculated by solving simultaneously the palaeomagnetic equations below.

$$\sin \lambda_p = \sin \lambda_x \sin\lambda + \cos \lambda_x \cos \lambda \cos D \qquad (3.1)$$

$$\sin (\phi_p - \phi_x) = \frac{\cos \lambda \sin D}{\cos \lambda_p} \quad \textit{for} \sin \lambda \geq \sin \lambda_p \sin \lambda_x \qquad (3.2)$$

$$\sin (180 + \phi_p - \phi_x) = \frac{\cos \lambda \sin D}{\cos \lambda_p} \quad \textit{for} \sin \lambda < \sin \lambda_p \sin \lambda_x \qquad (3.3)$$

and

$$\tan I = 2 \tan \lambda \qquad (3.4)$$

where λ_x is the site's present geographic latitude, ϕ_x the site's present geographic longitude, λ_p the geographic latitude of the palaeomagnetic pole, and ϕ_p the geographic longitude of the palaeomagnetic pole. In this investigation, the above equations were solved using a simple spreadsheet calculation.

TABLE 3.3 The median ages of the Cretaceous geological stages

STAGE	AGE OF BOUNDARIES (MA)$		ERROR (MA)*		MEDIAN $+e_+/-e_-$	$\bar{e}$
	UPPER$	LOWER$	UPPER*	LOWER*	(MA)	(MA)
MAASTRICTIAN	65.0	74.0	2.3	2.8	69.5 +5.3/-5.1	5.2
CAMPANIAN	74.0	83.0	2.8	3.6	78.5 +5.8/-5.3	5.5
SANTONIAN	83.0	86.6	3.6	3.0	84.8 +3.5/-4.0	3.8
CONIACIAN	86.6	88.5	3.0	1.8	87.6 +2.0/-3.1	2.6
TURONIAN	88.5	90.4	1.8	1.6	89.5 +1.9/-2.0	1.9
CENOMANIAN	90.4	97	1.6	2.0	93.7 +3.9/-3.7	3.8
ALBIAN	97	112	2.0	1.8	104.5 +7.7/-7.8	7.7
APTIAN	112	124.5	1.8	12.5	118.3 +14.0/-6.5	10.2
BARREMIAN	124.5	131.8	12.5	7.5	128.2 +8.3/-13.0	10.7
HAUTERIVIAN	131.8	135	7.5	6.9	133.4 +7.1/-7.7	7.4

$: the age of the stage's upper and lower stratigraphic boundaries. * : the chronogram errors at the stage's upper and lower boundaries (Harland et al., 1990). "Median $+e^+/-e^-$" means that the most probable absolute age of the stage should have a value between (Median + e^+) and (Median − e^-). e^+ and e^- are the most probable values of errors and are defined as

$$e^+ = \sqrt{(LOWER^*)^2 + (\frac{1}{2}(LOWER^\$ - UPPER^\$))^2}$$

and

$$e^- = \sqrt{(UPPER^*)^2 + (\frac{1}{2}(LOWER^\$ - UPPER^\$))^2}$$

respectively. However, the simpler form $\bar{e} = \frac{1}{2}(e^+ + e^-)$ will be used in further calculations.

TABLE 3.4 The ages of specimens

SITE/SPECIMEN	STAGE[1]	MEDIAN ± $\bar{e}$ (MA)	SITE'S MEAN AGE MEAN(MA)	STD(MA)
167				
167-62-4-64	ALBIAN	104.5± 7.7	115.7	14.8
167-63-4-75	ALBIAN	104.5± 7.7		
167-65-3-42	ALBIAN	104.5± 7.7		
167-67-3-36	ALBIAN	104.5± 7.7		
167-69-4-133	APTIAN	118.3±10.2		
167-71-2-63	BARREMIAN	128.2±10.7		
167-72-2-63	BARREMIAN	128.2±10.7		
167-73-2-121	HAUTERIVIAN	133.4± 7.4		
288A				
288A-21-2-98	TURONIAN ?	89.5± 1.9	91.9	6.1
288A-21-3-18	TURONIAN ?	89.5± 1.9		
288A-22-2-82	TURONIAN ?	89.5± 1.9		
288A-23-1-79	TURONIAN ?	89.5± 1.9		
288A-23-2-115	TURONIAN ?	89.5± 1.9		
288A-23-3-76	TURONIAN ?	89.5± 1.9		
288A-26-1-28	CENOMANIAN	93.7± 3.8		
288A-29-1-47	ALBIAN	104.5± 7.7		
315A				
315A-19-5-50	CAMPANIAN	78.5± 5.5	79.3	5.7
315A-20-2-21	CAMPANIAN	78.5± 5.5		
315A-20-2-131	CAMPANIAN	78.5± 5.5		
315A-20-5-17	CAMPANIAN	78.5± 5.5		
315A-21-2-11	CAMPANIAN	78.5± 5.5		
315A-21-5-8	CAMPANIAN	78.5± 5.5		
315A-21-6-108	CAMPANIAN	78.5± 5.5		
315A-26-2-123	SANTONIAN	84.8± 3.8		

TABLE 3.4 (Continued)

SITE/SPECIMEN	STAGE[§]	MEDIAN ± $\bar{e}$ (MA)	SITE'S MEAN AGE MEAN(MA)	STD(MA)
316				
316-19-2-108	MAASTRICHTIAN	69.5± 5.2	73.4	6.9
316-19-4-74	MAASTRICHTIAN	69.5± 5.2		
316-20-4-67	MAASTRICHTIAN	69.5± 5.2		
316-22-2-77	MAASTRICHTIAN	69.5± 5.2		
316-23-3-107	CAMPANIAN	78.5± 5.5		
316-24-3-59	CAMPANIAN	78.5± 5.5		
316-25-5-40	CAMPANIAN	78.5± 5.5		
462				
462-55-1-28	CAMPANIAN	78.5± 5.5	78.5	5.5
462-55-1-114	CAMPANIAN	78.5± 5.5		
462-55-2-128	CAMPANIAN	78.5± 5.5		
462-55-3-29	CAMPANIAN	78.5± 5.5		
462-55-3-132	CAMPANIAN	78.5± 5.5		
463				
463-58-1-31	ALBIAN	104.5± 7.7	107.9	10.3
463-58-2-82	ALBIAN	104.5± 7.7		
463-59-2-104	ALBIAN	104.5± 7.7		
463-60-2-33	ALBIAN	104.5± 7.7		
463-61-1-105	ALBIAN	104.5± 7.7		
463-64-1-60	ALBIAN	104.5± 7.7		
463-67-2-103	APTIAN	118.3±10.2		
463-70-1-78	APTIAN	118.3±10.2		

§ Winterer et al. (1973) for site 167; Andrews et al. (1975) for site 288; Schlanger et al. (1976a) for site 315; Schlanger et al. (1976b) for site 316; Larson et al. (1981) for site 462; Thiede et al. (1981b) for site 463. Site's mean age is calculated from the median ages of specimens within the site. While N is the number of specimen within the site, STD is the standard deviation and is defined as

$$STD = \sqrt{\frac{1}{N} \sum \left((\bar{e}_i)^2 + (MEDIAN_i - MEAN)^2 \right)} .$$

The observed remanence inclination at the site was calculated as the mean inclination of the characteristic remanence inclinations of the specimens at the site. Since the true azimuths of the specimens are unknown, it would not be appropriate to use the ordinary Fisher statistical analysis. Instead, a method proposed by McFadden and Reid (1982) was used. A numerical example of how this method was applied is given in Appendix 2.

Table 3.5 compares the observed characteristic remanence inclinations and the predicted palaeoinclinations from the APWP of the Pacific Plate for all sites. It shows that shallowing of remanence inclination (positive ΔI) occurs in all sites but site 463. Despite the limited number of specimens per site used in this investigation, the data are in good agreement with those reported or quoted by Tarduno (1990).

3.6 Discussion

The reliability of the method of estimating inclination shallowing of remanence described in the preceding section depends strongly on several factors.

First, it depends on the quality of the mean of the observed remanence inclinations, which is represented by the best estimate of the precision parameter, k, and by the 95 per cent confidence limit, I_{95} (Tarling, 1983). Table 3.5 shows that the values of k from the present investigation are mostly smaller and the values of I_{95} are higher than from the other sources listed. This lesser precision from the present study is expected because much fewer specimens per site were used in the present investigation.

TABLE 3.5 Palaeomagnetic data of the Pacific DSDP sites

SITE	AGE (MA)	I_{ob} (°)	k	I_{95} (°)	D_{pd} (°)	I_{pd} (°)	ΔI (°)	N	SOURCE
167	115.8	-25.4	31.4	10.4	23.3	-38.0	12.6	8	(1)
	115	-29.1	37	2.0			8.7	95	(2)
288A	91.9	-44.8	16.6	14.4	5.5	-56.7	11.9	8	(1)
	92	-41.6	49	2.6			14.7	41	(3)
315A	79.3	-15.8	51.4	8.1	13.5	-42.2	26.4	8	(1)
	78	-20.5	67	2.6			20.2	30	(3)
316	73.4	-26.8	39.7	10.3	9.6	-41.8	15.0	7	(1)
	70	-17.1	34	1.7			20.9	132	(3,4)
462	78.5	-16.8	160.5	7.1	-7.2	-39.8	23.0	5	(1)
	81	-11.1	87	3.7			32.1	13	(5)
463	108.0	-30.6	55.8	7.7	15.9	-18.7	-11.9	8	(1)
	108	-30.9	87	2.4			-12.4	28	(3)

I_{ob} is the observed inclination of each site (see Appendix 2), k the best estimate of precision parameter, I_{95} the 95 per cent confidence limit for I_{ob}, D_{pd} the predicted declination of each site, I_{pd} the predicted inclination of each site and ΔI the discrepancy between I_{ob} and I_{pd}. Data from other sources are also listed (shaded rows) for comparison. Sources of data: (1) This work; (2) Tarduno et. al (1989); (3) Tarduno (1990); (4) Cockerham (1979); (5) Steiner (1981). (2), (4), and (5) were quoted from (3).

The reliability also depends on how accurately one determines the predicted palaeoinclination of the Earth's field at each site. The predicted inclination is derived from the APWP assuming the magnetic pole propagated steadily in a straight path between known pole positions. This assumption is valid if the known pole positions are separated by short time intervals. In the APWP of the Pacific plate this interval varies from 13 to 31 MA. The reliability also depends on how accurately one calculates the age of specimens at a particular site (Table 3.4). Unfortunately, it is difficult to integrate these two sources of error. Hence, an error estimate for inclination shallowing ΔI is not given in Table 3.5. Nor was an error estimate for ΔI given by the previous workers listed in Table 3.5.

CHAPTER 4

MAGNETIC ANISOTROPY

4.1 Magnetic Anisotropy in Sediments

A sample with magnetic anisotropy has magnetic properties that depend on the direction in which they are measured (Cullity, 1971). Magnetic anisotropy is commonly expressed as either directional variability of magnetic susceptibility, remanent magnetization or energy of magnetization to saturation (see Hrouda, 1982).

In natural rocks that have never been exposed to high magnetic field prior to an anisotropy measurement, magnetic anisotropy is caused by shape anisotropy and/or magnetocrystalline anisotropy (Bathal, 1971; Hrouda, 1982). Shape anisotropy is due to preferred orientation of non-spherical ferromagnetic grains in rocks. It is displayed only by magnetic minerals with high intrinsic susceptibility, such as magnetite. In elongated magnetite grains, the maximum susceptibility is found approximately in the longest direction. In contrast, low susceptibility minerals, such as hematite, exhibit only magnetocrystalline anisotropy, which is anisotropy due to magnetization along certain crystallographic axes being easier than along other axes.

Except in red sediments, magnetite is the most prominent magnetic mineral in sedimentary rock (Piper, 1987). Thus, magnetic anisotropy in sediments depends mainly on the shape and the orientation of magnetite grains. This dependence makes magnetic anisotropy useful in reconstructing the depositional processes of sediments (Hamilton and Rees, 1970; Taira, 1989).

Few papers have been published on magnetic anisotropy studies in deep-sea sediments. Sayre (1981b) reported the use of anisotropy of magnetic susceptibility (AMS) in investigating the possible existence of depositional slopes and palaeocurrent activity in North Pacific DSDP sediments. Shor et al.(1984) showed the use of AMS in differentiating downslope and alongslope depositional processes on the Nova Scotia continental rise. Flood et al.(1985) demonstrated the use of AMS in recognizing primary and secondary magnetic fabrics in surficial deep-sea sediments of the Nova Scotia continental rise.

Magnetic anisotropy is also used widely in other research areas such as igneous petrology and structural geology. Hrouda (1982) and McDonald and Ellwood (1987) have reviewed the general applications of magnetic anisotropy.

4.2 Anisotropy of Anhysteretic Susceptibility

Use of anisotropy of anhysteretic susceptibility (AAS) was introduced to rock magnetism by McCabe et al.(1985). This method measures anisotropy in a rock specimen's ability to acquire an anhysteretic remanent magnetization (ARM).

A specimen acquires anhysteretic remanence when it is exposed to a weak direct field in the presence of a strong alternating field whose intensity is reduced slowly to zero. The intensity of anhysteretic remanence is proportional to the strength of the direct field. The proportionality constant was termed anhysteretic susceptibility by King et al. (1982). Although resembling initial or low field susceptibility, anhysteretic susceptibility contains no contribution from paramagnetic and diamagnetic components in the sample. Magnetically hard minerals such as hematite and geothite contribute minimally to anhysteretic susceptibility as their coercivities are typically higher than the range of alternating field applied. Thus, the contribution of magnetite is enhanced. Therefore, this method is important in studies involving rock specimens that contain a low magnetite concentration (e.g., limestone or shale).

These differences led McCabe et al.(1985) to suggest that AAS is more useful in geophysics than AMS. Potter and

Stephenson (1988) confirmed that remanence anisotropy (including AAS) in some rocks can be very high while anisotropy of susceptibility is weak or even zero.

Another difference between AAS and AMS is that AAS is more sensitive to the magnetite grain size of interest to palaeomagnetism. Whereas AMS tends to be dominated by less stable multi-domain and superparamagnetic grains in the sample, AAS tends to be dominated by the stable single-domain and pseudo single-domain grains (McCabe et al., 1985). In deep-sea sediments, where single-domain magnetite is often the carrier of stable remanence, AAS may be more effective than AMS. Although AMS does carry complementary information, it is often much more difficult to measure because of the very low magnetite content of many deep-sea sediments.

4.3 Calculation of Anisotropy Parameters

Throughout, it is assumed that the anhysteretic remanence intensity is a linear function of the direct field strength. The anhysteretic susceptibility tensor, χ, for an anisotropic medium is given by:

$$A_i = \chi_{ii} . H_i + \chi_{ij} . H_j + \chi_{ik} . H_k \qquad (4.1)$$

where **i,j,k** = 1,2,3 are the axes of the Cartesian coordinate system, A_i the component of anhysteretic remanence intensity in the **i** direction, H_i the component of direct field in the **i** direction and χ_{ij} the second order symmetric tensor ($\chi_{ij} = \chi_{ji}$), which represents the anhysteretic susceptibility.

Like any other second order symmetric tensor, the anhysteretic susceptibility tensor is characterized by six tensor components χ_{11}, χ_{22}, χ_{33}, χ_{31}, χ_{32}, χ_{12} that are normally non zero. However, there should exist a Cartesian coordinate system in which the non-diagonal components are zero. In such a coordinate system, anhysteretic susceptibility is expressed by only three components (χ_1, χ_2, χ_3) in three orthogonal directions. The components χ_1, χ_2, χ_3 are called the principal anhysteretic susceptibilities and their directions are called the principal directions. Such a coordinate system is obtained by solving the characteristic equations of matrix χ_{ij} as follows:

$$\mathbf{det}\ (\eta\delta_{ij} - \chi_{ij}) = 0 \qquad (4.2.a)$$

$$(\eta\delta_{ij} - \chi_{ij})\mathbf{x} = 0 \qquad (4.2.b)$$

where **det** is the determinant function, η the eigenvalue of matrix χ_{ij}, **x** the eigenvector corresponding to η and δ_{ij} the Kronecker delta. Based on their eigenvalues, the principal anhysteretic susceptibilities χ_1, χ_2, χ_3 are respectively called the maximum, intermediate and minimum anhysteretic susceptibility. Geometrically, they represent the principal axes of an ellipsoid.

Girdler (1961) proposed a procedure to calculate the susceptibility tensor in AMS calculations. The six AAS tensor components χ_{11}, χ_{22} . . .χ_{12} can also be determined using the same procedure. An ARM is given to a rock specimen along certain axes using the same strength of direct field and the remanence intensities are measured. The measured remanence intensities can then be considered as the corresponding anhysteretic susceptibility tensor components in Equation 4.1.

Three orthogonal axes, OX_1, OX_2, and OX_3 that indicate the orientation of the specimen with respect to geographic north (1 = North, 2 = East, and 3 = Down), are used as the reference coordinate system. Generally, the anhysteretic susceptibility along an arbitrary axis OX_m denoted by **m** is given by

$$A_m = c_{mi}\, c_{mj}\, \chi_{ij} \qquad (4.3)$$

where c_{mi} and c_{mj} are the direction cosines of **m** relative to the reference axes i and j respectively and A_m the measured remanence intensity in the **m** direction.

Girdler (1961) proposed using measurements along the nine axes shown in Figure 4.1. The direction cosines of these axes with respect to the reference axes (N, E, D) are:

A_1 (1, 0, 0)	A_4 $(1/\sqrt{2}, 1/\sqrt{2}, 0)$	A_7 $(-1/\sqrt{2}, 1/\sqrt{2}, 0)$
A_2 (0, 1, 0)	A_5 $(1/\sqrt{2}, 0, 1/\sqrt{2})$	A_8 $(-1/\sqrt{2}, 0, 1/\sqrt{2})$
A_3 (0, 0, 1)	A_6 $(0, 1/\sqrt{2}, 1/\sqrt{2})$	A_9 $(0, -1/\sqrt{2}, 1/\sqrt{2})$

According to Equation 4.3, the anhysteretic susceptibilities in the nine measured directions are:

$$
\begin{aligned}
A_1 &= \chi_{11} \\
A_2 &= \chi_{22} \\
A_3 &= \chi_{33} \\
A_4 &= \tfrac{1}{2}\chi_{11} + \tfrac{1}{2}\chi_{22} + \chi_{12} \\
A_5 &= \tfrac{1}{2}\chi_{11} + \tfrac{1}{2}\chi_{33} + \chi_{31} \\
A_6 &= \tfrac{1}{2}\chi_{22} + \tfrac{1}{2}\chi_{33} + \chi_{23} \\
A_7 &= \tfrac{1}{2}\chi_{11} + \tfrac{1}{2}\chi_{22} - \chi_{12} \\
A_8 &= \tfrac{1}{2}\chi_{11} + \tfrac{1}{2}\chi_{33} - \chi_{31} \\
A_9 &= \tfrac{1}{2}\chi_{22} + \tfrac{1}{2}\chi_{33} - \chi_{23}
\end{aligned}
$$

The above equations can be written in matrix notation as:

$$\mathbf{A} = \theta\, \mathbf{X} \tag{4.4}$$

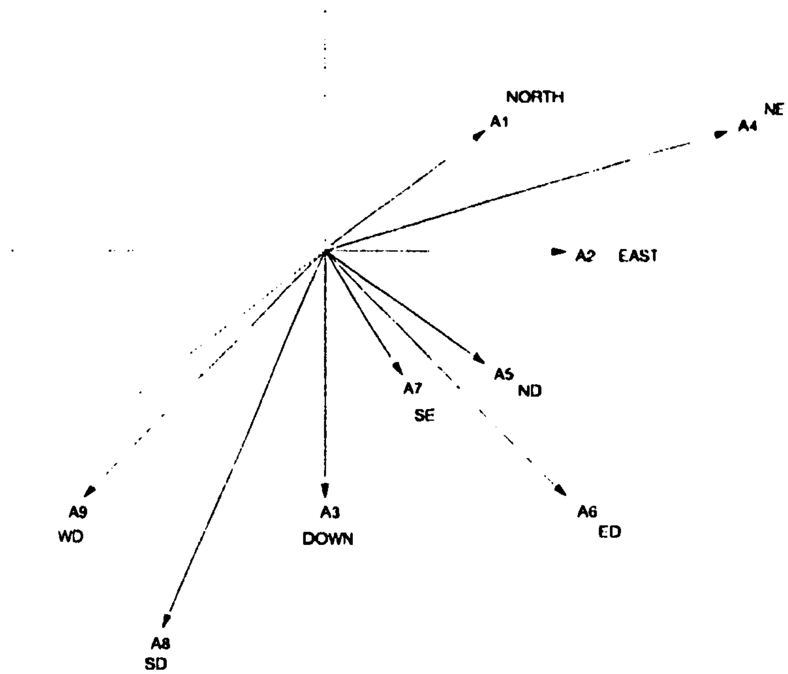

Fig. 4.1 Directions along which the anhysteretic remanences are given and measured.

where

$$\mathbf{A} = \begin{vmatrix} A_1 \\ A_2 \\ A_3 \\ A_4 \\ A_5 \\ A_6 \\ A_7 \\ A_8 \\ A_9 \end{vmatrix}, \quad \boldsymbol{\theta} = \begin{vmatrix} 1 & 0 & 0 & 0 & 0 & 0 \\ 0 & 1 & 0 & 0 & 0 & 0 \\ 0 & 0 & 1 & 0 & 0 & 0 \\ \frac{1}{2} & \frac{1}{2} & 0 & 0 & 0 & 1 \\ \frac{1}{2} & 0 & \frac{1}{2} & 0 & 1 & 0 \\ 0 & \frac{1}{2} & \frac{1}{2} & 1 & 0 & 0 \\ \frac{1}{2} & \frac{1}{2} & 0 & 0 & 0 & -1 \\ \frac{1}{2} & 0 & \frac{1}{2} & 0 & -1 & 0 \\ 0 & \frac{1}{2} & \frac{1}{2} & -1 & 0 & 0 \end{vmatrix}, \textit{and } \mathbf{X} = \begin{vmatrix} \chi_{11} \\ \chi_{22} \\ \chi_{33} \\ \chi_{23} \\ \chi_{31} \\ \chi_{12} \end{vmatrix}.$$

The problem can be classified as an overdetermined problem where the number of observations (A_n) exceed the number of unknown parameters (χ_{ij}). The best fit anisotropy tensor is determined using a least squares method, which gives

$$\mathbf{X} = (\theta_t \theta)^{-1} \theta_t \mathbf{A} \qquad (4.5.a)$$

where θ_t is the transpose of θ and $(\theta_t\theta)^{-1}$ is the reciprocal of $(\theta_t\theta)$. Equation 4.5.a gives

$$\begin{Vmatrix} \chi_{11} \\ \chi_{22} \\ \chi_{33} \\ \chi_{23} \\ \chi_{31} \\ \chi_{12} \end{Vmatrix} = \frac{1}{18} \begin{Vmatrix} 10 & -2 & -2 & 4 & 4 & -2 & 4 & 4 & 2 \\ -2 & 10 & -2 & 4 & -2 & 4 & 4 & -2 & 4 \\ -2 & -2 & 10 & -2 & 4 & 4 & -2 & 4 & 4 \\ 0 & 0 & 0 & 0 & 0 & 9 & 0 & 0 & -9 \\ 0 & 0 & 0 & 0 & 9 & 0 & 0 & -9 & 0 \\ 0 & 0 & 0 & -9 & 0 & 0 & -9 & 0 & 0 \end{Vmatrix} \begin{Vmatrix} A_1 \\ A_2 \\ A_3 \\ A_4 \\ A_5 \\ A_6 \\ A_7 \\ A_8 \\ A_9 \end{Vmatrix} \qquad (4.5.b)$$

By substituting the six components of χ_{ij} into Equations 4.2.a and 4.2.b, one can calculate the magnitudes and directions of the principal anyhsteretic susceptibilities of the specimen.

The anisotropy of anhysteretic susceptibility data can be represented by the same parameters as the AMS data. Ellwood et al. (1988) suggested that for instruments such as the cryogenic magnetometer that directly measure the elements of the total susceptibility ellipsoid, the anisotropy parameters should be based on the ratio of the principal susceptibilities. The following are the ratio-based parameters that are widely used:

$P = \chi_1/\chi_3$ often called the degree of anisotropy;

$L = \chi_1/\chi_2$ often called magnetic lineation;

$F = \chi_2/\chi_3$ often called magnetic foliation.

If P = 1, the specimen is magnetically isotropic. As P increases the specimen becomes magnetically more anisotropic. A specimen is called magnetically lineated if the long-axes of its non-spherical magnetic grains are oriented along a certain axis or magnetically foliated if these long axes are distributed in a plane.

In a group of specimens, the orientation of their maximum susceptibility axes may indicate the controlling processes during their formation. For example, magnetic lineation in sediments may indicate deposition in a water current, whereas magnetic foliation may be enhanced by sediment compaction.

Although P, L and F of the AAS and AMS were calculated and listed in the appendices, parameters p% and T, which are simpler to understand, will be used in the following chapters of this thesis.

Instead of the ratio-based parameter $P = \chi_1/\chi_3$, for degree of anisotropy, the percent anisotropy parameter p% will be used and is defined as

$$p\% = ((\chi_1/\chi_3) - 1) \times 100 \text{ per cent.}$$

A degree of anisotropy expressed as p%= 15.5% is easier to understand than when expressed as P = 1.155.

Instead of the two parameters, magnetic lineation L and magnetic foliation F, the single shape factor T will be used to represent the shape of the susceptibility ellipsoid. This parameter was introduced by Jelinek (1981) and is defined as

$$T = (\ln F - \ln L)/(\ln F + \ln L)$$

where ln F and ln T are the natural logarithms of F and L repectively. The interpretation of T is summarized in Table 4.1. Positive values of T indicate that magnetic foliation dominates and negative values of T indicate that magnetic lineation dominates.

TABLE 4.1 Interpretation of shape factor T

$T = -1$	only magnetic lineation is developed
$-1 < T < 0$	magnetic lineation is dominant
$T = 0$	magnetic lineation and foliation equally developed
$0 < T < 1$	magnetic foliation is dominant
$T = 1$	only magnetic foliation is developed

CHAPTER 5

ANISOTROPY MEASUREMENTS

5.1 Anisotropy of Anhysteretic Susceptibility Measurements

The anhysteretic susceptibility of each specimen can be determined by measuring anhysteretic remanence along nine directions in the specimen. The theory of anhysteretic susceptibility measurement was discussed in the last chapter and the practice will now be described.

Prior to giving an anhysteretic remanent magnetization (ARM) to the first measured direction, the rock specimen was demagnetized using an alternating field of 70 mT or higher to ensure that natural remanence was usually reduced to 5% or less. The Schonstedt GDS-1 AF demagnetizer used for the demagnetizations was then used to produce an ARM. For this purpose, the demagnetizer was modified by winding an additional layer of turns of wire around the primary coil of the demagnetizer. This additional coil was used to apply a direct field of 0.2 mT to the sample while the main coil applied an alternating field of 70 mT, which was slowly reduced to zero. The direct field of 0.2 mT was generated by a current of 300 mA supplied from a 12 volt car battery and was monitored by a digital multimeter (Phillips type FM 2421). The resulting anhysteretic remanence was then measured with the superconducting magnetometer using the same procedure as described in Section 4.2.

The sample was then demagnetized along the ARM direction and two other directions perpendicular to it using the same alternating field of 70 mT or higher in all demagnetizations. This reduced the ARM to 1% or less. Each time the specimen was demagnetized, the sequence was changed, i.e., the measured direction being demagnetized alternately first or last to minimize bias domain configuration. The specimen was then given an identical ARM in the reverse direction by repeating the above magnetization steps with the 0.2 mT direct field reversed. Remeasuring and then averaging the anhysteretic remanence intensity for normal and reverse field removes the small contribution (usually less than 1% of ARM) from natural remanence that had survived.

The whole procedure was then repeated for other directions until all nine directions described in Section 4.3 had been measured. The ARM intensities along the nine directions could be reproduced to 1% error.

The mean anhysteretic remanence intensity values for the nine directions were then used to determine the six anhysteretic susceptibility tensor components (Equation

4.5.a). Next, these six tensor components were used to recalculate the remanences in the nine directions (Equation 4.4). The discrepancies between the observed and the calculated remanences are used to estimate the quality of the data. Small discrepancies mean that the data are of high quality and that anisotropy can be reliably described by a triaxial ellipsoid. The six tensor components of each specimen were then used as the inputs for computer program ND11R5 (Appendix 3) to solve Equations 4.2.a and 4.2.b. This program is modified from program D11R1 (Vetterling et al., 1987) and its routine JACOBI (Press et al., 1987). The output is the magnitude and direction of the three principal susceptibilities.

5.2 Declination Adjustment

So far, the orientation of the principal susceptibilities in the horizontal plane has been only nominal because the azimuth of the specimens is unknown. The horizontal plane orientations of the principal susceptibilities were then adjusted using a simple calculation. It was assumed that the characteristic declination of the natural remanence of each specimen (Column 4 of Table 4.1) coincided with the palaeo-declination of the Earth's field at its site predicted from the APWP (Column 6 of Table 4.4). The orientation of the principal susceptibility axes in the horizontal plane was adjusted accordingly.

For example: the characteristic remanence of specimen 167-62-4-64 has an inclination of -32.0° and a nominal declination of 197.8° (see Table 3.1). Anisotropy measurement shows that the axis of maximum susceptibility has an inclination of -13.3° and a declination of 7.6° (see Appendix 4). The predicted palaeodeclination of site 167 is 23.3° (see Table 3.4). Therefore the adjusted declination of the maximum axis is (7.6 - 197.8 + 23.3)° = -166.9° = 193.1°.

The above maximum susceptibility axis also can be represented in its opposite sense with declination of (193.1 - 180) = 13.1° and inclination of -(- 13.3°) = + 13.3°. This representation with positive inclination is chosen so the axis can be plotted in the lower hemisphere of the equal area projection. A similar adjustment is also applied to the minimum susceptibility axis.

5.3 Results

Specimen 463-70-1-78 was rejected from AAS measurement because its anhysteretic remanence is weak and inconsistent. The observed and the calculated anhysteretic remanence intensity values for the nine directions as well as their discrepancies are listed for all other specimens in Appendix 4. The six anhysteretic susceptibility tensor components and the magnitude and direction of the three principal susceptibilities for these specimens are also listed in Appendix 4. The discrepancies between the observed and the calculated remanences of the specimens are often very small, suggesting that the anisotropy is well described by a triaxial ellipsoid. These results of AAS measurements are summarized in Table 5.1.

In Table 5.1, the degree of anisotropy is expressed as p%, while magnetic lineation and foliation are represented by the shape factor T. Parameters p% and T were described in Section 4.3. Table 5.1 also lists the directions of the principal susceptibilities of each specimen. The declination of these axes has been adjusted using the method described in Section 5.2. The maximum and minimum axes of specimens within a particular site are plotted in Figure 5.1 in equal area projection onto the lower hemisphere (positive or downward inclination). Following the convention suggested by Ellwood et al. (1988), the maximum axes of AAS are shown by filled squares (with the degree of anisotropy p% given beside them). The minimum axes are shown by filled circles. The results for each site are summarized as follows:

SITE 167 (Fig.5.1.a)

The degree of anisotropy p% varies from 2.7% to 23.0% (the mean is 10.5% with a standard deviation of 6.3%). The minimum axes are always nearly vertical and the maximum axes are all nearly horizontal. The mean of 0.71 and a standard deviation of 0.17 for shape factor T indicates that most specimens of this site are magnetically foliated rather than lineated. Nevertheless, the maximum axes tend to cluster along a NNW-SSE axis suggesting a possible weak lineation in that direction.

SITE 288 HOLE A (Fig.5.1.b)

The degree of anisotropy p% varies from 1.0% to 15.1% (the mean is 9.3% with a standard deviation of 3.8%). For all but two specimens (23-1-79 and 23-2-115), the minimum axes are nearly vertical, whereas their maximum and intermediate axes are nearly horizontal and dispersed in declination consistent with strong magnetic foliation. The mean of 0.71 and a standard deviation of 0.20 (specimen 23-1-79 is excluded) for shape factor T indicates that most specimens are magnetically foliated. Specimen 23-1-79 has an extremely low degree of anisotropy (1.0%) making the directions of its maximum and minimum axes very inaccurate and of little significance. On the contrary, specimen 23-2-115 has a sizeable anisotropy

(12.1%) making it definitely anomalous that its maximum axis is nearly vertical and its minimum axis nearly horizontal.

SITE 315 HOLE A (Fig.5.1.c)

The degree of anisotropy p% in all specimens is relatively high varying from 12.5% to 35.2% with a mean of 20.5% and a standard deviation of 6.4%. Minimum axes are always nearly vertical whereas and maximum axes are nearly horizontal. The mean of 0.89 and a standard deviation of 0.08 for shape factor T indicates that most specimens have magnetic foliation. Nevertheless, the alignment of the maximum axes suggests a weak NE-SW lineation.

SITE 316 (Fig.5.1.d)

The anisotropy results are very similar to those from site 315A. The degree of anisotropy p% in all specimens is high varying from 9.3% to 36.1% with a mean of 24.1% and a standard deviation of 7.9%. The minimum axes are all nearly vertical whereas the maximum axes are all nearly horizontal. The shape factor T averages 0.90 (with a standard deviation of 0.05), which is the highest among the sites, indicating a strong average magnetic foliation. Nevertheless, the alignment of maximum axes suggests a weak NNE-SSW lineation.

TABLE 5.1 The results of AAS measurements

SITE/SPECIMEN	p% (%)	T	χ_1		χ_2		χ_3	
			DEC	INC	DEC	INC	DEC	INC
167								
167-62-4-64	6.6	0.79	13.1	13.3	105.3	9.2	229.0	73.7
167-63-4-75	13.3	0.73	9.2	3.2	99.2	0.8	203.4	86.7
167-65-3-42	14.7	0.87	156.5	2.1	246.6	4.6	42.0	85.0
167-67-3-36	12.4	0.75	7.4	0.6	277.3	5.2	104.1	84.8
167-69-4-133	2.7	0.57	115.8	11.7	23.6	10.7	252.2	74.1
167-71-2-63	23.0	0.95	271.6	0.1	1.6	3.3	179.2	86.7
167-72-2-63	8.3	0.62	169.0	23.9	264.6	12.2	19.3	62.8
167-73-2-121	3.3	0.37	162.3	1.5	72.3	2.4	283.1	87.2
288A								
288A-21-2-98	7.6	0.81	99.1	0.8	189.1	4.2	357.9	85.7
288A-21-3-18	9.0	0.80	12.4	2.7	282.1	7.6	121.8	82.0
288A-22-2-82	15.1	0.86	287.9	13.5	197.3	2.6	96.7	76.3
288A-23-1-79	1.0	-0.86	43.5	54.5	267.6	27.1	166.2	21.1
288A-23-2-115	12.1	0.40	177.2	84.3	328.2	5.0	58.4	2.8
288A-23-3-76	9.0	0.95	329.0	0.9	59.0	4.4	227.8	85.6
288A-26-1-28	11.3	0.43	295.5	6.1	25.6	1.1	125.7	83.8
288A-29-1-47	9.2	0.73	58.8	4.7	328.2	7.3	181.2	81.3
315A								
315A-19-5-50	22.2	0.90	202.5	2.0	112.5	1.0	355.7	87.7
315A-20-2-21	20.2	0.98	17.9	1.1	287.8	3.6	124.8	86.2
315A-20-2-131	18.9	0.87	50.8	6.8	320.8	0.2	229.0	83.2
315A-20-5-17	14.5	0.86	40.0	4.2	310.0	0.2	217.8	85.8
315A-21-2-11	35.2	0.98	270.7	0.6	0.8	10.1	177.4	79.9
315A-21-5-8	22.2	0.90	261.3	1.5	351.4	5.5	155.7	84.3
315A-21-6-108	12.5	0.69	38.3	0.5	128.3	3.9	301.2	86.1
315A-26-2-123	18.4	0.90	84.5	2.0	354.5	0.8	242.3	87.8

TABLE 5.1 (Continued)

SITE/SPECIMEN	p% (%)	T	χ_1 DEC	χ_1 INC	χ_2 DEC	χ_2 INC	χ_3 DEC	χ_3 INC
316								
316-19-2-108	23.6	0.85	202.2	1.0	292.2	2.2	87.1	87.6
316-19-4-74	31.9	0.90	201.5	4.5	111.5	0.2	18.6	85.5
316-20-4-67	9.3	0.91	337.5	3.2	247.2	5.8	95.9	83.4
316-22-2-77	23.2	0.89	243.4	0.5	153.4	2.0	348.6	87.9
316-23-3-107	36.1	0.82	22.5	1.9	112.5	1.0	230.9	87.9
316-24-3-59	21.3	0.94	232.6	2.6	322.7	1.9	88.1	86.8
316-25-5-40	23.0	0.97	227.1	3.2	317.2	0.8	60.8	86.7
462								
462-55-1-28	10.7	0.71	253.8	2.0	163.8	1.0	47.1	87.8
462-55-1-114	8.1	0.82	343.9	8.5	252.1	11.6	109.5	75.6
462-55-2-128	7.0	0.68	345.2	4.5	255.2	0.0	164.8	85.5
462-55-3-29	26.7	0.85	142.3	2.8	52.3	0.2	317.5	87.2
462-55-3-132	24.1	0.90	87.8	4.8	177.9	1.6	285.9	85.0
463								
463-58-1-31	1.9	-0.38	101.0	85.4	277.7	4.6	7.7	0.3
463-58-2-82	3.2	0.14	48.0	3.0	315.5	39.6	141.6	50.3
463-59-2-104	2.7	-0.14	139.9	25.5	44.3	11.7	291.7	61.7
463-60-2-33	1.9	-0.36	108.1	68.7	8.2	3.8	276.7	21.0
463-61-1-105	11.8	0.76	120.0	4.0	29.8	2.2	91.6	85.5
463-64-1-60	2.2	-0.46	221.8	85.0	82.3	3.8	352.1	3.2
463-67-2-103	2.3	-0.13	160.8	79.2	291.8	7.2	22.8	8.1

p% is the degree of anisotropy $\{((\chi_1/\chi_3) - 1) \times 100$ per cents$\}$ and T the shape factor $\{(\ln F - \ln L)/(\ln F + \ln L)\}$. T is positive when magnetic foliation dominates and is negative when magnetic lineation dominates.

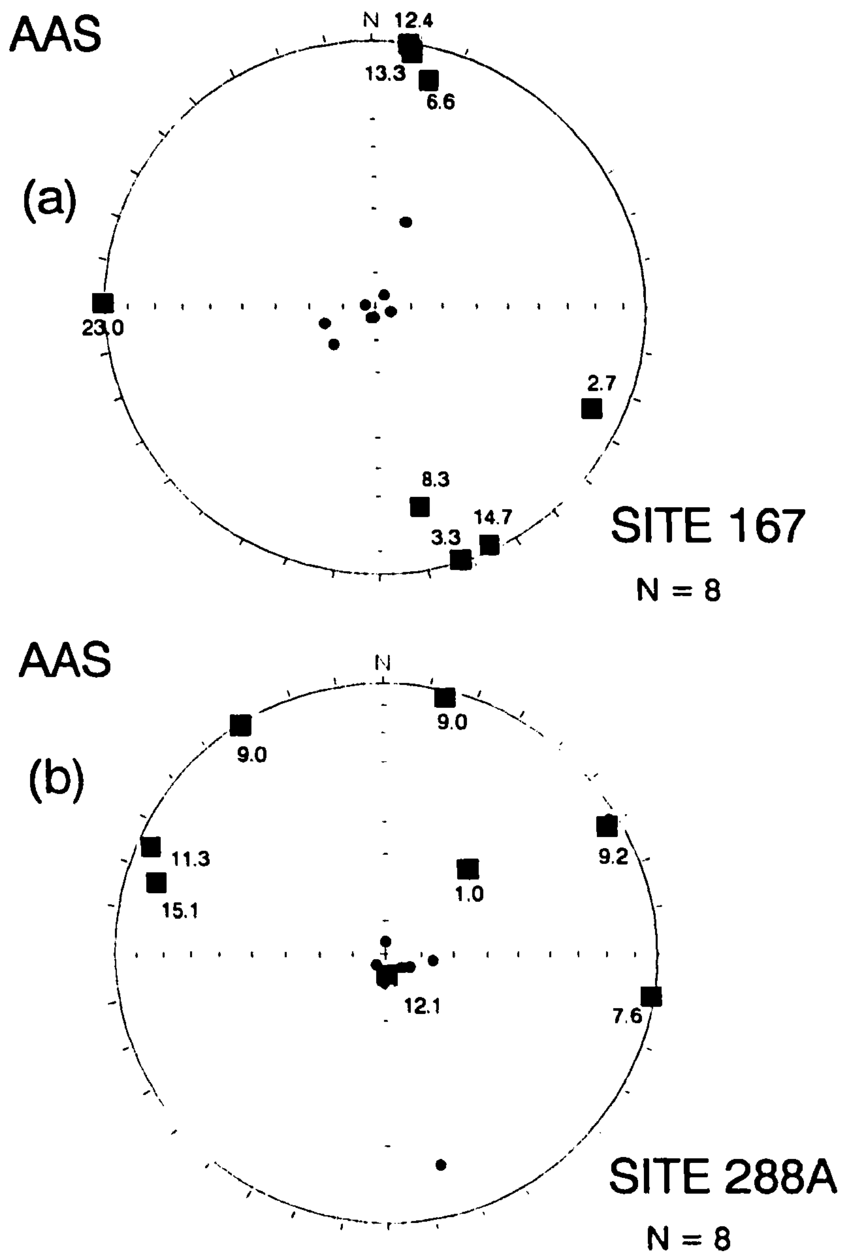

Fig.5.1 Equal area projections of directions of maximum (large filled squares) and minimum (small filled circles) axes of AAS in specimens of sites (a) 167, (b) 288 hole A, (c) 315 hole A, (d) 316, (e) 462, and (f) 463. Numbers indicate the degree of anisotropy (p%) in per cent.

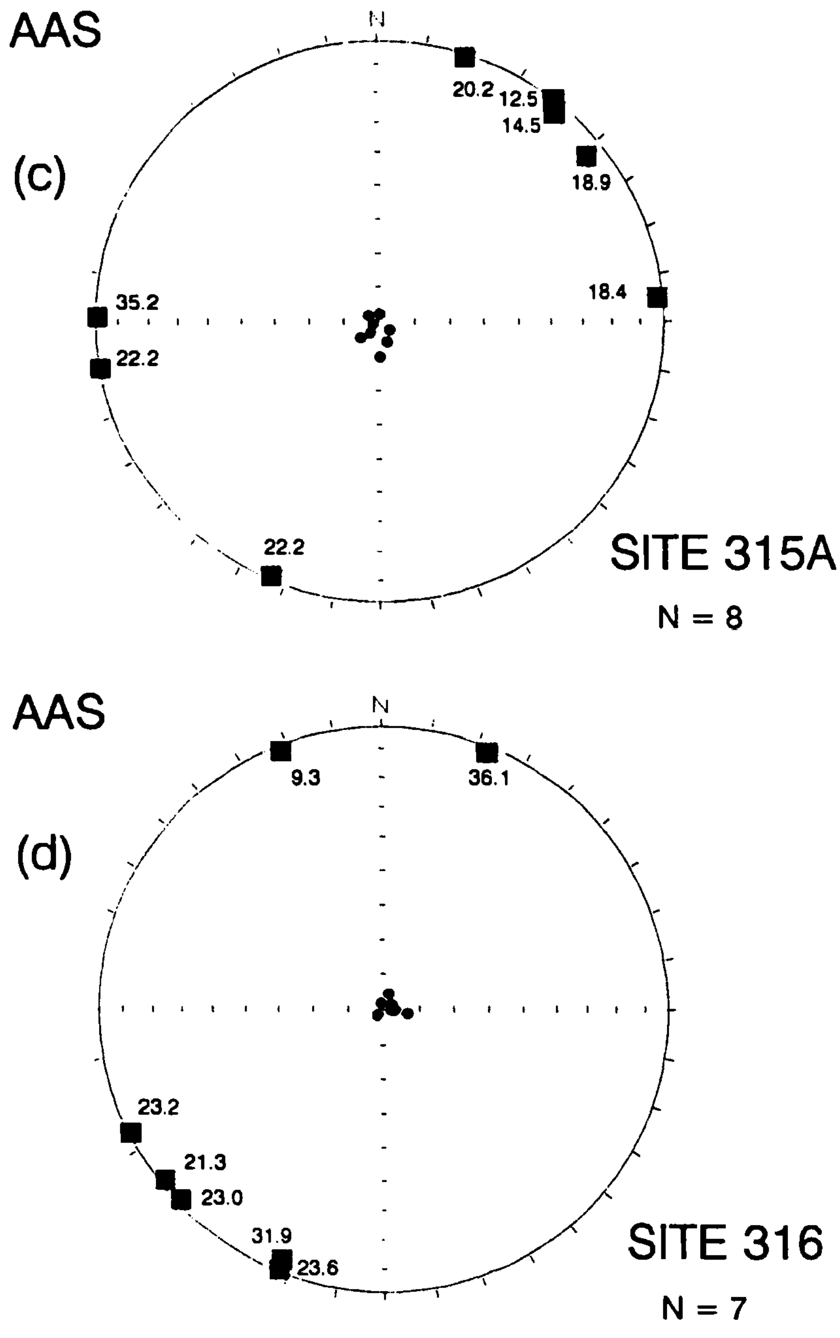
AAS
N
20.2
12.5
14.5
18.9
(c)
35.2
18.4
22.2
22.2
SITE 315A
N = 8
AAS
N
9.3
36.1
(d)
23.2
21.3
23.0
31.9
23.6
SITE 316
N = 7

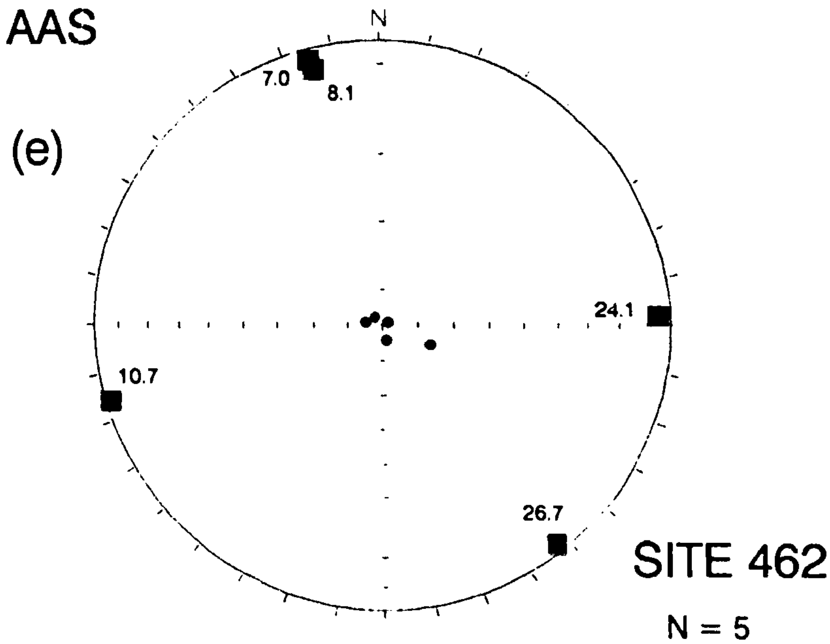
AAS
N
(e)
7.0
8.1
24.1
10.7
26.7
SITE 462
N = 5

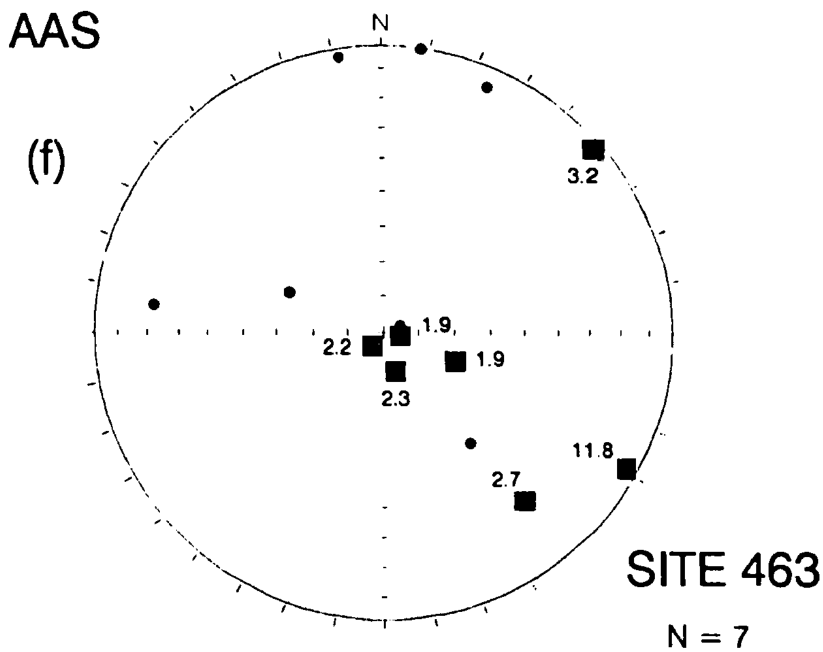
AAS
N
(f)
3.2
1.9
2.2
1.9
2.3
11.8
2.7
SITE 463
N = 7

SITE 462 (Fig.5.1.e)

The degree of anisotropy p% varies from 7.0% to 26.7% with a mean of 15.3% and a standard deviation of 8.4%. The shape factor T averages 0.79 (with a standard deviation of 0.08) indicating a strong magnetic foliation. The minimum axes are all nearly vertical whereas the maximum and intermediate axes are all nearly horizontal. All the maximum axes disperse in declination consistent with strong foliation.

SITE 463 (Fig.5.1.f)

The degree of anisotropy p% in all but one specimen (61-1-105) is low varying from 1.9% to 3.2% with a mean of 2.4% and a standard deviation of 0.5%. Excluding specimen 61-1-105, the shape factor T has a mean of -0.22 (with a standard deviation of 0.20) suggesting a weak dominance of magnetic lineation over foliation. However, because the degree of anisotropy is very low except for one specimen, the observed great scatter in directions of maximum and minimum axes may have little significance. Specimen 61-1-105 is the exception and has a degree of anisotropy of 11.8%. Like specimens of strong anisotropy from other sites, its maximum axis is nearly horizontal and its minimum axis is nearly vertical.

5.4 Anisotropy of Magnetic Susceptibility Measurements

In this investigation, AMS was also measured to compare with AAS. The AMS measurements were performed in the Department of Geology, University of Toronto, using a Bartington Magnetic Susceptibility Meter model MS2. The instrument consists of a sensor coil (type MS2B) with internal diameter of 36 mm connected to a meter by a co-axial cable. The sensor produces a low frequency 0.1 mT alternating magnetic field. When the specimen is placed inside the sensor, it produces a changes in frequency, which is then converted to a magnetic susceptibility measurement. The measurement is displayed on the meter. The measuring range of the instrument is 1 to 9999 x 10^{-6} cgs units or 1.26 x 10^{5} to 1.26 x 10^{1} SI units.

The measurement began by inserting the specimen into the sensor coil with the direction to be measured being placed parallel to the sensor coil's axis. A reading was then taken through the meter which is connected to an on-line computer. This was then repeated for other directions by changing the orientation of specimen. All the readings were controlled by the computer program called AMS-BAR provided by Morris Magnetics Incorporated. There are three modes of measurement offered by the program. All three modes measure six orientations (X , Y, Z, XY, XZ, YZ) of the specimen. The first mode requires six readings (one reading for each orientation) while the second and third modes require 12 and 24 readings (two and four readings for each orientation) respectively.

In the present investigation, the 12 readings mode was used for all the specimens. The program calculates the magnitudes and directions of the three principal susceptibility axes as well as other anisotropy parameters. One of the parameters is the average susceptibility (A_v) defined as

$$A_v = (K_1 + K_2 + K_3)/3,$$

where K_1, K_2 and K_3 are the magnitudes of the maximum, intermediate and minimum susceptibilities. Specimens 462-55-3-29 and 462-55-3-132 were excluded because they cracked prior to AMS measurement. Appendix 5 lists the detailed AMS data of the specimens.

The average susceptibility for most specimens was found to be very weak (see Table 5.2). Some of the specimens have an average susceptibility close to the lowest end of the measuring range of the instrument. This leads to high RMS (root mean square) % error in calculation of principal axes. The program AMS-BAR defines RMS % error as the square root of the sums of the squares of the differences between repeat measurements of the same matrix element divided by the average susceptibility and multiplied by 100. RMS % error of more than 1 per cent indicates that the susceptibility of the specimen cannot be represented reliably by triaxial axes (Hale, 1991, personal discussion). The AMS results of specimens whose RMS% error is much greater than 1% were then rejected on the basis that their magnetic susceptibility is too low to be measured reliably by this instrument. Table 5.2 also shows that the average susceptibility of specimens from sites 315A, 316 and 462 are higher than from other sites. This suggests that the sedimentary rocks from these three sites have higher magnetite content.

Table 5.3 lists the anisotropy parameters as well as the directions of maximum and minimum axes of specimens whose RMS % error is approximately 1 per cent or less. Like the corresponding AAS data, the AMS data of these specimens show a positive shape factor T that indicates the domination of magnetic foliation over lineation. The AMS degree of anisotropy, is always smaller than its AAS correlative. The ratio of AMS to AAS degree of anisotropy vary from 0.14 to 0.77 with a mean of 0.37 and a standard deviation of 0.16.

Figures 5.2.a and 5.2.b show the stereographic projections of the AMS maximum and minimum axes of specimens

TABLE 5.2 The AMS average susceptibility and RMS% error

SITE/SPECIMEN	A_v (SI unit)	RMS% error (%)	SITE/SPECIMEN	A_v (SI unit)	RMS% error (%)
167			**316**		
167-62-4-64	1.71e-03	0.86	316-19-2-108	1.75e-03	0.66
167-63-4-75	2.61e-03	0.65	316-19-4-74	1.76e-03	0.80
167-65-3-42	2.05e-03	0.81	316-20-4-67	7.67e-04	2.85
167-67-3-36	7.67e-04	4.72	316-22-2-77	1.65e-03	1.08
167-69-4-133	5.40e-04	2.25	316-23-3-107	6.87e-03	0.17
167-71-2-63	1.43e-03	3.34	316-24-3-59	1.78e-03	0.81
167-72-2-63	4.78e-04	7.03	316-25-5-40	1.95e-03	1.03
167-73-2-121	2.01e-04	14.41			
288A			**462**		
288A-21-2-98	7.41e-04	1.87	462-55-1-28	3.98e-03	0.47
288A-21-3-18	9.17e-04	6.93	462-55-1-114	7.67e-04	1.57
288A-22-2-82	1.68e-03	2.15	462-55-2-128	2.02e-03	0.46
288A-23-1-79	1.63e-04	4.38			
288A-23-2-115	6.16e-04	5.03			
288A-23-3-76	1.07e-03	2.25			
288A-26-1-28	2.40e-03	0.60			
288A-29-1-47	1.48e-03	2.64			
315A			**463**		
315A-19-5-50	4.26e-03	0.38	463-58-1-31	8.80e-05	13.02
315A-20-2-21	7.36e-03	1.05	463-58-2-82	2.14e-04	6.06
315A-20-2-131	1.13e-02	0.23	463-59-2-104	1.13e-04	14.51
315A-20-5-17	2.84e-03	0.78	463-60-2-33	1.88e-04	6.45
315A-21-2-11	5.20e-03	0.61	463-61-1-105	5.78e-04	1.72
315A-21-5-8	2.44e-03	0.18	463-64-1-60	1.01e-04	14.61
315A-21-6-108	1.65e-03	1.29	463-67-2-103	2.76e-04	4.42
315A-26-2-123	3.00e-03	0.34			

TABLE 5.3 The results of AMS measurements for selected specimens

SITE/SPECIMEN	p% (%)	T	K_1		K_2		K_3	
			DEC	INC	DEC	INC	DEC	INC
167								
167-62-4-64	5.0	0.06	279.8	9.1	103.9	80.9	9.9	0.6
167-63-4-75	3.3	-0.68	108.9	14.4	9.3	32.8	219.1	53.4
167-65-3-42	4.4	-0.02	24.5	19.8	293.8	2.1	198.0	70.1
288A								
288A-26-1-28	3.0	0.28	92.3	20.3	355.0	19.0	225.4	61.6
315A								
315A-19-5-50	11.4	0.62	334.7	0.8	244.6	7.0	71.5	82.9
315A-20-2-21	7.3	0.84	199.7	1.4	289.7	2.3	77.7	87.3
315A-20-2-131	6.9	0.83	180.9	0.2	270.9	2.7	85.7	87.3
315A-20-5-17	7.5	0.86	323.2	5.7	232.7	5.0	102.1	82.4
315A-21-2-11	6.3	0.75	125.5	3.7	35.3	4.1	257.5	84.5
315A-21-5-8	8.3	0.86	230.3	1.0	140.3	1.7	350.6	88.0
315A-21-6-108	8.3	0.61	192.8	2.2	282.9	2.1	56.7	86.9
315A-26-2-123	5.0	0.30	16.2	2.8	286.0	3.3	146.0	85.7
316								
316-19-2-108	7.7	0.62	339.4	9.1	247.9	9.0	113.9	77.2
316-19-4-74	4.3	0.29	128.4	10.2	37.1	7.0	273.2	77.6
316-22-2-77	8.0	-0.13	321.8	9.0	231.0	4.7	113.6	79.9
316-23-3-107	8.3	0.76	161.3	0.4	251.3	0.6	40.8	89.3
316-24-3-59	6.0	0.16	145.3	5.0	53.7	17.4	250.8	71.9
316-25-5-40	5.2	0.54	200.8	14.9	109.3	5.5	359.7	74.1
462								
462-55-1-28	4.7	0.86	180.2	0.0	270.2	0.0	47.2	90.0
462-55-2-128	4.3	0.59	268.3	0.0	358.3	0.0	116.0	90.0

from sites 315A and 316. Like the AAS results, the AMS results also show that the maximum axes are often nearly horizontal whereas their minimum axes are mostly vertical. However, the directions of the AMS maximum and intermediate axes often disagree with those of AAS. For example: the AAS principal axes plot of site 315A (Fig. 5.1.c) suggests a NE-SW lineation while its corresponding AMS plot (Fig.5.2.a) suggests a NNW-SSE lineation. Similarly, the AAS principal axes plot of site 316 (Fig. 5.1.d) shows a NE-SW lineation whereas its corresponding AMS plot (Fig. 5.2.b) suggests a NNW-SSE lineation. These differences may be due to differences in magnetite grain size that dominate each type of anisotropy. As was mentioned earlier (Section 4.2), the AMS is likely dominated by multi-domain and superparamagnetic grains in the sample whereas AAS is likely dominated by single-domain and pseudo single-domain grains.

Another factor may be that in the present investigation the specimens had all been subjected to strong alternating fields in the AAS measurements before the AMS measurements. This may have given the specimens a preferred domain orientation. Recent study by Potter and Stephenson (1990) showed that the application of strong alternating or direct magnetic fields could effect the measured AMS of weakly anisotropic samples. This puts the reliability of the present

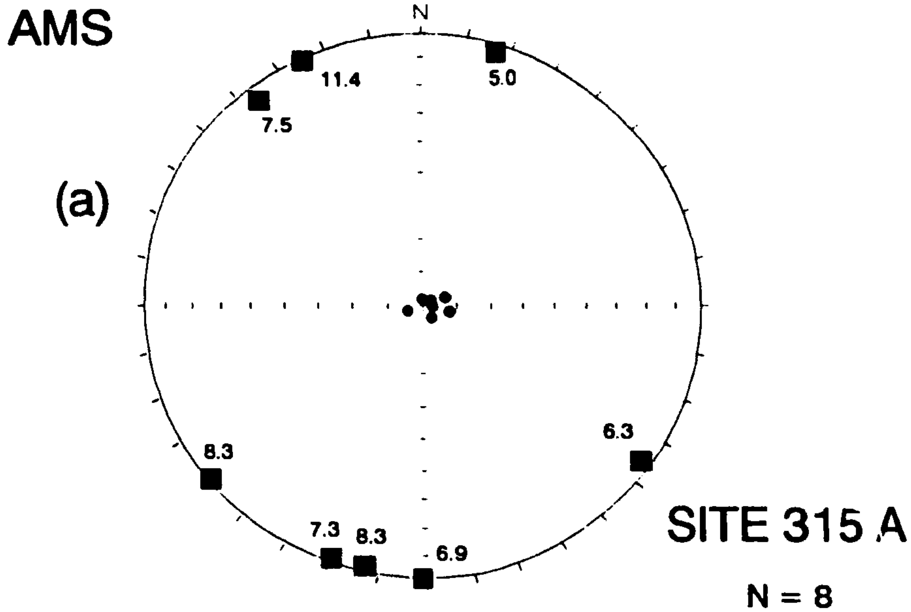

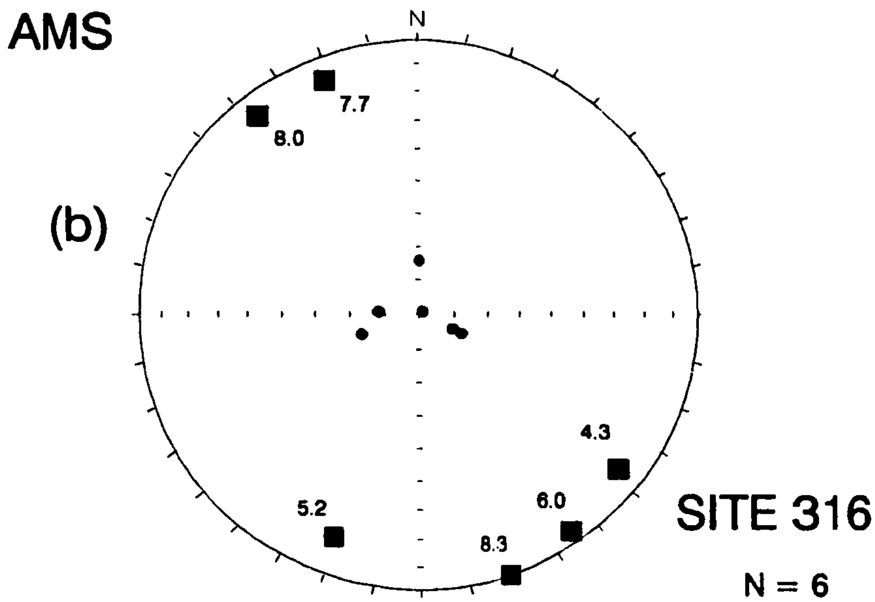

Fig.5.2 Equal area projections of directions of maximum (large filled squares) and minimum (small filled circles) axes of AMS in specimens of sites (a) 315 hole A and (b) 316. Numbers indicate the degree of anisotropy (p%) in per cent.

AMS data in question. The AMS should have been measured prior to the AAS measurements or AF demagnetization should have been carried out while tumbling the sample rather than demagnetizing one axis at a time as in the present study (Potter and Stephenson, 1990).

In conclusion, the AMS results for most specimens are not reliable because the magnetic susceptibility is too weak for its anisotropy to be measured with the magnetic susceptibility meter used in this investigation. The stronger specimens, on the other hand, show a reasonable degree of anisotropy as well as magnetic foliation with minimum axes vertical and maximum axes horizontal. However, the AMS degree of anisotropy of these specimens is found to be always smaller than the corresponding AAS. A similar conclusion was reported earlier by Kodama and Sun (1990) for artificial sediments (see Section 1.4).

Although AAS is more effective than AMS in samples of low magnetite content, measuring AAS is much more time consuming. To measure a single specimen, AAS took 3 to 4 hours whereas AMS takes only 15 minutes. Therefore, AAS is probably not suitable for studies involving great numbers of samples unless the measurement procedure can be greatly speeded up.

CHAPTER 6

DISCUSSION AND CONCLUSIONS

6.1 Inclination Shallowing and Its Possible Causes

The present investigation has demonstrated that remanence at all sites studied except site 463 has shallower inclination than expected confirming what had been pointed out by Gordon (1990). Gordon (1990) suggested several mechanisms that could be responsible for this inclination shallowing observed in Pacific plate Cretaceous DSDP sediments (See Section 1.3).

Gordon pointed out that the Cretaceous deep-sea rotary cores from the equatorial Pacific exhibit an inclination shallowing whereas the younger (Neogene) near-surface piston cores from the same area do not. However, Gordon admitted that the coring process was a less likely cause of inclination shallowing than were the age-dependent or burial-dependent mechanisms now to be discussed.

One of Gordon's suggested mechanisms for inclination shallowing was that a viscous overprint of shallow inclination may have been acquired when the sites moved closer to the equator as the Pacific plate drifted northward. Alternating field (AF) demagnetization shows that this mechanism is unlikely. Vector plots demonstrate that some specimens do steepen inclination upon AF demagnetization as a shallow remanence component of low coercivity is removed (For example, see Figures 3.1.a, d, and f). However, this low coercivity component is removed by alternating fields of 20 mT and further demagnetization suggests only a single-component remanence remains.

Another of Gordon's suggested mechanisms for inclination shallowing was delayed magnetization. That is, the sediments might not have acquired their primary magnetization until long after they were deposited. Since the Pacific plate moved northwards moving the sites closer to the equator in the Cretaceous, the delayed magnetization would be of lower inclination than at the latitude of deposition. Using Equation 3.4 and assuming that the sediments were deposited at about 20°S but only acquired stable magnetization 5 million years later, the inclination error would be only about 5° because the Pacific Plate, from 110 to 43 MA, moved northward at the rate of only 7 cm/year or about 0.6°/m.y. (Zonenshain et al., 1987). Thus, it is unlikely that the observed inclination error of more than 20° at sites 315A and 462, for example, is due to this mechanism alone, unless the time lag between deposition and magnetization is about 20 million years or more. This great time lag seems very unlikely since recent soft deep-sea sediments acquired stable remanence in much less than 1 million years recording the Brunhes-Matuyama boundary at 0.7 million years for example.

Gordon also suggested that sediment compaction might be responsible for inclination shallowing. Laboratory experiments (Anson and Kodama, 1987; Kodama and Sun, 1990) and palaeomagnetic reexamination of the Cretaceous DSDP sediments (Tarduno, 1990) have supported sediment compaction as the most likely cause of inclination error. The present investigation has studied the magnetic anisotropy of the Pacific Plate DSDP sediments to further test the hypothesis of compaction-induced inclination shallowing.

6.2 Tests of Hypothesis of Compaction-Induced Inclination Shallowing

6.2.1 Anisotropy Magnitude and Relation to Bedding Plane

In the present investigation, measurements of anisotropy of anhysteretic susceptibility (AAS) show that most specimens from sites other than site 463 are strongly anisotropic (the degree of magnetic anisotropy averages 15.8% with a standard deviation of 8.8%). The AAS measurements also show that these specimens are strongly foliated (the shape factor T averages 0.75 with a standard deviation of 0.31) with their minimum anhysteretic susceptibility axes nearly perpendicular to the bedding plane. As observed earlier in artificial sediment (Kodama and Sun, 1990), strong anisotropy, strong magnetic foliation and vertical minimum axes can result from sediment compaction.

6.2.2 Inclination Shallowing as a Function of Latitude

Some papers (Anson and Kodama, 1987; Arason and Levi, 1990b) have suggested theoretical models of compaction-induced inclination shallowing. These models describe the degree of inclination shallowing or inclination error as

$$\Delta I = I_i - \tan^{-1}((1 - a\,\Delta V)\tan I_i) \qquad (6.1)$$

where ΔI is the inclination shallowing, I_i is the initial (or palaeo-) inclination, ΔV is the degree of compaction and a is a constant chosen to fit the data from laboratory experiments and natural sediments. Using a synthetic sediment comprised of kaolinite, distilled water and magnetite, Anson and Kodama (1987) showed that a depends on the shape of magnetite grains.

Figure 6.1 shows the plot of absolute palaeoinclination versus inclination error for the six DSDP sites and the theoretical curves for various values of $a\Delta V$. Since the

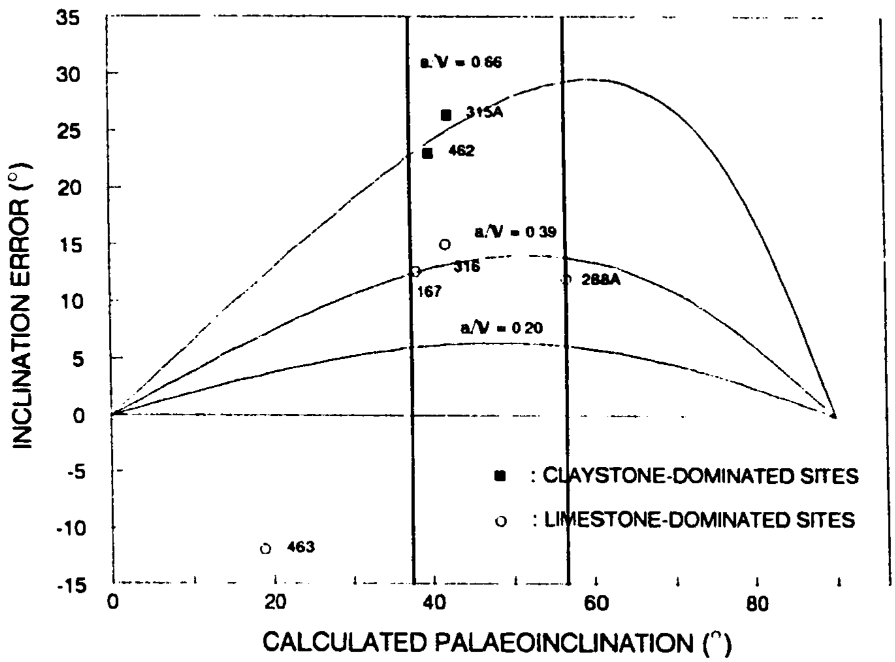

Fig. 6.1 Inclination error as a function of calculated palaeoinclination for the six DSDP sites and the theoretical curves for various values of aΔV. Parallel solid lines show that the palaeoinclinations of all sites but site 463 are confined to a narrow range.

palaeoinclinations of all sites but site 463 are confined to a narrow range (38.0° to 56.7°), it is difficult to test whether the data are distributed along the theoretical curves. However, this narrow range of palaeoinclination also implies that the dependency of inclination shallowing on palaeoinclination at these sites can be ignored to first order approximation. Figure 6.1 also shows that inclination error for claystone-dominated sites, i.e., sites 315A and 462, is higher than for limestone-dominated sites. Theoretically, this high inclination error for claystone might indicate that the degree of compaction for claystones is higher than for limestones assuming that the values of *a* are similar for both claystones and limestones.

6.2.3 Correlation between Anisotropy and Inclination Error

To test whether magnetic anisotropy and inclination shallowing in the DSDP samples might be due to sediment compaction, a correlation between inclination shallowing and degree of anisotropy was looked for. Specimens from site 463 are excluded because they do not show inclination shallowing and are only weakly anisotropic perhaps because early silicification prevented compaction as suggested by Tarduno (1990).

Figure 6.2 examines the correlation between degree of inclination shallowing and degree of anisotropy (p%) of all specimens except those from site 463. The inclination error of a specimen is defined as the difference between its characteristic remanence inclination and the palaeoinclination of the Earth's field at the corresponding site calculated from the APW path. Correlations were performed separately for the two rock types studied - limestone and claystone. The claystones include all five specimens from site 462, the four claystone specimens of site 315A, the four clayey-limestone specimens from site 315A (20-2-21, 20-2-131, 21-5-8, and 21-6-108) and two marly limestone specimens from site 167 (62-4-64 and 63-4-75). All the other specimens are categorized as limestones.

Figure 6.2.a shows that the degree of inclination shallowing for claystone does seem to increase with degree of anisotropy as expected if both were induced by sediment compaction. However, the regression line intersects the Y (inclination error) axis above the origin suggesting that about 12° of the inclination error is probably a systematic error not related to sediment compaction. This systematic error also seems to be present in the limestones since the regression line in Figure 6.2.b also cuts the Y axis above the origin. This systematic error may be due to initial anisotropy when the sediments were deposited, or to delayed magnetization, or to systematic error in the APW path.

The correlation between inclination shallowing and anisotropy in Fig. 6.2.a suggests that anisotropy may be useful in estimating the reliability of deep-sea claystone specimens for palaeomagnetic study. For example, if the maximum tolerable error of remanence inclination in a palaeomagnetic study is 5°, then specimens whose degree of anisotropy is about 15% or more, may not be reliable for such study at mid-palaeolatitude (since an error of 4° in palaeo-latitude could be expected).

Kodama and Sun (1990) observed that degree of anisotropy, magnetic foliation, and shallowing of remanence inclination increased with compaction pressure in their experiments with artificial clay-rich sediments. For their 5% magnetite samples, the degree of anisotropy p% increased from 13.4% at initial pressure of 0.0184 MPa to 43.8% at 0.1884 MPa, while remanence inclination decreased from 45° to about 35°. That is a 29% increase in degree of anisotropy accompanied a 10° inclination shallowing. This is in reasonable agreement with the results of the present investigation of DSDP claystones, where a 22.8% (±8.4%) increase in degree of anisotropy accompanies a 14° inclination shallowing (Figure 6.2.a).

Figure 6.2.b shows that the degree of inclination shallowing for limestones does not seem to be related to the degree of anisotropy. A possible cause for this lack of correlation might be that the limestones acquired remanence earlier in the compaction process than the claystones. This could give the limestones an anisotropy similar to claystones but with less inclination shallowing (assuming that the magnetite causing anisotropy is coarser than that carrying the characteristic remanence direction).

(a)

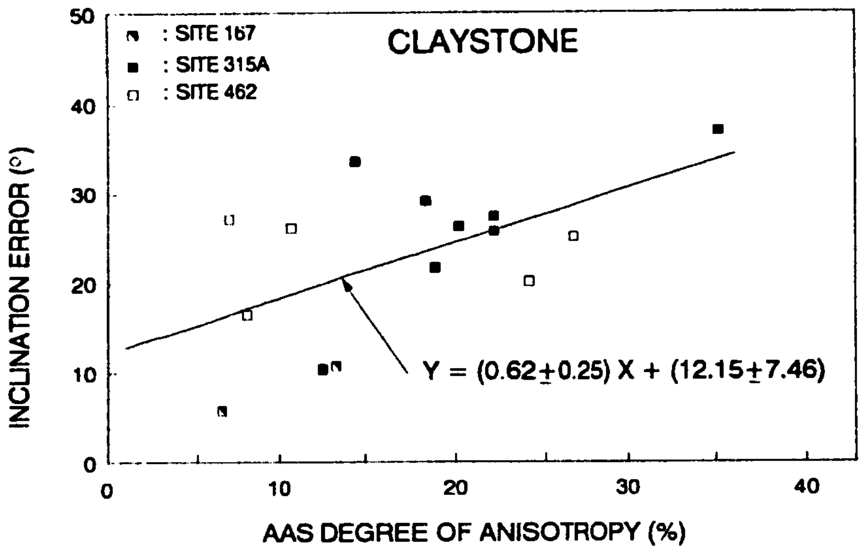

(b)

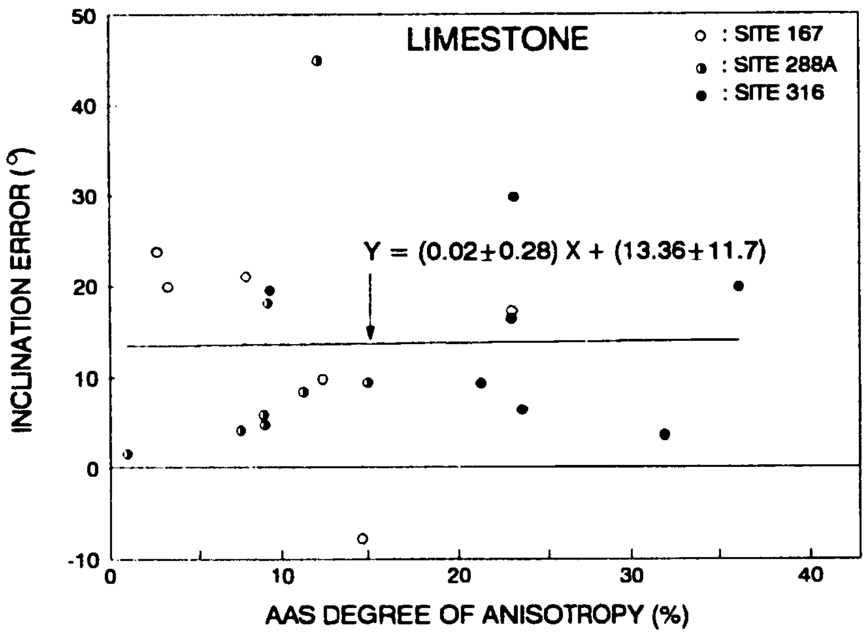

Fig. 6.2 Correlations between degree of anhysteretic susceptibility anisotropy and inclination error for (a) claystones and (b) limestones. Squares and circles are data for claystones and limestones respectively. Solid lines are the regression lines. The quality of each correlation is indicated by the standard errors in its regression equation.

6.2.4 Correlation between Anisotropy and Density

To further test the causal relation between degree of anisotropy and sediment compaction, Figure 6.3 examines the correlation between degree of anisotropy and density. Density should increase with degree of compaction assuming that the specimens of each group are alike in mineral composition and grain size and shape. The density of specimens was obtained by measuring their dimensions with calipers, calculating their volumes, and then weighing. The data are listed in Table 6.1.

Figure 6.3 shows that the degree of anisotropy for both claystones and limestones seems to increase with density suggesting a compaction-induced anisotropy. However, this correlation between density and degree of anisotropy is less obvious in limestones than in claystones.

6.3 Anisotropy, Bedding Plane and Palaeocurrents

Both AAS and AMS methods show that in most anisotropic specimens there is a strong magnetic foliation in the horizontal plane with the minimum axes perpendicular to the bedding plane. This implies that magnetic anisotropy measurements may be useful in finding the bedding plane in sedimentary specimens whose bedding is not visible. The accuracy will depend on the specimen's degree of anisotropy.

TABLE 6.1 Density of the specimens

SITE/SPECIMEN	DENSITY ($g.cm^{-3}$)	SITE/SPECIMEN	DENSITY ($g.cm^{-3}$)
167		**316**	
167-62-4-64	1.58	316-19-2-108	2.26
167-63-4-75	2.00	316-19-4-74	2.22
167-65-3-42	2.08	316-20-4-67	2.01
167-67-3-36	2.12	316-22-2-77	2.28
167-69-4-133	2.15	316-23-3-107	2.23
167-71-2-63	2.16	316-24-3-59	2.22
167-72-2-63	2.23	316-25-5-40	2.06
167-73-2-121	2.23		
288A		**462**	
288A-21-2-98	1.96	462-55-1-28	1.63
288A-21-3-18	1.86	462-55-1-114	1.64
288A-22-2-82	1.98	462-55-2-128	1.60
288A-23-1-79	1.97	462-55-3-29	1.80
288A-23-2-115	1.94	462-55-3-132	1.92
288A-23-3-76	1.87		
288A-26-1-28	1.79		
288A-29-1-47	2.17		
315A		**463**	
315A-19-5-50	2.08	463-58-1-31	2.16
315A-20-2-21	2.05	463-58-2-82	2.00
315A-20-2-131	2.19	463-59-2-104	1.86
315A-20-5-17	1.92	463-60-2-33	2.15
315A-21-2-11	2.13	463-61-1-105	2.16
315A-21-5-8	2.12	463-64-1-60	2.15
315A-21-6-108	1.93	463-67-2-103	2.03
315A-26-2-123	1.98		

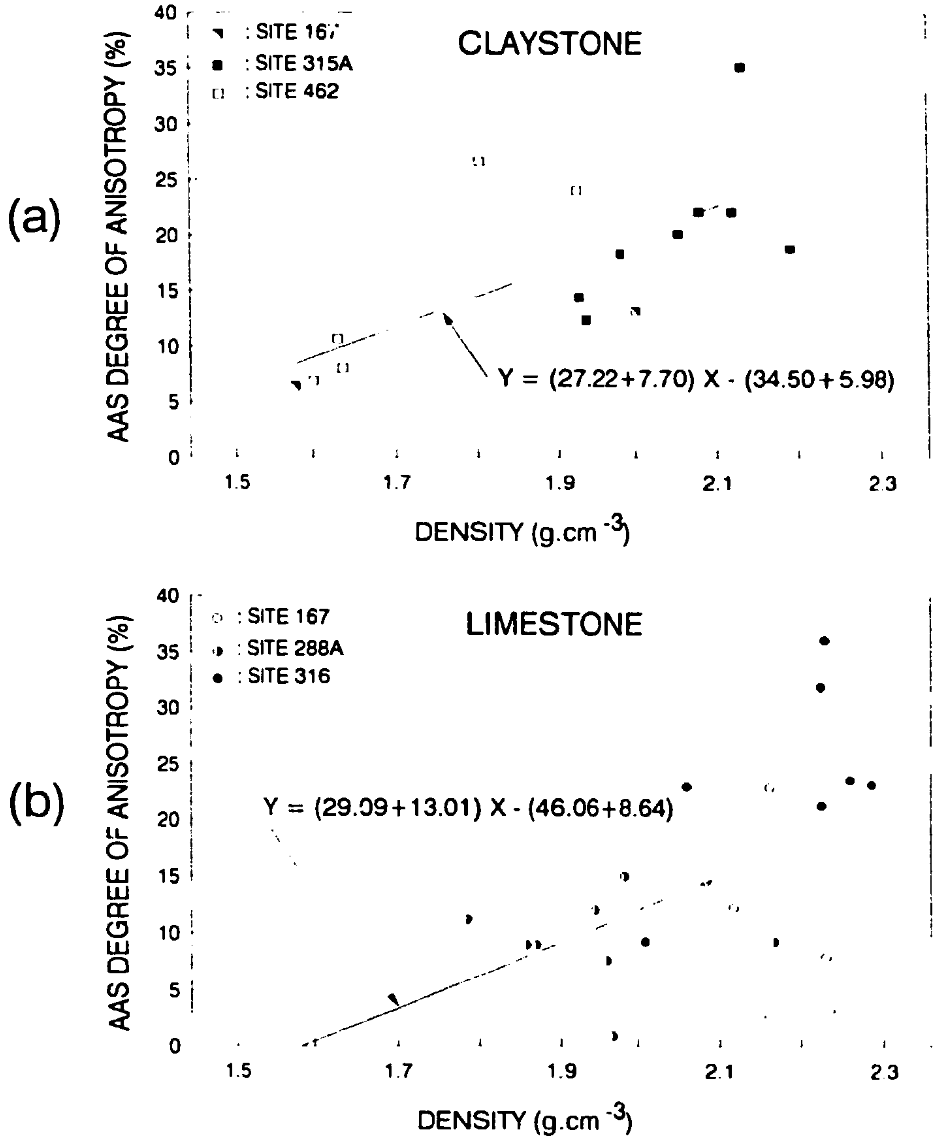

Fig. 6.3 Correlations between degree of anhysteretic susceptibility anisotropy and density for (a) claystones and (b) limestones. Squares and circles are data for claystones and limestones respectively. Solid lines are the regression lines. The quality of each correlation is indicated by the standard errors in its regression equation.

In artificial sediments, Kodama and Sun (1990) observed that the minimum axes came closer to vertical orientation as pressure and the AAS degree of anisotropy increased. The minimum axes were about vertical at a pressure of 0.09 MPa, which produced an AAS degree of anisotropy of about 19%. This is consistent with what is observed in the DSDP specimens. Table 6.2 lists the mean deviation of minimum axes from vertical orientation for various ranges of AAS degree of anisotropy. Specimens with AAS degree of anisotropy of less than 5% as well as the anomalous specimens 288A-23-2-115 and 463-61-1-105 are excluded. Table 6.2 shows that as the AAS degree of anisotropy increases the minimum axes come closer to vertical orientation. For AAS degree of anisotropy between 10 and 20%, the minimum axis of a specimen can be expected to lie about 5° (± 3°) from vertical.

At some sites (for example sites in Figures 5.1.c and 5.1.d), the maximum susceptibility axes cluster along a certain horizontal axis. It is possible that this is a palaeocurrent axis. However, the lack of strong magnetic lineation and the lack of any independent evidence about palaeocurrents at the sites make this suggestion speculative. Nevertheless, the potential use of AAS to determine palaeo-current axes should be further investigated because it could be an important tool in palaeooceanography.

TABLE 6.2 The mean deviation of minimum axes from vertical for various ranges of AAS degree of anisotropy

$p\%_{AAS}$	N	MEAN DEV.	STD
5 to 10%	9	10.7°	7.5°
10 to 20%	10	5.3°	3.2°
> 20%	13	3.9°	2.1°

$p\%_{AAS}$ is the range of the AAS degree of anisotropy and N the number of specimens from each range. MEAN DEV. is the mean deviation of minimum axes' inclination from vertical orientation for each range of AAS degree of anisotropy. STD is the statistical standard deviation of MEAN DEV..

6.4 Conclusions

(1) Cretaceous limestones and claystones from six equatorial DSDP Pacific sites were studied. Except for site 463, remanence inclination was found to be shallower than expected from the apparent polar wander path of the Pacific plate (Table 3.5), as shown earlier by Gordon (1990) and Tarduno (1990).

(2) Careful stepwise AF demagnetization of the specimens was used to show that the remanence inclination shallowing was not likely due to a shallow overprint.

(3) The anisotropy of anhysteretic susceptibility (AAS) measurements show that most specimens (except those from site 463) have a high degree of anisotropy. The average degree of

anisotropy is 15.8% with a standard deviation of 8.8% (excluding site 463). This strong anisotropy accompanied by strong horizontal bedding plane magnetic foliation and vertical minimum axes (Figures 5.1.a to 5.1.e) suggest that the anisotropy was enhanced by sediment compaction during burial.

(4) Correlation found between degree of anisotropy and density (particularly for the claystones) further supports anisotropy enhancement by sediment compaction (Figure 6.3).

(5) In the claystones, a correlation between degree of inclination shallowing and degree of anisotropy was found (Figure 6.2.a). This suggests that the shallowing of remanence inclination as well as the degree of anisotropy were enhanced by sediment compaction in the claystones. However, in the limestones the degree of inclination shallowing and the degree of anisotropy were not found to be correlated. This may be due partly to inclination shallowing being less in the limestones than in the claystones, and also to the limestones perhaps magnetizing earlier in the compaction process.

(6) An inclination error independent of degree of anisotropy also seems to be present in both claystone and limestone specimens (Figure 6.2). This systematic inclination error (of 12°±7° in the claystones) is not caused by sediment

compaction. It may be due to initial anisotropy when the sediments were deposited or to delay in magnetization after deposition or to inaccuracies in the APW path.

(7) The magnetic susceptibilities of most specimens used in the present investigation are too weak for the anisotropy of magnetic susceptibility (AMS) to be reliably measured. For the stronger specimens, AMS resembles AAS in showing strong foliation in the horizontal bedding plane with vertical minimum axes. However, the ratio of AMS to AAS degree of anisotropy is always smaller than 1 averaging 0.37 (with a standard deviation of 0.16).

(8) The axis of minimum anhysteretic susceptibility deviates an average of 5° ± 3° from perpendicular to bedding in the DSDP specimens with about 15% anisotropy making AAS potentially useful in locating the bedding plane in specimens in which bedding is not visible.

(9) The possibility that axes of maximum anhysteretic susceptibility sometimes indicate palaeocurrent axes requires testing since this could make AAS an important tool in palaeo-oceanography.

REFERENCES

ANDREWS, J.E., G. PACKHAM, J.V. EADE, et al. (The Shipboard Scientific Party), Site 288, *Initial Rep. Deep Sea Drill. Proj., 30,* 175-229, 1975.

ANSON, G.L. and K.P. KODAMA, Compaction-induced Inclination Shallowing of the Post-depositional Remanent Magnetization in a Synthetic Sediment, *Geophys. J.R. Astron. Soc., 88,* 673-692, 1987.

ARASON, P. and S. LEVI, Compaction and Inclination Shallowing in Deep-Sea Sediments From the Pacific Ocean, *J. Geophys. Res., 95,* 4,501-4,510, 1990a.

ARASON, P. and S. LEVI, Models of Inclination Shallowing During Sediment Compaction, *J. Geophys. Res., 95,* 4,481-4,499, 1990b.

BATHAL, R.S., Magnetic Anisotropy in Rocks, *Earth-Sci. Rev., 7,* 227-253, 1971.

BORNHOLD, B.D. and M. BONARDI, Magnetic Spherules in Arctic Ocean Sediments, *Can. J. Earth Sci., 16,* 1,778-1,788, 1979.

CELAYA, M.A. and B.M. CLEMENT, Inclination Shallowing in Deep Sea Sediments from the North Atlantic, *Geophys. Res. Lett., 15,* 52-55, 1988.

CHANG, S.R. and J.L. KIRSCHVINK, Magnetofossils, the Magnetization of Sediments, and the Evolution of Magnetite Biomineralization, *Ann. Rev. Earth Planet. Sci., 17,* 169-195, 1989.

CHESTER, R., *Marine Geochemistry,* 698 pp., Unwin Hyman Ltd., London, 1990.

COCKERHAM, R.S. and R.D. JARRAD, Palaeomagnetism of Some Leg 33 Sediments and Basalts, *Initial Rep. Deep Sea Drill. Proj., 33,* 631-646, 1976.

COCKERHAM, R.S., A Palaeomagnetic and Magnetic Property Study of the DSDP Pacific Basalts and Sediments of Cretaceous Age, *Eos Trans. AGU, 60,* 239, 1979.

CONDIE, K.C., *Plate Tectonics & Crustal Evolution,* 2nd Ed., 310 pp., Pergamon Press Inc., New York, 1982

COX, A. and R.B. HART, *Plate Tectonics: How It Works,* 392 pp., Blackwell Scientific Publications, Palo Alto, 1986.

COX, A., M.G. DEBICHE and D.C. ENGEBRETSON, Terrane Trajectories and Plate Interactions along Continental Margins in the North Pacific Basin, In: Z. Ben-Avraham (Editor), *The Evolution of the Pacific Ocean Margins,* Oxford Mon. Geol. Geophys. no.8, pp. 20-35, 1989.

CULLITY, B.D., *Introduction to Magnetic Materials,* 666 pp., Addison-Wesley, Massachusetts, 1971.

DEAMER, G.A. and K.P. KODAMA, Compaction-Induced Inclination Shallowing in Synthetic and Natural Clay-Rich Sediments, *J. Geophys. Res., 95,* 4,511-4,529, 1990.

DIETZ, R.S., and J.C. HOLDEN, Reconstruction of Pangaea: Breakup and Dispersion of Continents, Permian to Present, *J. Geophys. Res., 75,* 4,939-4,956, 1970.

ELLWOOD, B.B, F. HROUDA, and J.J. WAGNER, Symposia on Magnetic Fabrics: Introductory Comments, *Phys. Earth Planet. Inter., 51,* 249-252, 1988.

ENGEBRETSON, D.C., A. COX, and M.G. DEBICHE, Reconstructions, Plate Interactions, and Trajectories of Oceanic and Continental Plates in the Pacific Basin, In: J.W.H. Monger and J. Francheteau (Editors), *Circum-Pacific Orogenic Belts and Evolution of the Pacific Ocean Basin,* Am. Geophys. Union Geodynamic Series vol. 18, pp. 19-27, 1987.

FLOOD, R.D., D.V. KENT, A.N. SHOR and F.R. HALL, The Magnetic Fabric of Surficial Deep-Sea Sediments in the HEBBLE Area (Nova Scotian Continental Rise), *Marine Geology, 66,* 149-167, 1985.

FOSTER, J.H. and N.D. OPDYKE, Upper Miocene to Recent Magnetic Stratigraphy in Deep-Sea Sediments, *J. Geophys. Res., 75,* 4,465-4,473, 1970.

FOWLER, C.M.R, *The Solid Earth: An Introduction to Global Geophysics,* 472 pp., Cambridge University Press, Cambridge, 1990.

GIRDLER, R.W., The Measurement and Computation of Anisotropy of Magnetic Susceptibility of Rocks, *Geophys. J.R. Astron. Soc., 5,* 34-44, 1961.

GORDON, R.G. and A. COX, Calculating Palaeomagnetic Poles for Oceanic Plates, *Geophys. J.R. Astron. Soc., 63,* 619-640, 1980.

GORDON, R.G, Late Cretaceous Apparent Polar Wander of the Pacific Plate: Evidence for a Rapid Shift of the Pacific Hotspots with Respects to the Spin Axis, *Geophys. Res. Lett., 10,* 709-712, 1983.

GORDON, R.G., Test for Bias in Palaeomagnetically Determined Palaeolatitudes from Pacific Plate Deep Sea Drilling Project Sediments, *J. Geophys. Res., 95,* 8,397-8,404, 1990.

HAMILTON, N. and A.I. REES, The Use of Magnetic Fabric in Palaeocurrent Estimation, In: S.K. Runcorn (Editor), *Palaeogeophysics,* pp. 445-464, Academic Press, London, 1970.

HARLAND, W.B., R.L. ARMSTRONG, A.V. COX et al., *A Geologic Time Scale 1989,* 263 pp., Cambridge University Press, Cambridge, 1990.

HILDE, T.W.C., S. UYEDA and L. KROENKE, Evolution of the Western Pacific and Its Margin, *Tectonophysics, 38,* 145-165, 1977.

HROUDA, F., Magnetic Anisotropy of Rocks and Its Application in Geology and Geophysics, *Geophys. Surv., 5,* 37-82, 1982.

JARRAD, R.D., Palaeomagnetism of Leg 17 Sediment Cores, *Initial Rep. Deep Sea Drill. Proj., 17,* 365-375, 1973.

JELINEK, V., Characterization of the Magnetic Fabrics of Rocks, *Tectonophysics, 79,* T63-T67, 1981.

JOHNSON, E.A., T. MURPHY and O.W. TORRESON, Pre-History of the Earth's Magnetic Field, *Terr. Magn. Atmos. Elec., 53,* 349-372, 1948.

KENNETT, J.P., *Marine Geology,* 813 pp., Prentice-Hall, Englewood Cliffs, 1982.

KING, J., S.K. BANERJEE, J. MARVIN and Ö. ÖZDEMIR, A Comparison of Different Magnetic Methods for Determining the Relative Grain Size of Magnetite in Natural Sediments: Some Results from Lake Sediments, *Earth and Planet. Sci. Lett., 59,* 404-419, 1971.

KODAMA, K.P. and W.W. SUN, SEM and Magnetic Fabric Study of a Compacting Sediment, *Geophys. Res. Lett., 17,* 795-798, 1990.

KONO, M., Statistics of Palaeomagnetic Inclination Data, *J. Geophys. Res., 85,* 3,878-3,882, 1980.

KROENKE, L.W., *Geology of the Ontong Java Plateau,* 119 pp., Ph.D Thesis, University of Hawaii, 1972.

LARSON, R.L. and S.O. SCHLANGER, Geological Evolution of The Nauru Basin, and Regional Implication, *Initial Rep. Deep Sea Drill. Proj., 61,* 841-862, 1981.

LARSON, R.L., S.O. SCHLANGER, R. BATIZA et al. (The Shipboard Scientific Party), Site 462: Nauru Basin, Western Pacific Ocean, Deep Sea Drilling Project Leg 61, *Initial Rep. Deep Sea Drill. Proj., 61,* 19-394, 1981.

LEVI, S. and S. BANERJEE, On the Origin of Inclination Shallowing in Redeposited Sediments, *J. Geophys. Res., 95,* 4,383-4,389, 1990.

LØVLIE, R., W. LOWRIE, and M. JACOBS, Magnetic Properties and Mineralogy of Four Deep-Sea Cores, *Earth and Planet. Sci. Lett., 15,* 157-168, 1971.

McCABE, C., M. JACKSON, and B.B. ELLWOOD, Magnetic Anisotropy in the Trenton Limestone: Results of a New Technique, Anisotropy of Anhysteretic Susceptibility, *Geophys. Res. Lett., 12,* 333-336, 1985.

McDONALD, W.D. and B.B. ELLWOOD, Anisotropy of Magnetic Susceptibility: Sedimentological, Igneous, and Structural-Tectonic Applications, *Rev. Geophys., 25,* 905-909, 1987.

McFADDEN, P.L. and A.B. REID, Analysis of Palaeomagnetic Inclination Data, *Geophys. J.R. Astron. Soc., 69,* 307-319, 1982.

NAGATA, T., *Rock Magnetism,* 350pp., Maruzen Company Ltd., Tokyo, 1961.

OGG, J.G., Palaeolatitudes and Magnetostratigraphy of Cretaceous and Lower Tertiary Sedimentary Rocks, Deep Sea Drilling Project Site 585, Mariana Basin, Western Central Pacific, *Initial Rep. Deep Sea Drill. Proj., 59,* 629-645, 1986.

OPDYKE, N.D. and J.D. PHILLIPS, Palaeomagnetic Stratigraphy of Sites 1-7 (Leg 1) Preliminary Report, *Initial Rep. Deep Sea Drill. Proj., 1,* 501-517, 1969.

OPDYKE, N.D., Palaeomagnetism of Deep-Sea Cores, *Rev. Geophys. Space Phys., 10,* 213-249, 1972.

OPDYKE, N.D., L.H. BRUCKLE, and A. TODD, The Extension of the Magnetic Time Scale in Sediments of the Central Pacific Ocean, *Earth and Planet. Sci. Lett., 22,* 300-306, 1974.

PEIRCE, J.W., Assessing the Reliability of DSDP Palaeolatitudes, *J. Geophys. Res., 81,* 4,173-4,187, 1976.

PIPER, J.D.A., *Palaeomagnetism and the Continental Crust,* 434 pp., Open University Press, Milton Keynes, 1987.

POTTER, D.K. and A. STEPHENSON, The Detection of Fine Particles of Magnetite Using Anhysteretic and Rotational Remanent Magnetizations, *Geophys. J.R. Astron. Soc., 87,* 569-582, 1986.

POTTER, D.K. and A. STEPHENSON, Single-Domain Particles in Rocks and Magnetic Fabric Analysis, *Geophys. Res. Lett., 15,* 1,097-1,100, 1988.

POTTER, D.K. and A. STEPHENSON, Field-Impressed Anisotropies of Magnetic Susceptibility and Remanence in Minerals, *J. Geophys. Res., 95,* 15,573-15,588, 1990.

PRESS, W.H., B.P. FLANNERY, S.A. TEUKOLSKY, and W.T. VETTERLING, *Numerical Recipes The Art of Scientific Computing,* 818 pp., Cambridge University Press, Cambridge, 1987.

SAGER, W.W. AND M.S. PRINGLE, Mid-Cretaceous to Early Tertiary Apparent Polar Wander Path of the Pacific Plate, *J. Geophys. Res., 93,* 11,753-11,771, 1988.

SAYRE, W.O., Preliminary Report on Palaeomagnetism of Aptian and Albian Limestones and Trachytes from the Mid-Pacific Mountains and Hess Rise, Drilled During Deep Sea Drilling

Project Leg 62, *Initial Rep. Deep Sea Drill. Proj., 62,* 983-994, 1981a.

SAYRE, W.O., Preliminary Report on the Magnetic Fabric of Aptian and Albian Limestones from the Mid-Pacfic Mountains and Hess Rise, Drilled During Deep Sea Drilling Project Leg 62, *Initial Rep. Deep Sea Drill. Proj., 62,* 977-981, 1981b.

SCHLANGER, S.O., E.D. JACKSON, R.E. BOYCE et al. (The Shipboard Scientific Party), Site 315, *Initial Rep. Deep Sea Drill. Proj., 33,* 37-104, 1976a.

SCHLANGER, S.O., E.D. JACKSON, R.E. BOYCE et al. (The Shipboard Scientific Party), Site 316, *Initial Rep. Deep Sea Drill. Proj., 33,* 105-159, 1976b.

SCLATER, J.G. and A. COX, Palaeolatitudes from JOIDES Deep Sea Sediment Cores, *Nature, 226,* 934-935, 1970.

SHOR, A.N., D.V. KENT and R.D. FLOOD, Contourite or Turbidite?: Magnetic Fabric of Fine-Grained Quaternary Sediments, Nova Scotia Continental Rise, In: D.A.V. Stow and D.J.W. Piper (Editors), *Fine-Grained Sediments: Deep-Water Processes and Facies,* 247-273, Geol. Soc., London, 1984.

STEINER, M.B., Palaeomagnetism of the Cretaceous Section, Site 462, *Initial Rep. Deep Sea Drill. Proj., 61,* 711-716, 1981.

STOLZ, J.F., D.R. LOVLEY, and S.E. HAGGERTY, Biogenic Magnetite and the Magnetization of Sediments, *J. Geophys. Res., 95,* 4,355-4,361, 1990.

TAIRA, A., Magnetic Fabrics and Depositional Processes, In: A. Taira and F. Masuda (Editors), *Sedimentary Facies in the Active Plate Margin,* pp. 43-77, TERRAPUB, Tokyo, 1989.

TARDUNO, J.A., Absolute Inclination Value from Deep Sea Sediments: A Reexamination of the Cretaceous Pacific Record, *Geophys. Res. Lett., 17,* 101-104, 1990.

TARLING, D.H., *Palaeomagnetism: Principles and Applications in Geology, Geophysics and Archaeology,* 379 pp., Chapman and Hall Ltd., London, 1983.

THIEDE, J., W.E. DEAN, D.K. REA, T.L. VALLIER and C.G. ADELSECK, The Geologic History of the Mid-Pacific

Mountains in the Central North Pacific Ocean-A Synthesis of Deep-Sea Drilling Studies, *Initial Rep. Deep Sea Drill. Proj., 62,* 1073-1120, 1981a.

THIEDE, J., T.L. VALLIER and C.G.ADELSECK et al. (The Shipboard Scientific Party), Site 463: Western Mid-Pacific Mountains, *Initial Rep. Deep Sea Drill. Proj., 62,* 33-156, 1981b.

VEROSUB, K.L., Depositional and Postdepositional Processes in the Magnetization of Sediments, *Rev. Geophys. Space Phys., 15,* 129-143, 1977.

VETTERLING, W.T., S.A. TEUKOLSKY, W.H. PRESS, and B.P. FLANNERY, *Numerical Recipes Example Book (FORTRAN)*, 179 pp., Cambridge University Press, Cambridge, 1987.

WINTERER, E.L., J.I. EWING, R.G. DOUGLAS et al. (The Shipboard Scientific Party), Site 167, *Initial Rep. Deep Sea Drill. Proj., 17,* 145-234, 1973.

WINTERER, E.L., Bathymetry and Regional Tectonic Setting of the Line Islands Chain, *Initial Rep. Deep Sea Drill. Proj., 33,* 731-747, 1976.

WORM, H.U. and N. WEINREICH, Rock Magnetism of Pelagic Sediments from the Equatorial Pacific, *Earth and Planet. Sci. Lett., 89,* 184-192, 1988.

ZONENSHAIN, L.P., M.V. KONONOV and L.A. SAVOSTIN, Pacific and Kula/Eurasia Relative Motions During the Last 130 Ma and Their Bearing on Orogenesis in Northeast Asia, In: J.W.H. Monger and J. Francheteau (Editors), *Circum-Pacific Orogenic Belts and Evolution of the Pacific Ocean Basin,* Am. Geophys. Union Geodynamic Series vol. 18, pp. 29-47, 1987.

APPENDIX 1

DETAILED PALAEOMAGNETIC DATA

The following table presents the detailed data of step-wise alternating field demagnetization for all specimens. The first column gives the magnitude of the alternating magnetic field. The second column gives the nominal declination of remanence after the corresponding demagnetization. The third column gives the inclination of remanenc((bedding is assumed horizontal perpendicular to the drill core axis). The fourth column gives the intensity of remanence and the fifth the intensity of remanence as a ratio of NRM.

FIELD(mT)	DEC.(°)	INC.(°)	MOMENT($A.m^2$)	M/M_0
SITE : 167		SPECIMEN : 62-4-64		
0.0	208.2	-15.3	1.104e-07	1.000
2.5	202.9	-13.6	1.198e-07	1.085
5.0	174.5	-21.0	9.496e-08	0.860
7.5	198.9	-26.3	8.140e-08	0.737
10.0	198.0	-28.1	7.135e-08	0.646
12.5	196.1	-31.6	6.125e-08	0.555
15.0	198.6	-31.6	5.366e-08	0.486
17.5	199.2	-30.8	4.613e-08	0.418
20.0	200.0	-32.6	4.335e-08	0.393
25.0	197.8	-35.3	3.050e-08	0.276
30.0	195.5	-28.4	2.292e-08	0.208
35.0	199.0	-35.4	1.499e-08	0.136
40.0	185.6	-33.8	1.008e-08	0.091
50.0	187.5	-12.6	7.319e-09	0.066
60.0	214.6	-33.5	2.277e-09	0.021

FIELD(mT)	DEC.(°)	INC.(°)	MOMENT(A.m^2)	M/M$_o$
SITE : 167			SPECIMEN : 63-4-75	
0.0	5.5	3.4	4.543e-07	1.000
2.5	359.8	2.9	3.959e-07	0.871
5.0	3.9	-2.4	2.681e-07	0.590
7.5	1.8	-10.6	1.606e-07	0.354
10.0	2.7	-18.2	1.184e-07	0.261
12.5	3.3	-21.6	9.550e-08	0.210
15.0	5.9	-24.5	7.830e-08	0.172
17.5	359.9	-19.1	7.846e-08	0.173
20.0	7.8	-27.1	5.244e-08	0.115
25.0	6.5	-28.4	3.949e-08	0.087
30.0	2.1	-26.1	2.708e-08	0.060
SITE : 167			SPECIMEN : 65-3-42	
0.0	266.0	-66.0	8.273e-08	1.000
2.5	254.0	-63.1	7.718e-08	0.933
5.0	243.2	-59.2	8.292e-08	1.002
7.5	247.5	-57.7	7.221e-08	0.873
10.0	236.5	-45.2	9.549e-08	1.154
12.5	234.7	-42.2	9.874e-08	1.194
15.0	236.4	-41.7	9.861e-08	1.192
17.5	236.4	-40.8	9.388e-08	1.135
20.0	238.6	-42.3	8.828e-08	1.067
25.0	242.1	-44.4	7.220e-08	0.873
30.0	243.3	-45.0	5.638e-08	0.681
35.0	249.2	-47.4	4.458e-08	0.539
40.0	248.0	-49.5	2.983e-08	0.361
50.0	251.7	-43.2	1.876e-08	0.227
60.0	288.8	-54.2	1.390e-08	0.168
70.0	276.4	-68.0	8.852e-09	0.107
SITE : 167			SPECIMEN : 67-3-36	
0.0	22.3	-9.1	1.403e-07	1.000
2.5	24.7	-7.8	1.454e-07	1.036
5.0	24.7	-9.9	1.243e-07	0.886
7.5	25.4	-10.9	1.078e-07	0.768
10.0	28.6	-12.2	1.020e-07	0.727
12.5	27.7	-16.2	7.921e-08	0.565
15.0	28.8	-17.8	6.860e-08	0.489
17.5	29.9	-20.9	5.791e-08	0.413
20.0	31.2	-24.0	5.166e-08	0.368
25.0	35.9	-20.7	4.858e-08	0.346
30.0	35.9	-28.5	2.928e-08	0.209

FIELD(mT)	DEC.(°)	INC.(°)	MOMENT(A.m^2)	M/M$_0$
SITE : 167		SPECIMEN : 67-3-36 (Cont'd)		
35.0	34.5	-29.0	2.291e-08	0.163
40.0	38.7	-28.8	1.750e-08	0.125
50.0	39.0	-24.0	9.000e-09	0.064
SITE : 167		SPECIMEN : 69-4-133		
0.0	70.7	16.2	5.021e-08	1.000
2.5	69.3	18.8	4.190e-08	0.834
5.0	74.7	18.4	3.677e-08	0.732
7.5	79.7	16.1	3.098e-08	0.617
10.0	85.2	13.8	2.294e-08	0.457
12.5	89.4	13.4	1.785e-08	0.356
15.0	90.5	12.1	1.331e-08	0.265
17.5	86.4	13.1	9.509e-09	0.189
20.0	80.4	16.5	6.209e-09	0.124
25.0	44.2	28.3	3.904e-09	0.078
30.0	7.0	38.2	4.136e-09	0.082
35.0	352.9	29.1	5.308e-09	0.106
40.0	2.9	35.0	4.524e-09	0.090
SITE : 167		SPECIMEN : 71-2-63		
0.0	330.4	-12.0	1.854e-07	1.000
2.5	325.7	-11.8	1.825e-07	0.984
5.0	355.3	-15.3	1.370e-07	0.739
7.5	321.2	-12.1	1.587e-07	0.856
10.0	314.6	-12.9	1.388e-07	0.749
12.5	309.3	-13.7	1.240e-07	0.669
15.0	308.4	-14.4	1.149e-07	0.620
17.5	302.3	-16.6	9.833e-08	0.530
20.0	300.9	-17.9	8.654e-08	0.467
25.0	297.2	-20.1	6.736e-08	0.363
30.0	296.7	-20.8	5.010e-08	0.270
35.0	297.2	-20.2	3.807e-08	0.205
40.0	301.3	-23.8	2.581e-08	0.139
50.0	299.7	-11.5	1.452e-08	0.078
60.0	320.5	-18.5	1.338e-08	0.072
SITE : 167		SPECIMEN : 72-2-63		
0.0	27.8	-10.4	4.028e-08	1.000
2.5	27.8	-10.8	3.962e-08	0.984
5.0	29.1	-11.3	3.779e-08	0.938
7.5	29.6	-11.8	3.503e-08	0.870

FIELD(mT)	DEC.(°)	INC.(°)	MOMENT(A.m^2)	M/M$_0$
SITE : 167		SPECIMEN : 72-2-63 (Cont'd)		
10.0	33.6	-10.6	4.123e-08	1.024
12.5	31.9	-16.4	2.660e-08	0.660
15.0	27.6	-17.3	2.206e-08	0.548
17.5	27.8	-19.4	1.939e-08	0.481
20.0	27.6	-19.8	1.619e-08	0.402
25.0	26.5	-19.1	1.201e-08	0.298
30.0	26.7	-14.1	8.755e-09	0.217
35.0	20.8	-11.8	6.895e-09	0.171
40.0	28.8	-6.3	5.154e-09	0.128
50.0	32.6	37.7	3.349e-09	0.083
60.0	357.9	18.6	3.017e-09	0.075
SITE : 167		SPECIMEN : 73-2-121		
0.0	12.1	-4.4	9.077e-09	1.000
5.0	13.2	-7.4	7.125e-09	0.785
7.5	14.2	-10.7	6.224e-09	0.686
10.0	12.1	-12.6	5.377e-09	0.592
12.5	14.4	-14.9	4.590e-09	0.506
15.0	13.1	-14.5	4.044e-09	0.446
20.0	12.2	-19.0	2.916e-09	0.321
25.0	11.9	-20.5	2.129e-09	0.235
30.0	6.0	-16.6	1.397e-09	0.154
35.0	7.2	-17.1	1.066e-09	0.117
40.0	9.7	-13.6	8.741e-10	0.096
50.0	38.4	1.6	5.019e-10	0.055
SITE : 288A		SPECIMEN : 21-2-98		
0.0	41.4	-49.7	5.567e-08	1.000
2.5	43.4	-50.6	5.399e-08	0.970
5.0	54.2	-52.2	4.745e-08	0.852
7.5	69.7	-55.4	3.874e-08	0.696
10.0	75.8	-55.4	3.377e-08	0.607
12.5	82.3	-55.2	2.915e-08	0.524
15.0	83.0	-53.3	2.510e-08	0.451
17.5	89.3	-52.3	2.222e-08	0.399
20.0	90.1	-52.1	1.903e-08	0.342
25.0	94.3	-48.7	1.455e-08	0.261
30.0	93.2	-45.5	1.011e-08	0.182
35.0	92.9	-46.2	8.464e-09	0.152
40.0	97.9	-36.6	7.046e-09	0.127
50.0	98.7	-15.4	3.128e-09	0.056
60.0	67.5	-42.2	2.717e-09	0.049

FIELD(mT)	DEC.(°)	INC.(°)	MOMENT(A.m²)	M/M_0

SITE : 288A SPECIMEN : 21-3-18

0.0	193.2	-68.6	4.913e-08	1.000
2.5	193.4	-66.8	4.944e-08	1.006
5.0	192.4	-63.5	4.962e-08	1.010
7.5	190.7	-60.0	4.962e-08	1.010
10.0	169.0	-58.6	4.668e-08	0.950
12.5	186.6	-54.2	4.513e-08	0.919
15.0	183.7	-53.2	4.144e-08	0.843
17.5	184.3	-53.5	3.683e-08	0.750
20.0	182.9	-51.2	3.335e-08	0.679
25.0	179.4	-51.2	2.725e-08	0.555
30.0	178.2	-48.3	2.088e-08	0.425
35.0	176.7	-48.6	1.605e-08	0.327
40.0	169.8	-48.1	1.254e-08	0.255
50.0	166.3	-39.6	5.877e-09	0.120
60.0	166.5	-69.1	3.234e-09	0.066

SITE : 288A SPECIMEN : 22-2-84

0.0	56.3	-51.5	1.246e-07	1.000
2.5	57.1	-48.6	1.290e-07	1.035
5.0	68.1	-52.4	1.162e-07	0.933
7.5	75.6	-51.1	1.075e-07	0.863
10.0	81.5	-50.4	9.826e-08	0.789
12.5	84.7	-50.2	8.969e-08	0.720
15.0	86.2	-48.3	8.044e-08	0.646
17.5	89.3	-48.5	7.086e-08	0.569
20.0	90.1	-47.8	6.408e-08	0.514
25.0	89.7	-46.2	5.057e-08	0.406
30.0	90.2	-49.5	4.336e-08	0.348
35.0	88.4	-46.3	2.928e-08	0.235
40.0	89.8	-42.5	2.301e-08	0.185
50.0	92.7	-44.8	9.234e-09	0.074
60.0	72.2	-29.8	1.008e-08	0.081

SITE : 288A SPECIMEN : 23-1-79

0.0	145.6	-66.3	1.783e-08	1.000
5.0	145.8	-61.8	1.787e-08	1.002
7.5	145.9	-58.1	1.741e-08	0.976
10.0	144.1	-57.3	1.607e-08	0.901
12.5	142.7	-57.0	1.454e-08	0.815
15.0	142.1	-55.4	1.311e-08	0.735
17.5	142.0	-55.3	1.158e-08	0.649
20.0	140.2	-54.3	1.026e-08	0.575

FIELD(mT)	DEC.(°)	INC.(°)	MOMENT($A.m^2$)	M/M_o
SITE : 288A		SPECIMEN : 23-1-79 (Cont'd)		
25.0	138.5	-54.6	8.248e-09	0.463
30.0	141.0	-52.2	6.156e-09	0.345
35.0	137.8	-56.0	4.780e-09	0.268
40.0	128.2	-56.8	2.906e-09	0.163
50.0	135.7	-46.7	1.730e-09	0.097
SITE : 288A		SPECIMEN : 23-2-115		
0.0	334.5	-8.6	9.331e-08	1.000
2.5	333.3	-9.0	9.009e-08	0.965
5.0	330.8	-9.7	7.901e-08	0.847
7.5	329.9	-9.5	6.679e-08	0.716
10.0	330.6	-10.0	5.511e-08	0.591
12.5	334.6	-9.0	5.216e-08	0.559
15.0	333.1	-10.1	3.822e-08	0.410
17.5	334.0	-12.0	3.284e-08	0.352
20.0	336.4	-12.5	2.747e-08	0.294
25.0	338.5	-13.3	1.928e-08	0.207
30.0	337.7	-10.6	1.353e-08	0.145
35.0	340.1	-9.0	1.080e-08	0.116
40.0	347.0	-11.8	7.857e-09	0.084
50.0	343.7	5.8	4.294e-09	0.046
SITE : 288A		SPECIMEN : 23-3-76		
0.0	161.6	-69.0	1.119e-07	1.000
2.5	162.8	-67.3	1.135e-07	1.014
5.0	167.0	-61.4	1.140e-07	1.019
7.5	167.0	-58.1	1.119e-07	1.000
10.0	167.5	-55.1	1.045e-07	0.934
12.5	167.2	-54.1	9.797e-08	0.876
15.0	166.8	-53.1	9.008e-08	0.805
17.5	166.4	-52.2	8.147e-08	0.728
20.0	166.6	-51.3	7.408e-08	0.662
25.0	164.8	-51.2	5.933e-08	0.530
30.0	165.7	-49.6	4.604e-08	0.411
35.0	160.7	-49.9	3.145e-08	0.281
40.0	159.5	-51.0	2.622e-08	0.234
50.0	161.5	-46.5	1.401e-08	0.125
60.0	151.0	-55.9	7.574e-09	0.068
SITE : 288A		SPECIMEN :26-1-28		
0.0	217.8	-48.7	2.023e-07	1.000

SITE : 288A   SPECIMEN :26-1-28 (Cont'd)

FIELD(mT)	DEC.(°)	INC.(°)	MOMENT($A.m^2$)	M/M_0
2.5	218.0	-48.9	2.012e-07	0.995
5.0	215.8	-48.2	1.971e-07	0.974
7.5	217.2	-48.2	1.908e-07	0.943
10.0	216.6	-48.0	1.828e-07	0.904
12.5	215.7	-48.1	1.749e-07	0.865
15.0	216.3	-48.4	1.642e-07	0.812
17.5	216.2	-48.8	1.570e-07	0.776
20.0	216.3	-49.0	1.480e-07	0.732
25.0	215.0	-48.5	1.286e-07	0.636
30.0	214.4	-46.7	1.117e-07	0.552
35.0	214.9	-47.1	9.549e-08	0.472
40.0	219.6	-51.1	7.539e-08	0.373
50.0	210.6	-45.3	5.815e-08	0.287
60.0	216.8	-50.5	3.936e-08	0.195

SITE : 288A   SPECIMEN : 29-1-47

FIELD(mT)	DEC.(°)	INC.(°)	MOMENT($A.m^2$)	M/M_0
0.0	88.4	-55.2	1.433e-07	1.000
2.5	93.4	-56.2	1.391e-07	0.971
5.0	99.8	-54.5	1.377e-07	0.961
7.5	104.7	-52.3	1.337e-07	0.933
10.0	107.4	-50.1	1.289e-07	0.900
12.5	110.5	-49.3	1.222e-07	0.853
15.0	112.1	-46.0	1.133e-07	0.791
17.5	113.1	-45.7	1.061e-07	0.740
20.0	114.3	-44.2	9.869e-08	0.689
25.0	115.8	-43.2	8.350e-08	0.583
30.0	115.3	-42.2	7.136e-08	0.498
35.0	116.0	-39.8	5.926e-08	0.414
40.0	115.4	-40.8	4.959e-08	0.346
50.0	114.0	-35.9	3.703e-08	0.258
60.0	113.2	-34.8	2.475e-08	0.173

SITE : 315A   SPECIMEN : 19-5-50

FIELD(mT)	DEC.(°)	INC.(°)	MOMENT($A.m^2$)	M/M_0
0.0	217.4	-14.1	1.756e-07	1.000
2.5	212.9	-11.1	1.957e-07	1.114
5.0	214.5	-12.6	1.770e-07	1.008
7.5	214.0	-13.7	1.570e-07	0.894
10.0	215.0	-14.7	1.398e-07	0.796
12.5	215.5	-14.0	1.201e-07	0.684
15.0	217.1	-14.8	1.018e-07	0.580
17.5	215.9	-15.4	8.940e-08	0.509
20.0	217.0	-15.7	7.261e-08	0.413

FIELD(mT)	DEC.(°)	INC.(°)	MOMENT(A.m^2)	M/M$_0$
SITE : 315A		SPECIMEN : 19-5-50 (Cont'd)		
25.0	217.5	-18.4	5.242e-08	0.299
30.0	216.7	-12.8	4.438e-08	0.253
35.0	224.2	-16.9	2.388e-08	0.136
40.0	223.9	-22.5	1.864e-08	0.106
50.0	216.0	-8.7	2.721e-08	0.155
SITE : 315A		SPECIMEN : 20-2-21		
0.0	356.8	-10.8	3.246e-07	1.000
2.5	356.4	-9.9	2.956e-07	0.911
5.0	355.9	-10.7	2.526e-07	0.778
7.5	357.7	-13.4	2.184e-07	0.673
10.0	355.4	-15.5	1.829e-07	0.563
12.5	353.9	-15.5	1.552e-07	0.478
15.0	354.6	-15.9	1.344e-07	0.414
17.5	354.0	-16.6	1.093e-07	0.337
20.0	354.9	-15.5	1.024e-07	0.315
25.0	354.1	-15.8	8.500e-08	0.262
30.0	351.5	-18.4	5.687e-08	0.175
35.0	359.9	-18.4	4.840e-08	0.149
40.0	1.6	-12.4	4.437e-08	0.137
50.0	325.0	-16.0	1.767e-08	0.054
60.0	7.6	-10.4	2.100e-08	0.065
SITE : 315A		SPECIMEN : 20-2-131		
0.0	105.7	-24.8	3.324e-07	1.000
2.5	111.0	-14.1	3.123e-07	0.940
5.0	113.1	-16.4	2.889e-07	0.869
7.5	114.4	-15.7	2.549e-07	0.767
10.0	117.5	-16.2	2.153e-07	0.648
12.5	119.3	-16.0	1.905e-07	0.573
15.0	111.6	-16.7	1.629e-07	0.490
17.5	117.8	-17.2	1.393e-07	0.419
20.0	119.8	-21.3	1.194e-07	0.359
25.0	118.7	-18.7	9.604e-08	0.289
30.0	114.3	-20.3	7.426e-08	0.223
35.0	124.9	-19.3	6.266e-08	0.189
40.0	110.0	-21.8	5.492e-08	0.165
45.0	116.3	-29.0	3.463e-08	0.104
50.0	128.3	-18.6	4.583e-08	0.138
55.0	128.0	-18.6	4.413e-08	0.133
60.0	92.3	-21.2	2.963e-08	0.089

SITE : 315A SPECIMEN : 20-5-17

FIELD(mT)	DEC.(°)	INC.(°)	MOMENT($A.m^2$)	M/M_0
0.0	347.5	-10.8	1.988e-07	1.000
2.5	347.5	-8.5	1.884e-07	0.948
5.0	345.4	-9.6	1.650e-07	0.830
7.5	345.6	-9.8	1.463e-07	0.736
10.0	344.6	-10.1	1.248e-07	0.628
12.5	345.3	-11.2	1.050e-07	0.528
15.0	346.3	-9.9	9.564e-08	0.481
17.5	344.7	-12.3	7.328e-08	0.369
20.0	346.2	-13.4	6.183e-08	0.311
25.0	347.7	-10.1	4.363e-08	0.219
30.0	341.9	-9.1	3.224e-08	0.162
35.0	348.9	-8.8	2.617e-08	0.132
40.0	350.3	-6.9	2.032e-08	0.102
50.0	333.1	-5.6	1.592e-08	0.080

SITE : 315A SPECIMEN : 21-2-11

FIELD(mT)	DEC.(°)	INC.(°)	MOMENT($A.m^2$)	M/M_0
0.0	266.1	-5.4	5.010e-07	1.000
2.5	265.4	-5.1	4.973e-07	0.993
5.0	265.4	-5.0	4.928e-07	0.984
7.5	265.8	-5.0	4.838e-07	0.966
10.0	265.4	-4.8	4.766e-07	0.951
12.5	265.0	-4.8	4.630e-07	0.924
15.0	264.7	-5.1	4.503e-07	0.899
17.5	264.9	-5.2	4.385e-07	0.875
20.0	265.2	-5.1	4.257e-07	0.850
25.0	265.9	-5.3	3.978e-07	0.794
30.0	266.0	-5.7	3.679e-07	0.734
35.0	265.3	-5.6	3.345e-07	0.668
40.0	267.4	-6.2	2.999e-07	0.599
50.0	264.8	-6.1	2.483e-07	0.496
60.0	268.0	-7.2	2.023e-07	0.404
70.0	275.1	-8.2	1.712e-07	0.342

SITE : 315A SPECIMEN : 21-5-8

FIELD(mT)	DEC.(°)	INC.(°)	MOMENT($A.m^2$)	M/M_0
0.0	98.4	-15.6	1.330e-07	1.000
2.5	100.5	-14.4	1.321e-07	0.993
5.0	102.4	-13.8	1.351e-07	1.016
7.5	104.6	-14.4	1.229e-07	0.924
10.0	106.9	-15.0	1.154e-07	0.868
12.5	104.0	-14.5	1.119e-07	0.841
15.0	109.6	-14.8	1.008e-07	0.758
17.5	110.3	-15.3	9.261e-08	0.696

FIELD(mT)	DEC.(°)	INC.(°)	MOMENT(A.m^2)	M/M$_o$
SITE : 315A		SPECIMEN : 21-5-8 (Cont'd)		
20.0	112.2	-15.5	8.312e-08	0.625
25.0	110.9	-13.8	7.964e-08	0.599
30.0	110.9	-14.3	6.632e-08	0.499
35.0	113.4	-17.0	4.989e-08	0.375
40.0	114.8	-16.0	4.358e-08	0.328
50.0	110.0	-10.9	3.558e-08	0.268
60.0	108.6	-16.6	2.219e-08	0.167
SITE : 315A		SPECIMEN : 21-6-108		
0.0	138.0	-31.9	8.956e-08	1.000
2.5	135.6	-29.1	9.505e-08	1.061
5.0	140.2	-30.5	8.949e-08	0.999
7.5	141.6	-29.4	8.718e-08	0.973
10.0	138.3	-32.7	7.959e-08	0.889
12.5	142.0	-30.5	8.046e-08	0.898
15.0	143.0	-29.1	7.547e-08	0.843
17.5	142.8	-29.7	7.077e-08	0.790
20.0	142.6	-30.4	6.477e-08	0.723
25.0	142.6	-30.5	5.345e-08	0.597
30.0	144.1	-30.8	4.505e-08	0.503
35.0	144.1	-32.5	3.680e-08	0.411
40.0	143.6	-31.1	3.083e-08	0.344
50.0	140.3	-33.1	2.178e-08	0.243
60.0	140.9	-34.0	1.646e-08	0.184
70.0	143.3	-34.8	1.324e-08	0.148
SITE : 315A		SPECIMEN : 26-2-123		
0.0	75.8	-14.6	1.489e-07	1.000
2.5	76.3	-13.0	1.462e-07	0.982
5.0	74.8	-11.8	1.528e-07	1.026
7.5	75.0	-11.8	1.504e-07	1.010
10.0	77.0	-12.3	1.389e-07	0.933
12.5	77.4	-11.9	1.360e-07	0.913
15.0	78.2	-12.4	1.315e-07	0.883
17.5	78.3	-12.7	1.268e-07	0.852
20.0	79.1	-12.5	1.223e-07	0.821
25.0	78.9	-12.8	1.122e-07	0.754
30.0	79.8	-13.7	1.002e-07	0.673
35.0	77.5	-12.1	1.043e-07	0.700
40.0	81.8	-12.7	8.394e-08	0.564
50.0	81.3	-12.1	6.266e-08	0.421
60.0	80.9	-15.9	4.795e-08	0.322

FIELD(mT)	DEC.(°)	INC.(°)	MOMENT(A.m^2)	M/M$_0$
SITE : 316		SPECIMEN : 19-2-108		
0.0	342.8	29.5	9.159e-08	1.000
2.5	342.7	30.6	8.989e-08	0.981
5.0	341.3	30.4	8.721e-08	0.952
7.5	341.0	31.6	8.271e-08	0.903
10.0	340.9	30.8	7.834e-08	0.855
12.5	338.4	32.4	7.416e-08	0.810
15.0	338.6	32.5	6.971e-08	0.761
17.5	336.2	33.3	6.429e-08	0.702
20.0	336.2	34.0	5.975e-08	0.652
25.0	347.2	31.3	5.604e-08	0.612
30.0	335.5	36.1	4.414e-08	0.482
35.0	337.9	36.3	3.804e-08	0.415
40.0	341.7	34.1	3.365e-08	0.367
50.0	335.0	45.7	2.201e-08	0.240
60.0	347.2	34.1	1.928e-08	0.211
SITE : 316		SPECIMEN : 19-4-74		
0.0	338.4	4.5	5.625e-08	1.000
2.5	338.0	6.3	5.406e-08	0.961
5.0	335.8	6.0	5.164e-08	0.918
7.5	334.9	7.3	4.886e-08	0.868
10.0	333.2	8.3	4.662e-08	0.829
12.5	332.2	9.4	4.404e-08	0.783
15.0	329.5	9.7	4.246e-08	0.755
17.5	328.6	10.3	3.989e-08	0.709
20.0	329.1	12.3	3.707e-08	0.659
25.0	328.9	14.6	3.308e-08	0.588
30.0	327.3	17.7	2.733e-08	0.486
35.0	326.1	21.4	2.220e-08	0.395
40.0	326.2	23.8	1.869e-08	0.332
50.0	331.5	34.2	1.559e-08	0.277
60.0	328.7	34.7	1.356e-08	0.241
65.0	348.4	58.0	9.266e-09	0.165
70.0	320.5	43.0	1.038e-08	0.185
75.0	334.8	35.3	1.026e-08	0.182
80.0	256.6	17.5	4.676e-09	0.083
SITE : 316		SPECIMEN : 20-4-67		
0.0	354.6	14.6	7.345e-08	1.000
2.5	0.5	15.3	6.824e-08	0.929
5.0	353.6	17.1	5.751e-08	0.783
7.5	353.1	19.4	5.053e-08	0.688

FIELD(mT)	DEC.(°)	INC.(°)	MOMENT(A.m^2)	M/M$_o$
SITE : 316		SPECIMEN : 20-4-67 (Cont'd)		
10.0	351.8	19.3	4.540e-08	0.618
15.0	350.1	21.0	3.682e-08	0.501
20.0	350.5	21.3	3.016e-08	0.411
25.0	348.8	23.6	2.314e-08	0.315
30.0	348.6	22.7	1.901e-08	0.259
35.0	351.6	23.6	1.538e-08	0.209
40.0	350.1	30.7	1.176e-08	0.160
45.0	350.5	35.2	9.640e-09	0.131
50.0	352.2	25.7	9.221e-09	0.126
60.0	12.2	22.6	6.799e-09	0.093
SITE : 316		SPECIMEN : 22-2-27		
0.0	321.8	10.2	1.322e-07	1.000
2.5	320.8	10.6	1.290e-07	0.976
5.0	319.5	10.5	1.238e-07	0.936
7.5	317.2	10.3	1.167e-07	0.883
10.0	315.0	10.1	1.118e-07	0.846
12.5	314.4	11.0	1.031e-07	0.780
15.0	313.0	11.7	9.521e-08	0.720
17.5	311.9	11.7	8.552e-08	0.647
20.0	312.1	12.3	7.796e-08	0.590
25.0	312.5	12.3	6.447e-08	0.488
30.0	311.5	12.6	5.181e-08	0.392
35.0	310.4	11.7	4.155e-08	0.314
40.0	312.2	11.4	3.294e-08	0.249
50.0	303.9	16.4	2.020e-08	0.153
60.0	319.9	6.8	1.588e-08	0.120
SITE : 316		SPECIMEN : 23-3-107		
0.0	353.3	9.6	1.566e-07	1.000
2.5	352.7	10.3	1.393e-07	0.890
5.0	350.3	13.6	1.251e-07	0.799
7.5	343.5	16.7	1.100e-07	0.702
10.0	344.0	16.6	1.038e-07	0.663
12.5	338.5	19.5	8.371e-08	0.535
15.0	336.3	17.3	7.771e-08	0.496
17.5	336.8	19.7	6.892e-08	0.440
20.0	333.9	21.3	5.645e-08	0.360
25.0	334.0	24.2	4.071e-08	0.260
30.0	328.6	21.2	3.318e-08	0.212
35.0	331.3	21.1	2.076e-08	0.133
40.0	355.8	22.8	1.456e-08	0.093

FIELD(mT)	DEC.(°)	INC.(°)	MOMENT(A.m^2)	M/M$_0$
SITE : 316		SPECIMEN : 23-3-107 (Cont'd)		
50.0	0.0	25.6	1.227e-08	0.078
60.0	330.0	-38.8	3.480e-09	0.022
SITE : 316		SPECIMEN : 24-3-59		
0.0	70.2	-43.7	5.496e-08	1.000
2.5	73.1	-39.4	5.268e-08	0.959
5.0	79.3	-38.0	4.825e-08	0.878
7.5	86.7	-36.5	4.401e-08	0.801
10.0	93.5	-37.5	3.973e-08	0.723
12.5	96.1	-34.7	3.650e-08	0.664
15.0	100.2	-29.4	3.929e-08	0.715
17.5	105.8	-37.4	2.984e-08	0.543
20.0	106.2	-37.2	2.702e-08	0.492
25.0	108.5	-34.3	2.209e-08	0.402
30.0	113.4	-36.2	1.787e-08	0.325
35.0	110.5	-31.9	1.514e-08	0.275
40.0	100.8	-30.4	1.232e-08	0.224
50.0	135.7	-17.9	6.838e-09	0.124
60.0	90.9	-17.0	6.917e-09	0.126
SITE : 316		SPECIMEN : 25-5-40		
0.0	91.8	-21.2	2.519e-07	1.000
2.5	91.1	-20.8	2.576e-07	1.023
5.0	92.6	-21.3	2.492e-07	0.989
7.5	94.1	-21.7	2.435e-07	0.967
10.0	94.2	-22.6	2.355e-07	0.935
12.5	94.7	-23.0	2.266e-07	0.900
15.0	94.9	-23.5	2.150e-07	0.854
17.5	95.4	-24.0	2.023e-07	0.803
20.0	95.4	-23.4	1.967e-07	0.781
25.0	95.8	-24.9	1.630e-07	0.647
30.0	95.4	-25.6	1.126e-07	0.447
35.0	94.2	-25.1	9.365e-08	0.372
40.0	97.4	-25.4	5.945e-08	0.236
50.0	92.7	-26.9	4.389e-08	0.174
60.0	93.9	-27.4	3.133e-08	0.124
SITE : 462		SPECIMEN : 55-1-28		
0.0	81.9	-13.6	3.350e-07	1.000
2.5	81.1	-13.8	3.290e-07	0.982
5.0	82.2	-13.8	3.252e-07	0.971

FIELD(mT)	DEC.(°)	INC.(°)	MOMENT(A.m^2)	M/M$_0$
SITE : 462		SPECIMEN : 55-1-28 (Cont'd)		
7.5	83.6	-13.5	3.123e-07	0.932
10.0	82.8	-14.5	2.906e-07	0.867
12.5	81.5	-13.5	2.845e-07	0.849
15.0	83.5	-14.1	2.520e-07	0.752
17.5	84.1	-13.8	2.297e-07	0.686
20.0	84.2	-13.6	2.160e-07	0.645
25.0	84.3	-13.9	1.723e-07	0.514
30.0	80.5	-13.3	1.455e-07	0.434
35.0	82.5	-14.0	1.155e-07	0.345
40.0	84.0	-13.1	9.200e-08	0.275
50.0	83.8	-13.0	6.613e-08	0.197
60.0	85.6	-11.6	4.988e-08	0.149
SITE : 462		SPECIMEN : 55-1-114		
0.0	160.7	-21.6	6.329e-08	1.000
2.5	159.3	-22.1	6.373e-08	1.007
5.0	160.6	-21.7	6.409e-08	1.013
7.5	161.6	-22.6	6.176e-08	0.976
10.0	161.5	-22.1	5.995e-08	0.947
15.0	166.4	-24.4	5.061e-08	0.800
20.0	161.6	-22.6	4.454e-08	0.704
25.0	161.0	-23.8	3.726e-08	0.589
30.0	161.5	-22.2	3.097e-08	0.489
35.0	160.2	-24.0	2.407e-08	0.380
40.0	159.3	-24.7	1.961e-08	0.310
50.0	157.2	-23.8	1.343e-08	0.212
60.0	185.4	-24.7	9.557e-09	0.151
SITE : 462		SPECIMEN : 55-2-128		
0.0	19.4	-2.1	2.874e-07	1.000
2.5	16.7	-12.6	2.766e-07	0.962
5.0	17.0	-12.4	2.678e-07	0.932
7.5	16.2	-12.8	2.518e-07	0.876
10.0	17.1	-12.4	2.369e-07	0.824
12.5	16.5	-12.4	2.181e-07	0.759
15.0	18.5	-12.8	1.985e-07	0.691
17.5	17.6	-13.1	1.787e-07	0.622
20.0	17.4	-12.8	1.608e-07	0.559
25.0	16.6	-13.4	1.281e-07	0.446
30.0	15.7	-12.3	1.049e-07	0.365
35.0	16.9	-14.2	7.643e-08	0.266
40.0	17.7	-12.1	6.122e-08	0.213

FIELD(mT)	DEC.(°)	INC.(°)	MOMENT(A.m²)	M/M₀
SITE : 462		SPECIMEN : 55-2-128 (Cont'd)		
50.0	17.1	-11.3	3.391e-08	0.118
60.0	19.0	-12.3	2.431e-08	0.085
SITE : 462		SPECIMEN : 55-3-29		
0.0	204.5	13.1	8.679e-07	1.000
2.5	204.8	13.0	8.753e-07	1.009
5.0	204.9	13.0	8.931e-07	1.029
7.5	204.7	12.7	8.828e-07	1.017
10.0	204.9	12.0	8.530e-07	0.983
12.5	205.1	12.2	8.077e-07	0.931
15.0	204.9	11.6	7.452e-07	0.859
17.5	206.1	11.8	6.814e-07	0.785
20.0	205.3	13.7	6.074e-07	0.700
25.0	205.2	13.9	4.959e-07	0.571
30.0	205.7	14.6	3.961e-07	0.456
35.0	205.1	14.1	3.056e-07	0.352
40.0	204.2	15.7	2.394e-07	0.276
50.0	207.9	17.4	1.757e-07	0.202
60.0	202.9	19.9	1.059e-07	0.122
SITE : 462		SPECIMEN : 55-3-132		
0.0	287.8	12.1	1.157e-07	1.000
2.5	287.1	13.4	1.201e-07	1.038
5.0	277.8	14.2	1.235e-07	1.067
7.5	271.7	14.1	1.375e-07	1.188
10.0	265.8	15.5	1.389e-07	1.201
12.5	265.7	13.9	1.444e-07	1.248
15.0	263.3	14.3	1.376e-07	1.189
17.5	261.2	14.3	1.323e-07	1.143
20.0	260.7	16.1	1.213e-07	1.048
25.0	260.5	15.1	1.031e-07	0.891
30.0	265.5	17.3	8.861e-08	0.766
35.0	263.2	18.6	6.890e-08	0.596
40.0	261.3	18.8	5.586e-08	0.483
50.0	258.4	22.2	5.112e-08	0.442
60.0	269.2	28.3	2.566e-08	0.222
70.0	258.1	19.9	2.911e-08	0.252
SITE : 463		SPECIMEN : 58-1-31		
0.0	62.4	-20.4	8.798e-09	1.000
2.5	65.5	-20.6	8.597e-09	0.977

FIELD(mT)	DEC.(°)	INC.(°)	MOMENT($A.m^2$)	M/M_0
SITE : 463		SPECIMEN : 58-1-31 (Cont'd)		
5.0	67.5	-24 3	7.982e-09	0.907
7.5	68.1	-25.2	7.102e-09	0.807
10.0	70.0	-28.9	6.521e-09	0.741
12.5	69.7	-30.3	5.900e-09	0.671
15.0	72.0	-29.2	5.347e-09	0.608
17.5	73.5	-27.9	4.860e-09	0.552
20.0	72.8	-29.7	4.477e-09	0.509
25.0	75.1	-27.2	3.816e-09	0.434
30.0	74.8	-26.6	3.137e-09	0.357
35.0	74.9	-24.5	2.677e-09	0.304
40.0	78.4	-19.2	2.355e-09	0.268
50.0	75.2	-20.5	1.470e-09	0.167
60.0	74.2	-17.5	1.474e-09	0.168
SITE : 463		SPECIMEN : 58-2-82		
0.0	45.8	-20.2	1.280e-08	1.000
2.5	46.8	-20.8	1.250e-08	0.977
5.0	48.4	-23.9	1.154e-08	0.902
7.5	49.6	-28.3	1.054e-08	0.823
10.0	50.9	-31.3	9.665e-09	0.755
12.5	50.8	-31.6	9.048e-09	0.707
15.0	49.5	-34.6	8.467e-09	0.661
17.5	52.2	-34.2	7.786e-09	0.608
20.0	52.5	-34.1	7.298e-09	0.570
25.0	53.0	-34.6	6.426e-09	0.502
30.0	52.5	-36.4	5.695e-09	0.445
35.0	54.3	-34.8	5.359e-09	0.419
40.0	54.1	-34.2	4.860e-09	0.380
50.0	52.6	-35.9	4.375e-09	0.342
60.0	54.4	-35.6	4.317e-09	0.337
SITE : 463		SPECIMEN : 59-2-104		
0.0	298.7	-26.0	5.581e-09	1.000
2.5	292.3	-24.7	5.076e-09	0.910
5.0	282.1	-28.9	4.848e-09	0.869
7.5	271.4	-32.3	4.605e-09	0.825
10.0	262.3	-33.4	4.514e-09	0.809
12.5	258.1	-34.1	4.434e-09	0.794
15.0	254.9	-31.9	4.396e-09	0.788
17.5	254.1	-30.2	4.102e-09	0.735
20.0	250.2	-32.1	3.930e-09	0.704
25.0	234.7	-36.0	3.170e-09	0.568

FIELD(mT)	DEC.(°)	INC.(°)	MOMENT($A.m^2$)	M/M_0
SITE : 463		SPECIMEN : 59-2-104 (Cont'd)		
30.0	246.6	-31.3	3.188e-09	0.571
35.0	246.3	-29.2	2.765e-09	0.495
40.0	243.2	-33.2	2.453e-09	0.440
50.0	245.8	-25.9	2.138e-09	0.383
60.0	242.7	-26.5	1.891e-09	0.339
SITE : 463		SPECIMEN : 60-2-33		
0.0	39.8	22.5	2.088e-08	1.000
2.5	41.2	23.9	2.060e-08	0.987
5.0	42.6	25.6	1.844e-08	0.883
7.5	43.8	29.6	1.646e-08	0.788
10.0	43.1	31.3	1.462e-08	0.700
12.5	44.9	33.0	1.312e-08	0.628
15.0	43.7	33.5	1.190e-08	0.570
17.5	44.1	32.8	1.073e-08	0.514
20.0	44.1	32.1	1.001e-08	0.479
25.0	45.4	31.7	8.837e-09	0.423
30.0	44.1	29.5	7.559e-09	0.362
35.0	43.9	31.0	6.986e-09	0.335
40.0	45.0	28.2	6.306e-09	0.302
50.0	44.7	29.9	5.694e-09	0.273
60.0	44.6	27.0	5.164e-09	0.247
SITE : 463		SPECIMEN : 61-1-105		
0.0	341.7	-31.2	4.711e-08	1.000
2.5	324.9	-34.3	4.237e-08	0.899
5.0	319.6	-36.0	3.923e-08	0.833
7.5	313.0	-37.4	3.645e-08	0.774
10.0	306.8	-38.1	3.254e-08	0.691
12.5	298.8	-37.2	2.863e-08	0.608
15.0	294.6	-36.0	2.552e-08	0.542
17.5	291.1	-33.7	2.231e-08	0.474
20.0	288.5	-34.5	1.963e-08	0.417
25.0	289.7	-32.6	1.683e-08	0.357
30.0	280.7	-32.2	1.287e-08	0.273
35.0	281.1	-34.1	1.037e-08	0.220
40.0	280.0	-33.5	8.719e-09	0.185
50.0	275.3	-31.7	6.694e-09	0.142
60.0	280.1	-33.7	5.053e-09	0.107

FIELD(mT)	DEC.(°)	INC.(°)	MOMENT($A.m^2$)	M/M_0
SITE : 463		SPECIMEN : 64-1-60		
0.0	297.8	-18.6	1.074e-08	1.000
2.5	296.8	-19.7	1.072e-08	0.998
5.0	294.5	-23.4	9.977e-09	0.929
7.5	292.2	-29.9	8.888e-09	0.828
10.0	291.8	-35.2	8.196e-09	0.763
12.5	292.6	-38.3	7.456e-09	0.694
15.0	292.5	-41.2	6.922e-09	0.645
17.5	291.6	-42.1	6.315e-09	0.588
20.0	291.7	-41.5	5.787e-09	0.539
25.0	293.9	-43.6	4.955e-09	0.461
30.0	294.1	-44.4	4.364e-09	0.406
35.0	294.3	-42.9	3.896e-09	0.363
40.0	295.3	-45.6	3.451e-09	0.321
50.0	294.3	-45.5	3.201e-09	0.298
60.0	296.1	-46.0	2.995e-09	0.279
SITE : 463		SPECIMEN : 67-2-103		
0.0	147.1	-26.3	1.950e-09	1.000
2.5	154.3	-26.2	2.462e-09	1.263
5.0	157.6	-26.1	2.536e-09	1.301
7.5	160.0	-29.5	2.419e-09	1.241
10.0	162.5	-33.4	2.261e-09	1.159
12.5	166.0	-30.7	2.027e-09	1.039
15.0	164.9	-32.7	1.926e-09	0.988
17.5	164.2	-29.6	1.664e-09	0.853
20.0	164.2	-32.1	1.487e-09	0.763
25.0	165.0	-32.6	1.209e-09	0.620
30.0	168.7	-35.9	1.049e-09	0.538
35.0	156.3	-33.4	8.618e-10	0.442
40.0	161.0	-30.5	6.726e-10	0.345
SITE : 463		SPECIMEN : 70-1-78		
0.0	9.4	-29.1	4.672e-09	1.000
2.5	8.5	-28.3	4.526e-09	0.969
5.0	9.6	-27.6	4.366e-09	0.935
7.5	9.3	-26.5	4.136e-09	0.885
10.0	9.7	-24.6	3.896e-09	0.834
12.5	10.6	-23.8	3.717e-09	0.796
15.0	9.5	-23.5	3.542e-09	0.758
17.5	9.3	-22.3	3.362e-09	0.720
20.0	10.3	-24.5	3.310e-09	0.708
25.0	11.1	-21.8	3.103e-09	0.664

FIELD(mT)	DEC.(°)	INC.(°)	MOMENT(A.m^2)	M/M$_o$
SITE : 463		SPECIMEN : 70-1-78 (Cont'd)		
30.0	9.1	-18.9	2.921e-09	0.625
35.0	11.9	-21.4	2.833e-09	0.606
40.0	11.9	-24.5	2.256e-09	0.483
50.0	11.9	-25.5	2.428e-09	0.520
60.0	8.1	-17.2	2.191e-09	0.469
70.0	9.9	-19.7	2.047e-09	0.438
80.0	17.2	-30.3	1.929e-09	0.413
90.0	17.8	-27.0	1.741e-09	0.373

APPENDIX 2

NUMERICAL EXAMPLE OF STATISTICS OF PALAEOMAGNETIC INCLINATION DATA (McFADDEN AND REID, 1982)

The following is a numerical example of the method suggested by McFadden and Reid (1982) for calculating the inclination of the true mean direction of vertical borecore specimens assuming that the data are Fisher distributed. In the present investigation this method was applied using a spreadsheet program (LOTUS 1-2-3 version 2.2) and a table of F distribution. Here, data of site 315A are taken as an example.

The values of inclination data of site 315A are -16.5, -15.9, -20.6, -8.6, -5.2, -14.9, -31.8, and -13.1. Accordingly, the values of θ_i, the complement of the observed inclination of the i^{th} specimen, are -73.5, -74.1, -69.4, -81.4, -84.8, -75.1, -58.2, and -76.9 respectively. Hence

$\Sigma \cos \theta_i = 2.1589$ and $\Sigma \sin \theta_i = -7.6322$.

Substituting these values into Equation (19) in McFadden and Reid (1982), which is

$$N \cos\theta_o + (\sin^2\theta_o - \cos^2\theta_o) \, \Sigma \cos\theta_i$$
$$- 2 \sin\theta_o \cos\theta_o \, \Sigma \sin\theta_i = 0$$

where N is the number of specimens and θ_o is the maximum likelihood estimate for the complement of the inclination of the true mean direction. This gives

$$8 \cos\theta_o + 2.1598 \, (\sin^2\theta_o - \cos^2\theta_o) + 15.2644 \sin\theta_o \cos\theta_o = 0.$$

Solving this equation by iteration gives two values for θ_o, i.e., -25.09 and -74.06. Obviously, the second value is the correct one.

Next, θ_o = -74.06 gives

$C = \Sigma \cos(\theta_o - \theta_i) = 7.9319$ and

$S = \Sigma \sin(\theta_o - \theta_i) = 0.0192.$

I, the unbiased estimate for the inclination of the true mean direction is defined (in degrees) in equation (40) in McFadden and Reid (1982) as

$$I = (90° - \theta_o - \frac{180S}{\pi C}).$$

Substituting for θ_o, C, and S gives

$$I = (90 + 74.06 + \frac{3.456}{24.919})^o = 164.2^o.$$

or in the present case of negative inclination I = -15.8°.

The best estimate for the precision parameter κ is denoted by k, which is defined in equation (20) of McFadden and Reid (1982) as

$$k = \frac{N - 1}{2(N - \Sigma \cos(\theta_o - \theta_i))} = \frac{N - 1}{2(N - C)}.$$

Substituting for N and C gives

$$k = \frac{7}{2\ (8 - 7.9319)} = 51.4.$$

The angle of confidence is denoted by α, whose cosine is given in equation (42) in McFadden and Reid (1982) as

$$\cos\alpha = 1 - \frac{1}{2}\ (\frac{S}{C})^2 - \frac{f(N - C)}{C(N - 1)},$$

where f is the relevant critical value of F distribution with 1 and N-1 degrees of freedom. The 95 per cent confidence limit of I is obtained using a two-tailed test. Table of the F distribution for F = 0.975 with 1 and 7 degrees of freedom gives f = 8.07. This means that there is a probability of

0.025 that f will exceed 8.07. Subtituting f = 8.07 into the above equation gives

$$\cos\alpha = 1 - \frac{1}{2}\left(\frac{0.0192}{7.9319}\right)^2 - \frac{8.07(8 - 7.9319)}{7.9319(8 - 1)} = 0.9900.$$

Hence α is equal to 8.1°. This implies that the inclination of the true mean direction lies between (-15.8 + 8.1)° = -7.7° and (-15.8 - 8.1)° = -23.9° with 95 per cent confidence. The results from the other sites are listed in Table 3.5. Note that in that table I and α are listed respectively as I_{ob} and I_{95}.

APPENDIX 3

LISTING OF PROGRAM ND11R5

```
        PROGRAM ND11R5
C       Driver for routine JACOBI
C
*************************************************************
C    THIS FORTRAN 77 PROGRAM CALCULATES THE EIGENVALUES AND
C    THE EIGENVECTORS OF 3 x 3 MATRICES.
C    THE PROGRAM IS MODIFIED FROM PROGRAM D11R1 AND ITS
C    ROUTINE JACOBI (PRESS et al., NUMERICAL RECIPES - THE ART
C    OF SCIENTIFIC COMPUTING, 818 PP., CAMBRIDGE UNIVERSITY
C    PRESS, CAMBRIDGE, 1987 AND VETTERLING et al., NUMERICAL
C    RECIPES EXAMPLE BOOK (FORTRAN), 179 PP., CAMBRIDGE
C    UNIVERSITY PRESS, CAMBRIDGE, 1987).
C    MODIFICATION IS MADE BY SATRIA BIJAKSANA, DEPT. OF EARTH
C    SCIENCES MEMORIAL UNIVERSITY OF NEWFOUNDLAND.
*************************************************************
        PARAMETER(NP=10,NMAT=1)
        CHARACTER TEXT*15
        DIMENSION D(NP),V(NP,NP),R(NP),DM(NP),VM(NP,NP)
        DIMENSION A(3,3),E(NP,NP),NUM(1),DEC(NP),AINC(NP)
        DATA NUM/3/
        OPEN(UNIT=1, FILE='LPT1')
        PI=3.141592654
61      WRITE(*,*)'enter your data......'
        WRITE(*,*)' THE SPEC. NAME SHOULD BE WRITTEN BETWEEN'
        WRITE(*,*)' A PAIR OF SINGLE QUOTE'
        WRITE(*,*)'SPECIMEN : ? '
        READ(*,*) TEXT
        DO 44 KJ=1,3
            DO 43 KM=1,3
                    WRITE(*,'(2I2)') KJ,KM
                    READ(*,*) A(KJ,KM)
43          CONTINUE
44      CONTINUE
        DO 24 I=1,1
                DO 12 II=1,3
                    DO 11 JJ=1,3
                        E(II,JJ)=A(II,JJ)
11                  CONTINUE
12              CONTINUE
                CALL JACOBI(E,3,NP,D,V,NROT)
            IF (D(1).LT.D(2)) GOTO 91
```

```
      IF (D(2).LT.D(3)) GOTO 92
      DM(1)=D(1)
      DM(2)=D(2)
      DM(3)=D(3)
           DO 80 L=1,3
                VM(1,L)=V(L,1)
                VM(2,L)=V(L,2)
                VM(3,L)=V(L,3)
80         CONTINUE
      GOTO 99
91    IF (D(2).GT.D(3)) GOTO 93
      DM(1)=D(3)
      DM(2)=D(2)
      DM(3)=D(1)
           DO 81 L=1,3
                VM(1,L)=V(L,3)
                VM(2,L)=V(L,2)
                VM(3,L)=V(L,1)
81         CONTINUE
      GOTO 99
93    IF (D(1).GT.D(3)) GOTO 94
      DM(1)=D(2)
      DM(2)=D(3)
      DM(3)=D(1)
           DO 84 L=1,3
                VM(1,L)=V(L,2)
                VM(2,L)=V(L,3)
                VM(3,L)=V(L,1)
84         CONTINUE
      GOTO 99
94    DM(1)=D(2)
      DM(2)=D(1)
      DM(3)=D(3)
           DO 82 L=1,3
                VM(1,L)=V(L,2)
                VM(2,L)=V(L,1)
                VM(3,L)=V(L,3)
82         CONTINUE
      GOTO 99
92    IF (D(1).LT.D(3)) GOTO 95
      DM(1)=D(1)
      DM(2)=D(3)
      DM(3)=D(2)
           DO 85 L=1,3
                VM(1,L)=V(L,1)
                VM(2,L)=V(L,3)
                VM(3,L)=V(L,2)
85         CONTINUE
      GOTO 99
```

```
95          DM(1)=D(3)
            DM(2)=D(1)
            DM(3)=D(2)
                 DO 89 L=1,3
                    VM(1,L)=V(L,3)
                    VM(2,L)=V(L,1)
                    VM(3,L)=V(L,2)
89               CONTINUE
            GOTO 99
99              DO 79 L=1,3
                   PIO=0.0
                   C1=VM(L,1)
                   C2=VM(L,2)
                   C3=VM(L,3)
                   DE1=ATAN(C2/C1)
                   DEC(L)=(180/PI)*DE1
                   IF (C1.LT.PIO) DEC(L)=DEC(L)+180
                   IF (DEC(L).LT.PIO) DEC(L)=DEC(L)+360
                   AIN1=ASIN(C3)
                   AINC(L)=(180/PI)*AIN1
79             CONTINUE
      WRITE(*,'(/1X,A,I2)') 'Matrix Number',I
      WRITE(*,'(1X,A,I3)') 'Number of JACOBI rotations:',NROT
      WRITE(*,'(/1X,A)') 'Eigenvalues (MAX.,INTERMED.,MIN.):'
            DO 17 J=1,NUM(I)
                WRITE(*,'(1X,F11.5)') DM(J)
17          CONTINUE
      WRITE(*,'(/1X,A)') 'Eigenvectors : '
      WRITE(*,'(/1X,A)') 'Components (x,y,z) and directions:'
         DO 18 J=1,NUM(I)
           WRITE(*,'(1X,T5,A,I3)') 'Number',J
           WRITE(*,'(1X,5F11.5)') VM(J,1),VM(J,2),VM(J,3)
           WRITE(*,'(1X,T14,A,F7.2)') 'Declination: ',DEC(J)
           WRITE(*,'(1X,T14,A,F7.2)') 'Inclination: ',AINC(J)
18       CONTINUE
        WRITE(*,*)'Print the result ? (Y=1/N=2)'
        READ(*,*) Y
        IF(Y.EQ.2) GOTO 33
        WRITE(1,*) 'SPECIMEN :'
        WRITE(1,*) TEXT
        WRITE(1,'(/1X,A)') 'INPUT '
           DO 41 L=1,3
              WRITE(1,'(/1X,5F12.6)') A(L,1),A(L,2),A(L,3)
41         CONTINUE
      WRITE(1,'(/1X,A)') 'EIGENVALUES(MAX.,INTERMED., MIN.)'
      WRITE(1,'(/1X,5F12.6)') DM(1),DM(2),DM(3)
      WRITE(1,'(/1X,A)') 'EIGENVECTORS'
      WRITE(1,'(/1X,A)')
    * '      X          Y           Z            D         I'
```

```
          DO 40 J=1,3
      WRITE(1,'(1X,3F12.6,3F10.2)')
     *        VM(J,1),VM(J,2),VM(J,3),DEC(J),AINC(J)
40        CONTINUE
24     CONTINUE
33    WRITE(*,*) 'DO YOU WANT TO CONTINUE WITH THE NEXT
     * SPECIMEN ?'
      WRITE(*,*) '(Y=1/N=2)'
      READ(*,*) Y1
      IF (Y1.EQ.1) GOTO 61
      CLOSE(1)
      END
C
      SUBROUTINE JACOBI(A,N,NP,D,V,NROT)
      PARAMETER (NMAX=100)
      DIMENSION A(NP,NP),D(NP),V(NP,NP),B(NMAX),Z(NMAX)
       DO 32 IP=1,N
          DO 31 IQ=1,N
             V(IP,IQ)=0.
31        CONTINUE
       V(IP,IP)=1.
32     CONTINUE
       DO 33 IP=1,N
          B(IP)=A(IP,IP)
          D(IP)=B(IP)
          Z(IP)=0.
33     CONTINUE
       NROT=0.
       DO 44 I=1,50
          SM=0.0
          DO 35 IP=1,N-1
             DO 34 IQ=IP+1,N
                   SM=SM+ABS(A(IP,IQ))
34           CONTINUE
35        CONTINUE
           IF(SM.EQ.0.)RETURN
           IF(I.LT.4) THEN
                TRESH=0.2*SM/N**2
           ELSE
                TRESH=0.0
           ENDIF
             DO 42 IP=1,N-1
                DO 41 IQ=IP+1,N
                   G=100.*ABS(A(IP,IQ))
       IF((I.GT.4).AND.(ABS(D(IP))+G.EQ.ABS(D(IP)))
     *                  .AND.(ABS(D(IQ))+G.EQ.ABS(D(IQ))))THEN
                     A(IP,IQ)=0.
                   ELSE IF(ABS(A(IP,IQ)).GT.TRESH)THEN
                       H=D(IQ)-D(IP)
```

```
                         IF(ABS(H)+G.EQ.ABS(H))THEN
                            T=A(IP,IQ)/H
                          ELSE
                            THETA=0.5*H/A(IP,IQ)
                          T=1./(ABS(THETA)+SQRT(1.+THETA**2))
                            IF(THETA.LT.0.0)T=-T
                          ENDIF
                          C=1./SQRT(1+T**2)
                          S=T*C
                          TAU=S/(1.+C)
                          H=T*A(IP,IQ)
                          Z(IP)=Z(IP)-H
                          Z(IQ)=Z(IQ)+H
                          D(IP)=D(IP)-H
                          D(IQ)=D(IQ)+H
                          A(IP,IQ)=0.
                          DO 36 J=1,IP-1
                             G=A(J,IP)
                             H=A(J,IQ)
                             A(J,IP)=G-S*(H+G*TAU)
                             A(J,IQ)=H+S*(G-H*TAU)
36                        CONTINUE
                          DO 37 J=IP+1,IQ-1
                             G=A(IP,J)
                             H=A(J,IQ)
                             A(IP,J)=G-S*(H+G*TAU)
                             A(J,IQ)=H+S*(G-H*TAU)
37                        CONTINUE
                          DO 38 J=IQ+1,N
                             G=A(IP,J)
                             H=A(IQ,J)
                             A(IP,J)=G-S*(H+G*TAU)
                             A(IQ,J)=H+S*(G-H*TAU)
38                        CONTINUE
                          DO 39 J=1,N
                             G=V(J,IP)
                             H=V(J,IQ)
                             V(J,IP)=G-S*(H+G*TAU)
                             V(J,IQ)=H+S*(G-H*TAU)
39                        CONTINUE
                      NROT=NROT+1
               ENDIF
41                CONTINUE
42             CONTINUE
           DO 43 IP=1,N
               B(IP)=B(IP)+Z(IP)
               D(IP)=B(IP)
               Z(IP)=0.
43         CONTINUE
```

```
44      CONTINUE
        PAUSE '50 iterations should never happen'
        RETURN
        END
```

APPENDIX 4

DETAILED AAS DATA

The anisotropy of anhysteretis susceptibility (AAS) data for each specimen are listed as follows:

SITE :		SPECIMEN:		MULTI. :1.00e-07 $(A.m^2)$		
A_i	A_{ic}	Error	χ_{ij}	χ_i & P	D_i&I_i	D_{ia}&I_{ia}
A_1	A_{1c}	A_1-A_{1c}	χ_{11}	χ_1	D_1	D_{1a}
A_2	A_{2c}	A_2-A_{2c}	χ_{22}	χ_2	I_1	I_{1a}
A_3	A_{3c}	A_3-A_{3c}	χ_{33}	χ_3	D_2	D_{2a}
A_4	A_{4c}	A_4-A_{4c}	χ_{23}		I_2	I_{2a}
A_5	A_{5c}	A_5-A_{5c}	χ_{31}	P	D_3	D_{3a}
A_6	A_{6c}	A_6-A_{6c}	χ_{12}	L	I_3	I_{3a}
A_7	A_{7c}	A_7-A_{7c}		F		
A_8	A_{8c}	A_8-A_{8c}				
A_9	A_{9c}	A_9-A_{9c}				

A_i are the observed anhysteretic remanences/susceptibilities along each of the nine directions measured (Fig. 3.1). A_{ic} are the anhysteretic remanence/susceptibilities calculated from Eq. 3.4. "Error" is the discrepancy between each component of A_i and A_{ic}. χ_{ij} are the six AAS tensor components. χ_i & P are the magnitude of the maximum, intermediate and minimum anhysteretic susceptibilities followed by the degree of anisotropy (P), the magnetic lineation (L) and the magnetic foliation (F). D_i&I_i are the nominal declinations and the inclinations of the principal susceptibilities. D_{ia}&I_{ia} are the adjusted declinations and inclinations of the principal susceptibilitiess. "MULTI." is the multiplication factor of magnetic moment for all listed quantities except P, L, F, D_i, I_i, D_{ia}, and I_{ia}. In the above table, for example, A_1 = 1.021 means that the magnetic moment of the observed anhysteretic remanence is 1.021 x 1.00e-07 $A.m^2$.

SITE: 167 SPECIMEN: 62-4-64 MULTI. :1.00e-05 ($A.m^2$)

A_i	A_{ic}	Error	χ_{ij}	χ_i & P	D_i&I_i	D_{ia}&I_{ia}
1.037	1.029	0.008	1.029	1.032	7.6	13.1
1.032	1.023	0.008	1.023	1.025	-13.3	13.3
1.000	0.973	0.027	0.973	0.968	99.8	105.3
1.030	1.025	0.005	-0.011		-9.2	9.2
0.976	0.989	-0.013	-0.013	1.066	43.5	229.0
0.973	0.987	-0.014	-0.001	1.007	73.7	73.7
1.033	1.028	0.005		1.059		
1.001	1.014	-0.013				
0.995	1.009	-0.014				

SITE: 167 SPECIMEN: 63-4-75 MULTI. :1.00e-05 ($A.m^2$)

A_i	A_{ic}	Error	χ_{ij}	χ_i & P	D_i&I_i	D_{ia}&I_{ia}
1.266	1.260	0.006	1.260	1.261	349.1	9.2
1.258	1.241	0.017	1.241	1.240	3.2	3.2
1.147	1.113	0.034	1.113	1.113	79.1	99.2
1.251	1.246	0.005	0.002		0.8	0.8
1.184	1.195	-0.011	0.085	1.133	183.2	203.4
1.154	1.177	-0.023	-0.039	1.017	86.7	86.7
1.259	1.254	0.005		1.114		
1.167	1.178	-0.011				
1.154	1.177	-0.023				

SITE: 167 SPECIMEN: 65-3-42 MULTI. :1.00e-05 ($A.m^2$)

A_i	A_{ic}	Error	χ_{ij}	χ_i & P	D_i&I_i	D_{ia}&I_{ia}
1.357	1.352	0.005	1.352	1.353	18.5	156.5
1.360	1.341	-0.019	1.341	1.341	2.1	2.1
1.217	1.181	0.036	1.181	1.180	108.7	244.6
1.356	1.350	0.006	0.143		4.6	4.6
1.257	1.268	-0.011	0.019	1.147	264.1	42.0

SITE: 167 SPECIMEN: 65-3-42 (Cont'd)

1.250	1.275	-0.025	0.034	1.009	85.0	85.0
1.349	1.343	0.006		1.137		
1.254	1.265	-0.011				
1.222	1.247	-0.025				

SITE: 167 SPECIMEN: 67-3-36 MULTI. :1.00e-06 (A.m^2)

A_i	A_{ic}	Error	χ_{ij}	χ_i & P	D_i&I_i	D_{ia}&I_{ia}
5.599	5.591	0.008	5.591	5.602	20.5	7.4
5.562	5.529	0.033	5.529	5.522	0.6	0.6
5.110	4.991	0.119	4.991	4.986	110.5	277.3
5.627	5.588	0.039	-0.043		-5.2	5.2
5.268	5.314	-0.046	0.023	1.124	117.3	104.1
5.144	5.217	-0.073	0.028	1.014	84.8	84.8
5.571	5.532	0.039		1.108		
5.221	5.268	-0.047				
5.230	5.303	-0.073				

SITE: 167 SPECIMEN: 69-4-133 MULTI. :1.00e-06 (A.m^2)

A_i	A_{ic}	Error	χ_{ij}	χ_i & P	D_i&I_i	D_{ia}&I_{ia}
4.926	4.904	0.022	4.904	4.908	357.7	115.8
4.918	4.877	0.041	4.877	4.882	-11.7	11.7
4.907	4.790	0.117	4.790	4.781	85.4	23.6
4.920	4.893	0.027	0.019		10.7	10.7
4.774	4.823	-0.049	-0.024	1.027	314.1	252.2
4.785	4.853	-0.068	0.003	1.006	74.1	74.1
4.915	4.888	0.027		1.021		
4.821	4.871	-0.050				
4.747	4.814	-0.067				

SITE: 167 SPECIMEN: 71-2-63 MULTI. :1.00e-05 $(A.m^2)$

A_i	A_{ic}	Error	χ_{ij}	χ_i & P	D_i&I_i	D_{ia}&I_{ia}
1.428	1.424	0.004	1.424	1.424	5.9	271.6
1.428	1.416	0.012	1.416	1.417	-0.1	0.1
1.191	1.158	0.033	1.158	1.158	95.9	1.6
1.429	1.421	0.009	-0.015		-3.3	3.3
1.279	1.292	-0.013	0.001	1.230	93.5	179.2
1.253	1.273	-0.020	0.001	1.005	86.7	86.7
1.428	1.419	0.009		1.224		
1.278	1.290	-0.012				
1.282	1.302	-0.020				

SITE: 167 SPECIMEN: 72-2-63 MULTI. :1.00e-06 $(A.m^2)$

A_i	A_{ic}	Error	χ_{ij}	χ_i & P	D_i&I_i	D_{ia}&I_{ia}
4.297	4.288	0.009	4.288	4.346	353.7	169.0
4.319	4.272	0.047	4.272	4.280	-23.9	23.9
4.188	4.078	0.110	4.078	4.011	89.2	264.4
4.280	4.253	0.027	-0.042		-12.2	12.2
4.023	4.059	-0.036	-0.124	1.083	24.1	19.3
4.059	4.133	-0.074	-0.027	1.015	62.8	62.8
4.333	4.307	0.026		1.067		
4.271	4.307	-0.036				
4.143	4.217	-0.074				

SITE: 167 SPECIMEN: 73-2-121 MULTI. :1.00e-07 $(A.m^2)$

A_i	A_{ic}	Error	χ_{ij}	χ_i & P	D_i&I_i	D_{ia}&I_{ia}
6.961	6.956	0.005	6.956	6.974	329.2	162.3
6.974	6.922	0.052	6.922	6.905	-1.5	1.5
6.938	6.755	0.183	6.755	6.754	59.2	72.3
6.972	6.909	0.063	0.008		2.4	2.4
6.785	6.854	-0.069	-0.002	1.033	270.0	283.1

SITE: 167 SPECIMEN: 73-2-121 (Cont'd)

6.732	6.847	-0.115	-0.031	1.010	87.2	87.2
7.033	6.970	0.063		1.022		
6.788	6.857	-0.069				
6.716	6.830	-0.114				

SITE: 288A SPECIMEN:21-2-98 MULTI. :1.00e-06 ($A.m^2$)

A_i	A_{ic}	Error	χ_{ij}	χ_i & P	D_i&I_i	D_{ia}&I_{ia}
4.590	4.580	0.010	4.580	4.581	6.1	99.1
4.596	4.547	0.049	4.547	4.548	-0.8	0.8
4.393	4.260	0.133	4.260	4.258	96.2	189.1
4.604	4.567	0.037	-0.022		-4.2	4.2
4.371	4.418	-0.047	-0.002	1.076	84.9	357.9
4.296	4.382	-0.086	0.003	1.007	85.7	85.7
4.598	4.560	0.038		1.068		
4.375	4.422	-0.047				
4.339	4.425	-0.086				

SITE: 288A SPECIMEN: 21-3-18 MULTI. :1.00e-06 ($A.m^2$)

A_i	A_{ic}	Error	χ_{ij}	χ_i & P	D_i&I_i	D_{ia}&I_{ia}
5.696	5.669	0.027	5.669	5.672	8.2	12.4
5.673	5.619	0.054	5.619	5.624	-2.7	2.7
5.353	5.212	0.141	5.212	5.204	97.8	282.1
5.685	5.654	0.031	0.051		7.6	7.6
5.355	5.411	-0.056	-0.029	1.090	297.6	121.8
5.382	5.466	-0.084	0.010	1.009	82.0	82.0
5.664	5.634	0.030		1.081		
5.413	5.470	-0.057				
5.279	5.364	-0.085				

SITE: 288A SPECIMEN: 22-2-82 MULTI. :1.00e-06 $(A.m^2)$

A_i	A_{ic}	Error	χ_{ij}	χ_i & P	D_i&I_i	D_u&I_u
9.265	9.264	0.001	9.264	9.337	12.1	287.9
9.303	9.247	0.056	9.247	9.243	13.5	13.5
8.433	8.182	0.251	8.182	8.114	101.5	197.3
9.370	9.273	0.097	0.009		-2.6	2.6
8.906	9.004	-0.098	0.281	1.151	181.0	96.7
8.571	8.723	-0.152	0.017	1.010	76.3	76.3
9.336	9.239	0.097		1.139		
8.344	8.442	-0.098				
8.553	8.706	-0.153				

SITE: 288A SPECIMEN: 23-1-79 MULTI. :1.00e-06 $(A.m^2)$

A_i	A_{ic}	Error	χ_{ij}	χ_i & P	D_i&I_i	D_u&I_u
1.311	1.308	0.003	1.308	1.316	178.4	43.5
1.317	1.303	0.014	1.303	1.304	54.5	54.5
1.346	1.312	0.034	1.312	1.303	42.5	267.6
1.314	1.306	0.008	0.000		27.1	27.1
1.292	1.304	-0.012	-0.006	1.010	121.1	166.2
1.285	1.308	-0.023	0.000	1.010	-21.1	21.1
1.314	1.305	0.009		1.001		
1.305	1.316	-0.011				
1.284	1.307	-0.023				

SITE: 288A SPECIMEN: 23-2-115 MULTI. :1.00e-06 $(A.m^2)$

A_i	A_{ic}	Error	χ_{ij}	χ_i & P	D_i&I_i	D_u&I_u
4.243	4.250	-0.007	4.250	4.664	149.0	177.2
4.475	4.420	0.055	4.420	4.507	84.3	84.3
4.791	4.662	0.129	4.662	4.160	120.0	328.2
4.224	4.184	0.040	-0.000		-5.0	5.0
4.395	4.428	-0.033	-0.028	1.121	30.2	58.4

SITE: 288A SPECIMEN: 23-2-115 (Cont'd)

4.445	4.541	-0.096	-0.151	1.035	2.8	2.8
4.526	4.486	0.040		1.083		
4.451	4.484	-0.033				
4.446	4.541	-0.095				

SITE: 288A SPECIMEN: 23-3-76 MULTI. :1.00e-06 (A.m^2)

A_i	A_k	Error	χ_{ij}	χ_i & P	D_i&I_i	D_{ia}&I_{ia}
6.685	6.655	0.030	6.655	6.667	128.2	329.0
6.706	6.661	0.045	6.661	6.652	0.9	0.9
6.274	6.123	0.151	6.123	6.119	38.3	59.0
6.687	6.649	0.038	-0.019		-4.4	4.4
6.284	6.352	-0.068	-0.037	1.090	27.1	227.8
6.289	6.373	-0.084	-0.009	1.002	85.6	85.6
6.705	6.667	0.038		1.087		
6.358	6.426	-0.068				
6.326	6.410	-0.084				

SITE: 288A SPECIMEN: 26-1-28 MULTI. :1.00e-06 (A.m^2)

A_i	A_k	Error	χ_{ij}	χ_i & P	D_i&I_i	D_{ia}&I_{ia}
4.389	4.400	-0.011	4.400	4.445	326.3	295.5
4.286	4.352	-0.066	4.352	4.312	-6.1	6.1
4.021	3.998	0.023	3.998	3.992	56.4	25.6
4.366	4.316	0.050	0.022		-1.1	1.1
4.116	4.155	-0.039	-0.044	1.113	336.6	125.7
4.212	4.196	0.016	-0.060	1.031	83.8	83.8
4.485	4.435	0.050		1.080		
4.203	4.242	-0.039				
4.169	4.153	0.016				

SITE: 288A SPECIMEN: 29-1-47 MULTI. :1.00e-06 ($A.m^2$)

A_i	A_{ic}	Error	χ_{ij}	χ_i & P	D_i&I_i	D_{is}&I_{is}
5.356	5.345	0.011	5.345	5.349	348.3	58.8
5.314	5.282	0.032	5.282	5.287	-4.7	4.7
5.037	4.908	0.129	4.908	4.899	77.7	328.2
5.347	5.304	0.043	0.055		7.3	7.3
5.049	5.101	-0.052	-0.026	1.092	290.7	181.2
5.075	5.150	-0.075	-0.010	1.012	81.3	81.3
5.366	5.323	0.043		1.079		
5.100	5.152	-0.052				
4.964	5.040	-0.076				

SITE: 315A SPECIMEN: 19-5-50 MULTI. :1.00e-06 ($A.m^2$)

A_i	A_{ic}	Error	χ_{ij}	χ_i & P	D_i&I_i	D_{is}&I_{is}
9.106	9.052	0.054	9.052	9.102	47.5	202.5
9.138	9.061	0.077	9.061	9.014	2.0	2.0
7.618	7.451	0.167	7.451	7.449	317.5	112.5
9.118	9.100	0.018	0.024		1.0	1.0
8.240	8.312	-0.072	0.060	1.222	200.6	355.7
8.186	8.280	-0.094	0.043	1.010	87.7	87.7
9.032	9.014	0.018		1.210		
8.120	8.192	-0.072				
8.138	8.232	-0.094				

SITE: 315A SPECIMEN: 20-2-21 MULTI. :1.00e-05 ($A.m^2$)

A_i	A_{ic}	Error	χ_{ij}	χ_i & P	D_i&I_i	D_{is}&I_{is}
1.305	1.305	0.000	1.305	1.305	358.8	17.9
1.308	1.301	0.007	1.301	1.302	1.1	1.1
1.113	1.086	0.027	1.086	1.085	88.8	287.8
1.312	1.303	0.009	-0.014		-3.6	3.6
1.190	1.200	-0.010	-0.004	1.202	105.8	124.8

SITE: 315A SPECIMEN: 20-2-21 (Cont'd)

1.164	1.180	-0.016	0.000	1.002	86.2	86.2
1.312	1.303	0.009		1.199		
1.182	1.192	-0.010				
1.191	1.208	-0.017				

SITE: 315A SPECIMEN: 20-2-131 MULTI. :1.00e-05 ($A.m^2$)

A_i	A_{ic}	Error	χ_{ij}	χ_i & P	D_i&I_i	D_{ia}&I_{ia}
1.318	1.316	0.002	1.316	1.321	337.0	50.8
1.312	1.308	0.004	1.308	1.306	-6.8	6.8
1.140	1.114	0.026	1.114	1.111	67.0	320.8
1.318	1.308	0.010	0.010		0.2	0.2
1.180	1.192	-0.012	-0.023	1.189	335.1	229.0
1.207	1.221	-0.014	-0.004	1.011	83.2	83.2
1.327	1.316	0.011		1.176		
1.225	1.237	-0.012				
1.186	1.200	-0.014				

SITE: 315A SPECIMEN: 20-5-17 MULTI. :1.00e-06 ($A.m^2$)

A_i	A_{ic}	Error	χ_{ij}	χ_i & P	D_i&I_i	D_{ia}&I_{ia}
4.720	4.700	0.020	4.700	4.705	11.8	40.0
4.697	4.663	0.034	4.663	4.662	4.2	4.2
4.219	4.113	0.106	4.113	4.110	101.8	310.0
4.716	4.690	0.026	0.007		-0.2	0.2
4.403	4.449	-0.046	0.043	1.145	189.5	217.8
4.335	4.395	-0.060	0.008	1.009	85.8	85.8
4.700	4.674	0.026		1.134		
4.318	4.364	-0.046				
4.321	4.381	-0.060				

SITE: 315A SPECIMEN: 21-2-11 MULTI. :1.00e-06 ($A.m^2$)

A_i	A_{ic}	Error	χ_{ij}	χ_i & P	D_i&I_i	D_u&I_u
7.956	8.021	-0.065	8.021	8.031	342.7	270.7
7.971	7.951	0.020	7.951	8.004	-0.6	0.6
6.130	6.003	0.127	6.003	5.939	72.8	0.8
8.043	7.957	0.086	-0.334		-10.1	10.1
6.865	6.886	-0.021	-0.126	1.352	69.4	177.4
6.537	6.643	-0.106	-0.029	1.003	79.9	79.9
8.100	8.014	0.086		1.348		
7.117	7.138	-0.021				
7.205	7.311	-0.106				

SITE: 315A SPECIMEN: 21-5-8 MULTI. :1.00e-06 ($A.m^2$)

A_i	A_{ic}	Error	χ_{ij}	χ_i & P	D_i&I_i	D_u&I_u
4.950	4.949	0.001	4.949	4.949	358.9	261.3
4.910	4.892	0.018	4.892	4.899	1.5	1.5
4.145	4.057	0.088	4.057	4.049	89.0	351.4
4.951	4.917	0.034	0.081		5.5	5.5
4.494	4.529	-0.035	0.026	1.222	253.3	155.7
4.503	4.555	-0.052	-0.003	1.010	84.3	84.3
4.957	4.924	0.033		1.210		
4.443	4.477	-0.034				
4.341	4.394	-0.053				

SITE: 315A SPECIMEN: 21-6-108 MULTI. :1.00e-06 ($A.m^2$)

A_i	A_{ic}	Error	χ_{ij}	χ_i & P	D_i&I_i	D_u&I_u
1.609	1.609	0.000	1.609	1.610	347.8	38.3
1.593	1.582	0.011	1.582	1.581	-0.5	0.5
1.458	1.433	0.025	1.433	1.432	77.8	128.3
1.597	1.589	0.008	-0.010		-3.9	3.9
1.510	1.517	-0.007	-0.004	1.125	70.6	301.2

SITE: 315A SPECIMEN: 21-6-108 (Cont'd)

1.479	1.498	-0.018	-0.006	1.018	86.1	86.1
1.609	1.602	0.007		1.104		
1.517	1.524	-0.007				
1.499	1.517	-0.018				

SITE: 315A SPECIMEN: 26-2-123 MULTI. :1.00e-06 $(A.m^2)$

A_i	A_{ic}	Error	χ_{ij}	χ_i & P	D_i&I_i	D_{ia}&I_{ia}
4.777	4.781	-0.004	4.781	4.791	331.1	84.5
4.760	4.760	0.000	4.760	4.752	-2.0	2.0
4.130	4.047	0.083	4.047	4.046	61.0	354.5
4.799	4.755	0.044	0.021		0.8	0.8
4.356	4.396	-0.040	-0.018	1.184	308.8	242.3
4.382	4.425	-0.043	-0.016	1.008	87.8	87.8
4.831	4.787	0.044		1.175		
4.392	4.432	-0.040				
4.339	4.382	-0.043				

SITE: 316 SPECIMEN: 19-2-108 MULTI. :1.00e-06 $(A.m^2)$

A_i	A_{ic}	Error	χ_{ij}	χ_i & P	D_i&I_i	D_{ia}&I_{ia}
7.472	7.467	0.005	7.467	7.470	352.0	202.2
7.365	7.356	0.009	7.356	7.356	-1.0	1.0
6.203	6.046	0.157	6.046	6.044	82.1	292.2
7.466	7.395	0.071	-0.046		-2.2	2.2
6.648	6.724	-0.076	-0.032	1.236	57.0	87.1
6.575	6.655	-0.080	-0.017	1.016	87.6	87.6
7.500	7.428	0.072		1.217		
6.712	6.789	-0.077				
6.667	6.747	-0.080				

SITE: 316 SPECIMEN: 19-4-74 MULTI. :1.00e-06 $(A.m^2)$

A_i	A_{ic}	Error	χ_{ij}	χ_i & P	D_i&I_i	D_{is}&I_{is}
3.451	3.538	-0.087	3.538	3.548	340.8	201.5
3.447	3.505	-0.058	3.505	3.501	-4.5	4.5
2.685	2.696	-0.011	2.696	2.690	70.8	111.5
3.576	3.509	0.067	0.025		0.2	0.2
3.074	3.054	0.020	-0.063	1.319	337.9	18.6
3.116	3.126	-0.010	-0.013	1.014	85.5	85.5
3.602	3.535	0.067		1.301		
3.199	3.180	0.019				
3.066	3.075	-0.009				

SITE: 316 SPECIMEN: 20-4-67 MULTI. :1.00e-06 $(A.m^2)$

A_i	A_{ic}	Error	χ_{ij}	χ_i & P	D_i&I_i	D_{is}&I_{is}
4.046	4.038	0.008	4.038	4.045	318.0	337.5
4.064	4.032	0.032	4.032	4.029	3.2	3.2
3.814	3.706	0.108	3.706	3.702	47.7	247.2
4.060	4.026	0.034	-0.037		-5.8	5.8
3.822	3.864	-0.042	-0.008	1.093	76.4	95.9
3.767	3.832	-0.065	-0.009	1.004	83.4	83.4
4.078	4.044	0.034		1.088		
3.838	3.880	-0.042				
3.841	3.906	-0.065				

SITE: 316 SPECIMEN: 22-2-77 MULTI. :1.00e-06 $(A.m^2)$

A_i	A_{ic}	Error	χ_{ij}	χ_i & P	D_i&I_i	D_{is}&I_{is}
3.845	3.843	0.002	3.843	3.844	5.9	243.4
3.831	3.799	0.032	3.799	3.799	-0.5	0.5
3.209	3.121	0.088	3.121	3.120	95.9	153.4
3.854	3.826	0.028	0.023		2.0	2.0
3.444	3.473	-0.029	-0.009	1.232	291.1	348.6

SITE: 316 SPECIMEN: 22-2-77 (Cont'd)

3.424	3.483	-0.059	0.005	1.012	87.9	87.9
3.844	3.816	0.028		1.218		
3.462	3.491	-0.029				
3.378	3.437	-0.059				

SITE: 316 SPECIMEN: 23-3-107 MULTI. :1.00e-06 (A.m^2)

A_i	A_{ic}	Error	χ_{ij}	χ_i & P	D_i&I_i	D_{ia}&I_{ia}
8.344	8.360	-0.016	8.360	8.377	345.2	22.5
8.201	8.167	0.034	8.167	8.153	1.9	1.9
6.271	6.157	0.114	6.157	6.154	75.3	112.5
8.256	8.208	0.048	0.016		1.0	1.0
7.305	7.338	-0.033	0.079	1.361	193.7	230.9
7.096	7.178	-0.082	-0.055	1.027	87.9	87.9
8.368	8.319	0.049		1.325		
7.147	7.179	-0.032				
7.065	7.146	-0.081				

SITE: 316 SPECIMEN: 24-3-59 MULTI. :1.00e-06 (A.m^2)

A_i	A_{ic}	Error	χ_{ij}	χ_i & P	D_i&I_i	D_{ia}&I_{ia}
5.391	5.391	0.000	5.391	5.401	330.5	232.6
5.404	5.378	0.026	5.378	5.370	2.6	2.6
4.555	4.456	0.099	4.456	4.453	60.6	322.7
5.407	5.371	0.036	0.005		1.9	1.9
4.938	4.975	-0.037	0.052	1.213	186.0	88.1
4.859	4.921	-0.062	-0.013	1.006	86.8	86.8
5.434	5.398	0.036		1.206		
4.834	4.871	-0.037				
4.850	4.912	0.062				

SITE: 316 SPECIMEN: 25-5-40 MULTI. :1.00e-06 ($A.m^2$)

A_i	A_{ic}	Error	χ_{ij}	χ_i & P	D_i&I_i	D_{ii}&I_{ii}
6.713	6.692	0.021	6.692	6.706	132.7	227.1
6.727	6.695	0.032	6.695	6.685	-3.2	3.2
5.586	5.456	0.130	5.456	5.452	42.8	317.2
6.723	6.685	0.038	-0.040		0.8	0.8
6.074	6.133	-0.059	0.060	1.230	146.4	60.8
5.965	6.036	-0.071	-0.009	1.003	86.7	86.7
6.741	6.702	0.039		1.226		
5.955	6.015	-0.060				
6.045	6.115	-0.070				

SITE: 462 SPECIMEN: 55-1-28 MULTI. :1.00e-06 ($A.m^2$)

A_i	A_{ic}	Error	χ_{ij}	χ_i & P	D_i&I_i	D_{ii}&I_{ii}
4.187	4.190	-0.003	4.190	4.195	343.8	253.8
4.169	4.138	0.031	4.138	4.133	2.0	2.0
3.881	3.790	0.091	3.790	3.789	73.7	163.8
4.178	4.147	0.031	-0.010		-1.0	1.0
3.974	4.002	-0.028	0.012	1.107	137.0	47.1
3.892	3.954	-0.062	-0.016	1.015	87.8	87.8
4.211	4.180	0.031		1.091		
3.950	3.978	-0.028				
3.911	3.973	-0.062				

SITE: 462 SPECIMEN: 55-1-114 MULTI. :1.00e-06 ($A.m^2$)

A_i	A_{ic}	Error	χ_{ij}	χ_i & P	D_i&I_i	D_{ii}&I_{ii}
1.113	1.104	0.009	1.104	1.106	331.7	343.9
1.105	1.096	0.009	1.096	1.099	-8.5	8.5
1.059	1.028	0.031	1.028	1.023	59.9	252.1
1.104	1.098	0.006	0.019		11.6	11.6
1.048	1.063	-0.015	-0.003	1.081	277.3	109.5

SITE: 462 SPECIMEN: 55-1-114 (Cont'd)

1.065	1.081	-0.016	-0.003	1.007	75.6	75.6
1.109	1.103	0.006		1.074		
1.054	1.070	-0.016				
1.028	1.043	-0.015				

SITE: 462 SPECIMEN: 55-2-128 MULTI. :1.00e-06 $(A.m^2)$

A_i	A_{ic}	Error	χ_{ij}	χ_i & P	D_i&I_i	D_{ia}&I_{ia}
4.859	4.853	0.006	4.853	4.856	9.3	345.2
4.838	4.805	0.033	4.805	4.804	4.5	4.5
4.652	4.542	0.110	4.452	4.540	99.3	255.2
4.873	4.837	0.036	0.004		-0.0	0.0
4.680	4.721	-0.041	0.024	1.070	189.0	164.8
4.609	4.677	-0.068	0.008	1.011	85.5	85.5
4.857	4.821	0.036		1.058		
4.631	4.673	-0.042				
4.601	4.670	-0.069				

SITE: 462 SPECIMEN: 55-3-29 MULTI. :1.00e-05 $(A.m^2)$

A_i	A_{ic}	Error	χ_{ij}	χ_i & P	D_i&I_i	D_{ia}&I_{ia}
2.402	2.406	-0.004	2.406	2.408	354.8	142.3
2.386	2.367	0.019	2.367	2.367	2.8	2.8
1.947	1.901	0.046	1.901	1.900	84.8	52.3
2.399	2.383	0.016	-0.004		-0.2	0.2
2.167	2.178	-0.011	0.025	1.267	170.0	317.5
2.096	2.130	-0.034	-0.004	1.017	87.2	87.2
2.406	2.390	0.016		1.246		
2.117	2.129	-0.012				
2.104	2.138	-0.034				

SITE: 462 SPECIMEN: 55-3-132 MULTI. :1.00e-05 (A.m^2)

A_i	A_{ic}	Error	χ_{ij}	χ_i & P	D_i&I_i	D_m&I_m
1.471	1.471	0.000	1.471	1.473	358.2	87.8
1.469	1.457	0.012	1.457	1.457	4.8	4.8
1.218	1.189	0.029	1.189	1.187	88.3	177.9
1.471	1.463	0.008	0.007		1.6	1.6
1.345	1.354	-0.009	0.024	1.241	196.3	285.9
1.309	1.329	-0.020	-0.001	1.011	85.0	85.0
1.473	1.465	0.008		1.227		
1.298	1.306	-0.008				
1.296	1.316	-0.020				

SITE: 463 SPECIMEN: 58-1-31 MULTI. :1.00e-07 (A.m^2)

A_i	A_{ic}	Error	χ_{ij}	χ_i & P	D_i&I_i	D_m&I_m
2.498	2.495	0.003	2.495	2.530	160.6	101.0
2.529	2.484	0.045	2.484	2.497	85.4	85.4
2.625	2.530	0.095	2.530	2.482	337.2	277.7
2.508	2.484	0.024	0.001		4.6	4.6
2.482	2.510	-0.028	-0.003	1.019	67.2	7.7
2.439	2.508	-0.069	-0.005	1.013	0.3	0.3
2.519	2.495	0.024		1.006		
2.487	2.515	-0.028				
2.438	2.506	-0.068				

SITE: 463 SPECIMEN: 58-2-82 MULTI. :1.00e-07 (A.m^2)

A_i	A_{ic}	Error	χ_{ij}	χ_i & P	D_i&I_i	D_m&I_m
2.459	2.441	0.018	2.441	2.492	85.2	48.0
2.521	2.491	0.030	2.491	2.458	3.0	3.0
2.493	2.433	0.060	2.433	2.415	352.7	315.5
2.476	2.469	0.007	0.001		39.6	39.6
2.434	2.458	-0.024	0.021	1.032	178.7	141.6

SITE: 463 SPECIMEN: 58-2-82 (Cont'd)

2.428	2.463	-0.035	0.003	1.014	50.3	50.3
2.469	2.463	0.006		1.018		
2.391	2.415	-0.024				
2.425	2.461	-0.036				

SITE: 463 SPECIMEN: 59-2-104 MULTI. :1.00e-07 (A.m^2)

A_i	A_{ic}	Error	χ_{ij}	χ_i & P	D_i&I_i	D_{ia}&I_{ia}
3.180	3.193	-0.013	3.193	3.209	9.1	139.9
3.184	3.162	0.022	3.162	3.162	25.5	25.5
3.226	3.143	0.083	3.143	3.126	93.5	44.3
3.224	3.186	0.038	-0.002		-11.7	11.7
3.176	3.200	-0.024	0.032	1.027	161.0	291.7
3.092	3.151	-0.059	0.009	1.015	61.7	61.7
3.206	3.169	0.037		1.011		
3.111	3.136	-0.025				
3.096	3.155	-0.059				

SITE: 463 SPECIMEN: 60-2-33 MULTI. :1.00e-07 (A.m^2)

A_i	A_{ic}	Error	χ_{ij}	χ_i & P	D_i&I_i	D_{ia}&I_{ia}
4.048	4.048	0.000	4.048	4.102	136.6	108.1
4.082	4.040	0.042	4.040	4.051	68.7	68.7
4.204	4.092	0.112	4.092	4.027	36.7	8.2
4.085	4.050	0.035	0.018		3.8	3.8
4.017	4.053	-0.036	-0.017	1.019	125.2	276.7
4.008	4.084	-0.076	0.006	1.013	-21.0	21.0
4.072	4.037	0.035		1.006		
4.052	4.087	-0.035				
3.971	4.048	-0.077				

SITE: 463 SPECIMEN: 61-1-105 MULTI. :1.00e-06 $(A.m^2)$

A_i	A_{ic}	Error	χ_{ij}	χ_i & P	D_i&I_i	D_u&I_u
1.205	1.202	0.003	1.202	1.206	23.8	120.0
1.202	1.193	0.009	1.193	1.190	4.0	4.0
1.105	1.080	0.025	1.080	1.079	113.7	29.8
1.210	1.203	0.007	-0.000		-2.2	2.2
1.141	1.151	-0.010	0.010	1.118	175.5	91.6
1.119	1.136	-0.017	0.006	1.013	85.5	85.5
1.199	1.192	0.007		1.103		
1.122	1.131	-0.009				
1.120	1.136	-0.016				

SITE: 463 SPECIMEN: 64-1-60 MULTI. :1.00e-07 $(A.m^2)$

A_i	A_{ic}	Error	χ_{ij}	χ_i & P	D_i&I_i	D_u&I_u
3.234	3.234	0.000	3.234	3.285	140.4	221.8
3.251	3.215	0.036	3.215	3.234	85.0	85.0
3.372	3.285	0.087	3.285	3.215	1.0	82.3
3.251	3.225	0.026	0.004		3.8	3.8
3.230	3.256	-0.026	-0.003	1.022	90.8	352.1
3.193	3.254	-0.061	0.000	1.016	-3.2	3.2
3.251	3.225	0.026		1.006		
3.237	3.263	-0.026				
3.185	3.246	-0.061				

SITE: 463 SPECIMEN: 67-2-103 MULTI. :1.00e-08 $(A.m^2)$

A_i	A_{ic}	Error	χ_{ij}	χ_i & P	D_i&I_i	D_u&I_u
9.435	9.375	0.060	9.375	9.586	309.3	160.8
9.568	9.463	0.105	9.463	9.463	79.2	79.2
9.884	9.580	0.304	9.580	9.370	80.3	291.8
9.501	9.431	0.070	-0.020		7.2	7.2
9.375	9.505	-0.130	0.027	1.023	351.3	22.8

SITE: 463 SPECIMEN: 67-2-103 (Cont'd)

9.327	9.502	-0.175	0.012	1.013	-8.1	8.1
9.478	9.408	0.070		1.010		
9.321	9.450	-0.129				
9.366	9.541	-0.175				

APPENDIX 5

DETAILED AMS DATA

The aniostropy of magnetic susceptibility (AMS) data of each specimen are listed as follows:

SITE: SPECIMEN:

K_1, K_2, K_3	A_v	RMS (%)	P, L, F	D_i, I_i	D_{ia}, I_{ia}
K_1	A_v	RMS (%)	P	D_1	D_{1a}
K_2			L	I_1	I_{1a}
K_3			F	D_2	D_{2a}
				I_2	I_{2a}
				D_3	D_{3a}
				I_3	I_{3a}

K_1, K_2, K_3 are the magnitude of the maximum, intermediate and minimum magnetic susceptibilities expressed in SI units. A_v is the average susceptibility (= $(K_1 + K_2 + K_3)/3$). RMS (%) is the root- mean square error in per cent (see Section 5.4). P is the degree of anisotropy. L is the magnetic lineation. F is the magnetic foliation. D_i, I_i are the nominal declinations and the inclinations of the principal susceptibilities. D_{ia}, I_{ia} are the adjusted declination and inclination of the principal susceptibilities.

SITE: 167 SPECIMEN: 62-4-64

K_1, K_2, K_3	A_v	RMS(%)	P, L, F	D_i, I_i	D_{is}, I_{is}
1.750e-03	1.709e-03	0.86	1.050	94.3	279.8
1.710e-03			1.023	9.1	9.1
1.667e-03			1.026	278.4	103.9
				80.9	80.9
				184.4	9.9
				0.6	0.6

SITE: 167 SPECIMEN: 63-4-75

K_1, K_2, K_3	A_v	RMS(%)	P, L, F	D_i, I_i	D_{is}, I_{is}
2.665e-03	2.614e-03	0.65	1.032	88.8	108.9
2.595e-03			1.027	14.4	14.4
2.582e-03			1.005	349.2	9.3
				32.8	32.8
				199.0	219.1
				53.4	53.4

SITE: 167 SPECIMEN: 65-3-42

K_1, K_2, K_3	A_v	RMS(%)	P, L, F	D_i, I_i	D_{is}, I_{is}
2.093e-03	2.048e-03	0.81	1.044	246.6	24.5
2.047e-03			1.022	19.8	19.8
2.005e-03			1.021	155.9	293.8
				2.1	2.1
				60.1	198.0
				70.1	70.1

SITE: 167 SPECIMEN: 67-3-36

K_1, K_2, K_3	A_v	RMS(%)	P, L, F	D_i, I_i	D_{is}, I_{is}
8.006e-04	7.665e-04	4.72	1.089	276.7	263.5
7.636e-04			1.049	1.9	1.9
7.355e-04			1.038	9.8	356.6
				58.9	58.9
				185.5	172.3
				31.0	31.0

SITE: 167 SPECIMEN: 69-4-133

K_1, K_2, K_3	A_v	RMS(%)	P, L, F	D_i, I_i	D_{is}, I_{is}
5.514e-04	5.404e-04	2.25	1.042	200.1	138.3
5.403e-04			1.020	52.0	52.0
5.293e-04			1.021	45.0	343.2
				35.3	35.3
				306.2	244.4
				12.2	12.2

SITE: 167 SPECIMEN: 71-2-63

K_1, K_2, K_3	A_v	RMS(%)	P, L, F	D_i, I_i	D_{is}, I_{is}
1.474e-03	1.433e-03	3.34	1.051	243.4	329.1
1.421e-03			1.038	16.6	16.6
1.403e-03			1.013	351.7	77.4
				46.4	46.4
				139.5	225.2
				38.9	38.9

SITE: 167 SPECIMEN: 72-2-63

K_1, K_2, K_3	A_v	RMS(%)	P, L, F	D_i, I_i	D_{ia}, I_{ia}
4.961e-04	4.775e-04	7.03	1.108	2.1	357.3
4.887e-04			1.015	15.1	15.1
4.478e-04			1.091	252.9	248.1
				50.5	50.5
				103.1	98.3
				35.4	35.4

SITE: 167 SPECIMEN: 73-2-121

K_1, K_2, K_3	A_v	RMS(%)	P, L, F	D_i, I_i	D_{ia}, I_{ia}
2.333e-04	2.011e-04	14.41	1.462	59.1	72.2
2.104e-04			1.109	17.8	17.8
1.595e-04			1.319	198.3	211.4
				67.0	67.0
				324.5	337.6
				14.1	14.1

SITE: 288A SPECIMEN: 21-2-98

K_1, K_2, K_3	A_v	RMS(%)	P, L, F	D_i, I_i	D_{ia}, I_{ia}
7.627e-04	7.414e-04	1.87	1.052	346.1	259.1
7.364e-04			1.036	21.1	21.1
7.252e-04			1.015	82.6	355.6
				16.4	16.4
				207.5	120.5
				62.8	62.8

SITE: 288A SPECIMEN: 21-3-18

K_1, K_2, K_3	A_v	RMS(%)	P, L, F	D_i, I_i	D_u, I_u
9.940e-04	9.173e-04	6.93	1.256	96.7	281.0
9.665e-04			1.028	36.5	36.5
7.915e-04			1.221	273.4	97.7
				53.5	53.5
				5.5	189.8
				1.6	1.6

SITE: 288A SPECIMEN: 22-2-82

K_1, K_2, K_3	A_v	RMS(%)	P, L, F	D_i, I_i	D_u, I_u
1.766e-03	1.684e-03	2.15	1.089	339.6	255.4
1.665e-03			1.061	18.7	18.7
1.621e-03			1.027	73.9	349.7
				12.7	12.7
				196.2	112.0
				67.1	67.1

SITE: 288A SPECIMEN: 23-1-79

K_1, K_2, K_3	A_v	RMS(%)	P, L, F	D_i, I_i	D_u, I_u
1.863e-04	1.634e-04	4.38	1.303	280.4	145.5
1.608e-04			1.159	64.3	64.3
1.430e-04			1.124	53.7	278.8
				18.3	18.3
				149.6	14.7
				17.5	17.5

SITE: 288A SPECIMEN: 23-2-115

K_1, K_2, K_3	A_v	RMS(%)	P, L, F	D_i, I_i	D_{ia}, I_{ia}
6.642e-04	6.158e-04	5.03	1.142	326.5	354.7
6.013e-04			1.105	4.7	4.7
5.817e-04			1.034	80.9	109.1
				78.7	78.7
				235.6	263.8
				10.3	10.3

SITE: 288A SPECIMEN: 23-3-76

K_1, K_2, K_3	A_v	RMS(%)	P, L, F	D_i, I_i	D_{ia}, I_{ia}
1.094e-03	1.068e-03	2.25	1.045	243.0	83.8
1.064e-03			1.028	18.4	18.4
1.047e-03			1.017	134.3	335.1
				43.9	43.9
				349.4	190.2
				40.3	40.3

SITE: 288A SPECIMEN: 26-1-28

K_1, K_2, K_3	A_v	RMS(%)	P, L, F	D_i, I_i	D_{ia}, I_{ia}
2.432e-03	2.400e-03	0.60	1.030	303.1	92.3
2.407e-03			1.011	20.3	20.3
2.362e-03			1.019	205.8	355.0
				19.0	19.0
				76.2	225.4
				61.6	61.6

SITE: 288A SPECIMEN: 29-1-47

K_1, K_2, K_3	A_v	RMS(%)	P, L, F	D_i, I_i	D_{ta}, I_{ta}
1.528e-03	1.483e-03	2.64	1.059	97.3	347.8
1.478e-03			1.034	13.1	13.1
1.443e-03			1.024	6.4	256.9
				3.9	3.9
				260.0	150.5
				76.3	76.3

SITE: 315A SPECIMEN: 19-5-50

K_1, K_2, K_3	A_v	RMS(%)	P, L, F	D_i, I_i	D_{ta}, I_{ta}
4.440e-03	4.260e-03	0.38	1.113	179.6	334.7
4.351e-03			1.020	0.8	0.8
3.989e-03			1.091	89.5	244.6
				7.0	7.0
				276.4	71.4
				82.9	82.9

SITE: 315A SPECIMEN: 20-2-21

K_1, K_2, K_3	A_v	RMS(%)	P, L, F	D_i, I_i	D_{ta}, I_{ta}
7.551e-03	7.364e-03	1.05	1.073	180.6	199.7
7.507e-03			1.006	1.4	1.4
7.034e-03			1.067	270.6	289.7
				2.3	2.3
				58.6	77.7
				87.3	87.3

SITE: 315A SPECIMEN: 20-2-131

K_1, K_2, K_3	A_v	RMS(%)	P, L, F	D_i, I_i	D_{is}, I_{is}
1.155e-02	1.128e-02	0.23	1.069	287.0	180.9
1.149e-02			1.006	0.2	0.2
1.081e-02			1.063	17.0	270.9
				2.7	2.7
				191.8	85.7
				87.3	87.3

SITE: 315A SPECIMEN: 20-5-17

K_1, K_2, K_3	A_v	RMS(%)	P, L, F	D_i, I_i	D_{is}, I_{is}
2.913e-03	2.840e-03	0.78	1.075	295.0	323.2
2.899e-03			1.005	5.7	5.7
2.709e-03			1.070	204.5	232.7
				5.0	5.0
				73.9	102.1
				82.4	82.4

SITE: 315A SPECIMEN: 21-2-11

K_1, K_2, K_3	A_v	RMS(%)	P, L, F	D_i, I_i	D_{is}, I_{is}
5.321e-03	5.202e-03	0.61	1.063	17.5	125.5
5.281e-03			1.008	3.7	3.7
5.005e-03			1.055	287.3	35.3
				4.1	4.1
				149.5	257.5
				84.5	84.5

SITE: 315A SPECIMEN: 21-5-8

K_1, K_2, K_3	A_v	RMS(%)	P, L, F	D_i, I_i	D_u, I_u
2.507e-03	2.438e-03	0.18	1.083	327.9	230.3
2.493e-03			1.006	1.0	1.0
2.314e-03			1.077	237.9	140.3
				1.7	1.7
				88.2	350.6
				88.0	88.0

SITE: 315A SPECIMEN: 21-6-108

K_1, K_2, K_3	A_v	RMS(%)	P, L, F	D_i, I_i	D_u, I_u
1.698e-03	1.646e-03	1.29	1.083	322.3	192.8
1.672e-03			1.016	2.2	2.2
1.568e-03			1.066	52.4	282.9
				2.1	2.1
				186.2	56.7
				86.9	86.9

SITE: 315A SPECIMEN: 26-2-123

K_1, K_2, K_3	A_v	RMS(%)	P, L, F	D_i, I_i	D_u, I_u
3.069e-03	3.003e-03	0.34	1.050	82.7	16.2
3.018e-03			1.017	2.8	2.8
2.923e-03			1.032	352.5	286.0
				3.3	3.3
				212.5	146.0
				85.7	85.7

SITE: 316 SPECIMEN: 19-2-108

K_1, K_2, K_3	A_v	RMS(%)	P, L, F	D_i, I_i	D_{is}, I_{is}
1.798e-03	1.747e-03	0.66	1.077	309.2	339.4
1.773e-03			1.014	9.1	9.1
1.670e-03			1.061	217.7	247.9
				9.0	9.0
				83.7	113.9
				77.2	77.2

SITE: 316 SPECIMEN: 19-4-74

K_1, K_2, K_3	A_v	RMS(%)	P, L, F	D_i, I_i	D_{is}, I_{is}
1.793e-03	1.759e-03	0.80	1.043	87.8	128.4
1.766e-03			1.015	10.2	10.2
1.719e-03			1.028	356.4	37.1
				7.0	7.0
				232.5	273.2
				77.6	77.6

SITE: 316 SPECIMEN: 20-4-67

K_1, K_2, K_3	A_v	RMS(%)	P, L, F	D_i, I_i	D_{is}, I_{is}
7.939e-04	7.665e-04	2.85	1.077	360.0	19.5
7.686e-04			1.033	0.0	0.0
7.371e-04			1.043	90.0	1109.5
				26.0	26.6
				270.0	289.5
				63.4	63.4

SITE: 316 SPECIMEN: 22-2-77

K_1, K_2, K_3	A_v	RMS(%)	P, L, F	D_i, I_i	D_w, I_w
1.713e-03	1.646e-03	1.08	1.080	264.3	321.8
1.640e-03			1.045	9.0	9.0
1.586e-03			1.034	173.5	231.0
				4.7	4.7
				56.1	113.6
				79.9	79.9

SITE: 316 SPECIMEN: 23-3-107

K_1, K_2, K_3	A_v	RMS(%)	P, L, F	D_i, I_i	D_w, I_w
7.077e-03	6.874e-03	0.17	1.083	124.1	161.3
7.010e-03			1.010	0.4	0.4
6.535e-03			1.073	214.1	251.3
				0.6	0.6
				3.6	40.8
				89.3	89.3

SITE: 316 SPECIMEN: 24-3-59

K_1, K_2, K_3	A_v	RMS(%)	P, L, F	D_i, I_i	D_w, I_w
1.834e-03	1.784e-03	0.81	1.060	243.2	145.3
1.789e-03			1.025	5.0	5.0
1.730e-03			1.034	151.6	53.7
				17.4	17.4
				348.7	250.8
				71.9	71.9

SITE: 316 SPECIMEN: 25-5-40

K_1, K_2, K_3	A_v	RMS(%)	P, L, F	D_i, I_i	D_{ia}, I_{ia}
1.988e-03	1.948e-03	1.03	1.052	286.4	200.8
1.965e-03			1.012	14.9	14.9
1.890e-03			1.039	194.9	109.3
				5.5	5.5
				85.3	359.7
				74.1	74.1

SITE: 462 SPECIMEN: 55-1-28

K_1, K_2, K_3	A_v	RMS(%)	P, L, F	D_i, I_i	D_{ia}, I_{ia}
4.048e-03	3.984e-03	0.47	1.047	270.1	180.2
4.036e-03			1.003	0.0	0.0
3.866e-03			1.044	0.1	270.2
				0.0	0.0
				137.1	47.2
				90.0	90.0

SITE: 462 SPECIMEN: 55-1-114

K_1, K_2, K_3	A_v	RMS(%)	P, L, F	D_i, I_i	D_{ia}, I_{ia}
7.942e-04	7.665e-04	1.57	1.092	22.2	214.4
7.782e-04			1.021	6.9	6.9
7.272e-04			1.070	114.9	307.1
				21.7	21.7
				275.5	107.7
				67.2	67.2

SITE: 462 SPECIMEN: 55-2-128

K_1, K_2, K_3	A_v	RMS(%)	P, L, F	D_i, I_i	D_m, I_m
2.057e-03	2.023e-03	0.46	1.043	292.5	268.3
2.039e-03			1.009	0.0	0.0
1.973e-03			1.034	22.5	358.3
				0.0	0.0
				140.2	116.0
				90.0	90.0

SITE: 463 SPECIMEN: 58-1-31

K_1, K_2, K_3	A_v	RMS(%)	P, L, F	D_i, I_i	D_m, I_m
1.065e-04	8.796e-05	13.02	1.515	168.8	109.2
9.324e-05			1.142	28.2	28.2
7.030e-05			1.326	40.9	341.3
				48.8	48.8
				274.9	215.3
				27.3	27.3

SITE: 463 SPECIMEN: 58-2-82

K_1, K_2, K_3	A_v	RMS(%)	P, L, F	D_i, I_i	D_m, I_m
2.310e-04	2.136e-04	6.06	1.152	345.5	308.3
2.093e-04			1.104	45.8	45.8
2.006e-04			1.043	226.9	189.7
				25.0	25.0
				118.9	81.7
				33.7	33.7

SITE: 463 SPECIMEN: 59-2-104

K_1, K_2, K_3	A_v	RMS(%)	P, L, F	D_i, I_i	D_{is}, I_{is}
1.289e-04	1.131e-04	14.51	1.341	167.1	297.9
1.143e-04			1.128	59.6	59.6
9.614e-05			1.189	57.8	188.6
				11.0	11.0
				321.9	92.7
				27.9	27.9

SITE: 463 SPECIMEN: 60-2-33

K_1, K_2, K_3	A_v	RMS(%)	P, L, F	D_i, I_i	D_{is}, I_{is}
2.194e-04	1.885e-04	6.45	1.499	177.0	148.5
1.997e-04			1.099	74.7	74.7
1.464e-04			1.364	308.6	280.1
				10.3	10.3
				40.7	12.2
				11.2	11.2

SITE: 463 SPECIMEN: 61-1-105

K_1, K_2, K_3	A_v	RMS(%)	P, L, F	D_i, I_i	D_{is}, I_{is}
6.015e-04	5.781e-04	1.72	1.074	167.2	263.3
5.725e-04			1.051	8.7	8.7
5.601e-04			1.022	258.2	354.3
				6.6	18.1
				24.9	121.0
				79.1	79.1

SITE: 463 SPECIMEN: 64-1-60

K_1, K_2, K_3	A_v	RMS(%)	P, L, F	D_i, I_i	D_m, I_m
1.265e-04	1.005e-04	14.61	1.774	155.5	236.9
1.038e-04			1.219	63.0	63.0
7.130e-05			1.456	285.5	6.9
				18.1	18.1
				22.0	103.4
				19.3	19.3

SITE: 463 SPECIMEN: 67-2-103

K_1, K_2, K_3	A_v	RMS(%)	P, L, F	D_i, I_i	D_m, I_m
2.936e-04	2.765e-04	4.42	1.154	100.1	311.7
2.813e-04			1.044	46.9	46.9
2.544e-04			1.106	257.9	109.5
				40.9	40.9
				357.8	209.4
				11.3	11.3